X-RAY   STRUCTURAL   INVESTIGATIONS

OF

TRANSITION   METAL COMPLEXES.

A   THESIS

PRESENTED   FOR   THE   DEGREE   OF   DOCTOR   OF   PHILOSOPHY

in the

FACULTY   OF   SCIENCE   OF   THE   UNIVERSITY   OF   GLASGOW

by

ROBERT WALKER, B.Sc.

ACKNOWLEDGEMENTS

Glasgow, 1979   R. Walker.

SUMMARY

This thesis describes the single-crystal X-ray structure analyses of eleven inorganic compounds.

A brief account of X-ray diffraction theory and experimental techniques is presented in Chapter One, with emphasis on those aspects relevant to the above-mentioned structural studies.

Theoretical treatments and experimental methods pertaining to the trans-influence of ligands are outlined briefly in Chapter Two. The structure analyses of five platinum complexes are then described: a continuing theme here is the nature of the trans-influence of carbon-donor and phosphine ligands. Four specific points of structural interest arise.

(i)   The study of the complexes cis-$[PtCl_2(CO)(L)]$ (L = PPh_3 and PMe_2Ph) has shown that the trans-influence of carbon monoxide is very small, being comparable to that of chloride. The trans-influence of carbon-donor ligands is then considered in terms of a platinum-ligand bonding model. It is further observed that the metal-ligand bond lengths, and also related i.r. and n.m.r. spectroscopic data, indicate the possibility of carbon monoxide exerting a cis-influence on the Pt-Cl and Pt-P bonds in the complexes.

(ii) In cis-$[PtCl_2\{Ph_2PCH_2CH_2P(CF_3)_2\}]$ the electronic properties of the substituents on the phosphorus atoms exert a pronounced effect on the metal-ligand bonding. Thus, the Pt-P$(CF_3)_2$-bond is extremely short $[l(Pt-P) = 2.168(2)$ Å; cf. $l(Pt-PPh_2-) = 2.244(2)$ Å$]$ and is trans to an unusually short Pt-Cl bond. An extension of the model of the trans-influence of carbon-donor ligands is presented.

(iii) Chatt and co-workers concluded that when the complexes <u>cis</u>-
$[PtCl_2\{C(NHMe)_2\}(PEt_3)]$ and <u>trans</u>-$[PtCl_2\{C(NMe)_2\}(PEt_3)_2]ClO_4$
react with dichlorine a novel 2-metallation and 4-chlorination
of the phenyl ring occurs. This has been verified by the
X-ray analysis of the Pt(IV) carbenoid derivative $[PtCl_2\{C -$
$(Cl.C_6H_3NH)(NHMe)\}(PEt_3)_2]ClO_4$. The N-C(carbenoid) and
Pt-C(donor) distances suggest that the platinum(IV) carbenoid
bonding is very similar to that observed in platinum(II)
complexes, with the main interaction being overlap of the
vacant <u>p</u> orbital of the $\underline{sp}^2$ carbenoid carbon atom with the
filled <u>p</u> orbitals of the adjacent nitrogen atoms, which are
also $\underline{sp}^2$ hybridised. The Pt-Cl bond lengths lead to the <u>trans</u>-
influence order chloride $<$ carbenoid $<$ σ-phenyl, which is
identical to that in platinum(II) derivatives.

(iv) The analysis of the cyclooctyne complex $[Pt(C_8H_{12})(PPh_3)_2]$. —
$0.5C_6H_6$ was carried out in order to compare the structure with
those of the cyclooctyne molecule and of the analogous
cyclohexyne and cycloheptyne complexes of platinum. The metal
co-ordination geometry is found to be very similar to those in
the related cycloalkyne complexes. However, the cyclooctyne
conformation is a half-boat, which differs from that (a half-
chair) observed in free cyclooctyne in the gas phase.

In Chapter Three the molecular structures of a novel ligand, 1,1-
dimethyl-2,5-diphenyl-1-silacyclopentadiene (silole), and its tri-
carbonylruthenium complex are described. This is the first structural
study of the complexed and uncomplexed forms of the same hetero-
cyclopentadiene, where the hetero-atom belongs to the second short
period. It has enabled an assessment to be made of the changes in

bonding which occur when the silole molecule is attached to a transition metal. A rationalisation of the results is given in terms of a Hückel molecular orbital model.

Recently, Chatt and co-workers synthesised a series of isocyanide complexes trans-$[M(CNR)_2(dppe)_2]$(M = Mo or W; dppe = $Ph_2PCH_2CH_2PPh_2$; R = alkyl or aryl). They noted that the $\nu(NC)$ values are much lower than those for free isocyanides and close to the values for bridging isocyanides. Moreover, the ready protonation at the nitrogen atom is unusual. To examine the isocyanide bonding in these complexes, the analyses of two representative derivatives $[M = Mo, (I)$ or $M = W, (II); R = CH_3]$ have been carried out. Details are given in Chapter Four.

The metal co-ordination geometries in (I) and (II) are similar to that in trans-$[Mo(N_2)_2(dppe)_2]$. The most noteworthy feature is the C-N-C(Me) interbond angle in (I) of $155.1(5)^{o}$. Prior to the present study, no fully attested example of substantial bending at the nitrogen atom of co-ordinated isocyanide was available. However, recently a corresponding C-N-C angle of $130(2)^{o}$ has been reported in $[Ru(CNBu^t)_4(PPh_3)]$. The present C-N-C angle and the Mo-C(donor) distance are both consistent with a large contribution from the canonical form $M=C=\overset{..}{N}_R$. The tungsten isocyanide complex (II) is almost isostructural with (I) and has a C-N-C(Me) angle of $151(1)^{o}$.

Recently, Chatt and co-workers synthesised a range of novel five- and six- co-ordinate rhenium nitrosyl complexes. They noted difficulties in structural assignment. Thus, the spectral and magnetic properties of $[ReCl_2(NO)(PMePh_2)_2]$ (III) appear anomalous. The structure analysis of two representative complexes $[ReCl_2(NO)(CH_3OH)-$

$(PMe_2Ph)_2$] (IV) and [$ReCl_3(NO)(PMePh_2)_2$] (V) are described herein. In both (IV) and (V) a linear Re-N-O arrangement is found, and the Re-N distances appear normal. Compound (IV) appears to be derived from (III) by addition of solvent methanol during recrystallisation and this unexpected reaction frustrated an attempt to determine the structural basis of the unusual magnetic properties of (III).

CONTENTS

CONTENTS (continued)   Page

CONTENTS (continued)   Page

- 1 -

CHAPTER   ONE

Some Aspects of X-Ray Structure Analysis

of Single Crystals

1.1. HISTORICAL BACKGROUND

Morphological crystallography[1] was studied systematically as early as
the 17th century. In 1669 Steno carried out measurements on quartz
crystal and postulated the law of constancy of the interfacial angles
of a crystal.

In 1801 Haüy formulated the law of rational indices which can be
expressed as follows: the ratios of the indices of any face of a
crystal are rational and, in general, are the ratios of small integers.
It follows from this law that a crystal can possess proper or improper
rotation axes only of order 1, 2, 3, 4 or 6. Combinations of these
symmetry elements lead to 32 point groups which are classifiable to
7 crystal classes.

Bravais showed that only 14 distinct crystal lattices exist. In a
lattice additional symmetry operations are possible, namely screw
axes and glide planes which involve, respectively, rotations and
reflexion coupled with translation by simple fractions of a cell
edge. Combination of symmetry elements leads to 230 independent space
groups, which are mathematical representations of the only ways in
which identical objects can be arranged in an infinite lattice.

In 1912, following a suggestion by von Laue, Friedrich and Knipping
demonstrated the diffraction of X-rays by a crystal.[2] This phenomenon
was interprepted by von Laue in terms of scattering from a three-
dimensional grating. In the following year, W.L. Bragg showed that
the scattering of monochromatic X-rays from a crystal could be con-
sidered in terms of reflexion and derived the law which bears his
name.[3] This enabled the crystal structures of relatively simple
compounds (such as sodium chloride) to be determined. Since that

time, with the application of the Fourier technique   and the develop-
ment of direct methods of phase determination, the elucidation of the
crystal and molecular structures of complex molecules has become
feasible. In addition, with the advent of powerful digital computers,
the use of the least-squares method of structure refinement has become
commonplace. Moreover, it is now less laborious to apply corrections
for effects such as absorption and extinction; indeed, in many cases
(e.g. the analyses of platinum derivatives described in this thesis) it
is essential to apply such corrections in order to obtain precise
structural information.

1.2. DETERMINATION OF CELL DIMENSIONS AND SPACE GROUP

A preliminary examination of a crystal is usually undertaken with a
Weissenberg or precession camera.[4] From the X-ray photographs, one
can determine the crystal system and the unit-cell dimensions.
Final values of the cell constants can be obtained by a least-squares
treatment of diffractometer setting angles.[5] In addition, the
systematically-absent reflexions enable one either to assign the
crystal uniquely to one space group or to determine which space
groups are possible.[4,6]

1.3. DATA COLLECTION AND REDUCTION

For crystal-structure analysis, a comprehensive set of integrated
intensities, I_o, is required.   There are two main methods of
obtaining such a set: by photographic techniques[4] or with a computer-
controlled diffractometer.[7]   In the photographic method, the
intensities are estimated visually by use of a calibrated series of
intensities on photographic film or measured with a densitometer.

For the diffractometer, a number of instrument geometries are possible; the Hilger and Watts' Y290 diffractometer employs four circles (labelled θ, ω, χ and ϕ) which are capable of independent motion.

In the θ/ω scan mode,[7] the counter and crystal motions are coupled as the crystal is moved through the Bragg condition in a number of steps. The number of counts, in a fixed time, at each step is obtained electronically with a scintillation counter in conjunction with a pulse-height analyser. The integrated intensity is calculated from the relationship:

$$I_o = C - (B_1 + B_2)\, t_p/2t_B \qquad \ldots\ldots (1.1)$$

where C is the total number of counts obtained during the scan, B_1 and B_2 are the background counts at each end of the scan range, t_p is the total time spent counting the peak, and t_B is the time spent counting each background. The estimated standard deviation of I_o, $\sigma(I_o)$, is given by:

$$\sigma^2(I_o) = C + (B_1 + B_2)\, t_p^{\,2}/4t_B^{\,2} + q^2 I_o^{\,2} \quad \ldots (1.2)$$

The first two terms in this equation arise from counting statistics and the term $q^2 I_o^{\,2}$ is included because of additional errors:[8] it is well known that discrepancies of a few percent arise between observed intensities of symmetrically-equivalent reflexions, even for those of the (hkl) and ($\overline{\text{hkl}}$) planes of a centrosymmetric non-absorbing crystal; some of the variation is undoubtedly due to extinction effects and minor instrumental aberrations; moreover, when weights are derived directly from $\sigma(F_o)$ values [see equation 1.44] neglect of the empirical term leads to unrealistic estimates

for strong reflexions. A value of ca. 0.05 is usually assigned to the factor q.

From the observed intensities, the amplitude of the diffracted wave,[6] $|F_o|$, can be derived:

$$|F_o| = K(I_o E/(ALp))^{1/2} \qquad \qquad \ldots\ldots (1.3)$$

K is a scale factor which puts the structure amplitudes on an absolute scale. A crude value can be obtained from the empirical relationship:

$$K = 0.3\ F(000)\ /F' \qquad \qquad \ldots\ldots (1.4)$$

where F(000) is the total number of electrons in the unit cell and F' is the largest (unscaled) structure amplitude obtained from the diffraction experiment. A more reliable estimate of the scale factor can be obtained from a Wilson plot.[9] The final value of K is obtained from the least-squares refinement (see Section 1.8). A and E are, respectively, corrections for absorption and extinction (see section 1.5). The Lorentz factor, L, corrects for the differing times individual reflexions spend in the diffraction condition and is dependent on the experimental technique employed and on the Bragg angle, θ.[6] For the equi-inclination Weissenberg method, L is given by:

$$L = \sin\theta\ /\ \{\sin 2\theta \sqrt{(\sin^2\theta - \sin^2\mu)}\} \quad \ldots\ldots (1.5)$$

where μ is the equi-inclination setting angle. For the normal-beam diffractometer, L is given by:

$$L = 1/\sin 2\theta \qquad \qquad \ldots\ldots (1.6)$$

The polarisation factor, p,[6] corrects for the partial polarisation

of the unpolarised, incident X-ray beam upon scattering and is given

by:

$$p = (1 + \cos^2 2\theta) / 2 \qquad \ldots \ldots (1.7)$$

However, if a crystal monochromator has been used, the X-ray beam is

partially polarised. For a normal-beam diffractometer with a plane

crystal monochromator, as in the Y290 instrument, the appropriate

expression is:

$$p = (\cos^2 2\theta + \cos^2 2\theta_M) / (1 + \cos^2 2\theta_M) \qquad \ldots \ldots (1.8)$$

where θ_M is the Bragg angle of the reflecting plane of the monochro-

mating crystal.[10]

The estimated standard deviation of $|F_0|$, denoted $\sigma(F_0)$, can be

obtained from the relationship:

$$\sigma(F_0) / |F_0| = \sigma(I_0) / 2I_0 \qquad \ldots \ldots (1.9)$$

1.4. DEAD-TIME LOSSES

With electronic counting systems, intensity losses arise when the

counting rates become too great. For scintillation counters with

pulse-height discrimination (as on the Y290 diffractometer) dead-time

losses are significant at counting rates greater than ca. 10,000 counts

s^{-1}. For the Y290 instrument suitable attenuating foils were not

available: hence, an empirical correction for counting losses was

developed during the course of the present work. The integrated

intensities suspected of being affected by such losses and of a

representative sample of intensities with peak counting rates below

10,000 counts s^{-1} were remeasured at reduced X-ray generator settings.

A quadratic equation was found to give a satisfactory representation

of the relationship between I_o and the integrated intensity at reduced

settings, J_o. The coefficients, r and s, of the equation:

$$J_o = rI_o + sI_o^2 \qquad \qquad \cdots \cdots (1.10)$$

were obtained by the method of least-squares; the function minimised

was $\Sigma w \Delta^2$, where

$$w = 1/\sigma^2 (J_o) \qquad \qquad \cdots \cdots (1.11)$$

and

$$\Delta = J_o - rI_o - sI_o^2 \qquad \qquad \cdots \cdots (1.12)$$

The corrected intensities and their estimated standard deviations

were taken as J_o/r and $\sigma(J_o)/r$, respectively. Typically, for

reflexions having counting rates of 10,000 counts s^{-1}, the counting-

loss correction, expressed as a fraction of the corrected intensity,

was ca. 1-2% and, for intense reflexions with rates of ca. 100,000

counts s^{-1}, the correction was of the order of 20-40%.

1.5. SYSTEMATIC ERRORS: ABSORPTION, EXTINCTION AND MULTIPLE REFLEXION

When X-rays pass through solid matter they are absorbed, the amount of

absorption depending on the material and the X-ray wavelength. The

integrated intensity corrected for absorption, I_o', is given by:

$$I_o' = I_o V \Big/ \int exp \left[-\mu (r_p + r_d)\right] dv \qquad \cdots \cdots (1.13)$$

where V is the crystal volume, μ is the linear absorption coefficient,

and r_p and r_d are the path lengths in the crystal along the primary

and diffracted beams, respectively, for reflexion by the volume

element dv.[6]

The mass absorption coefficient is defined as μ/ρ , where ρ is the density of the material. For a composite, homogeneous material, to a very good approximation,

$$\mu/\rho \quad = \quad \sum_i \; g_i \; (\mu/\rho)_i \qquad\qquad \ldots\ldots (1.14)$$

where the summation is over all the constituent elements, and g_i is the mass fraction contributed by the ith element. Hence, from a knowledge of the crystal composition and density, one can calculate μ.

The integral in equation (1.13) can be evaluated numerically by Gaussian integration[11] or by the analytical method of de Meulenaer and Tompa.[12] For evaluation of the path lengths, r_p and r_d, the crystal faces must be indexed and crystal dimensions obtained. A suitable instrument for this purpose is a two-circle optical goniometer.

For heavy-metal complexes, significant X-ray absorption is expected. Consequently, one should calculate the magnitude of the correction for a representative sample of reflexions in order to determine whether or not to apply this correction to the complete set of intensities.

Another effect which reduces the observed intensities is extinction. Two types, primary and secondary, were defined by Darwin.[13] Primary extinction results from the reduction of the X-ray beam due to multiple reflexions as it passes through a crystal.
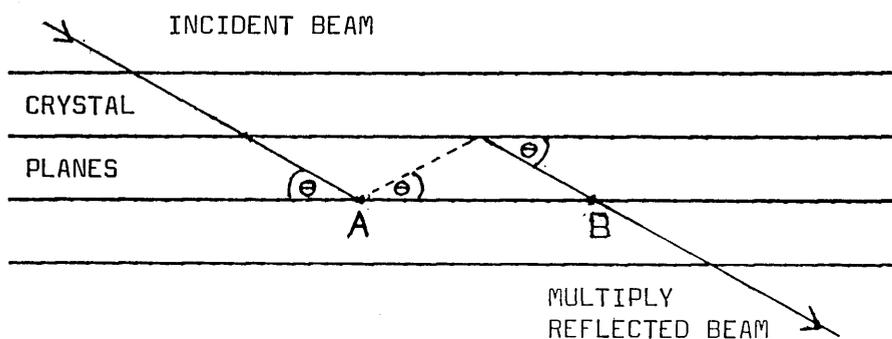
Fig. 1.1. Primary Extinction

In Figure 1.1. a reflected beam at A is at the correct angle for reflexion by the plane at B. On reflexion the phase of the reflected beam changes by 90°, so that the twice-reflected beam is 180° out of phase with the incident beam and destructive interference occurs. In general, a beam multiply reflected n times will be 180° out of phase from one reflected $(n-2)$ times. The net result is that I_o is proportional to $|F_o|$ rather than $|F_o|^2$ for an ideally perfect crystal. However, most crystals can be considered to consist of small mosaic blocks tilted slightly with respect to each other, so that the perfect planes extend over only small regions within the crystal. In general,

$$I_o \ \alpha \ |F_o|^n \qquad\qquad \ldots\ldots (1.15)$$

where $1 \leq n \leq 2$ and is usually closer to 2 for a mosaic crystal. Thus, for mosaic crystals, primary extinction effects are usually negligible.

Secondary extinction, which affects intense reflexions, is more commonly encountered. For strong reflexions, a significant proportion of the incident beam is reflected by the planes near the crystal surface so that deeper planes receive a diminished incident intensity and their contribution to the diffracted intensity is much less than it would otherwise have been. Darwin deduced that the observed intensities are related to the calculated intensities, I_c, by the equation:

$$I_o \ = \ I_c \cdot \exp(-2gI_c) \qquad\qquad \ldots\ldots (1.16)$$

where g is a constant for the crystal at a particular wavelength. To a good approximation, this relationship can be reduced to:

$$I_c/I_o = 1 + 2gI_c \qquad \ldots\ldots (1.17)$$

Hence, from a plot of I_c/I_o versus I_c, an estimate of g can be obtained. The corrected intensity, $\hat{I}_o$, is then given by:

$$\hat{I}_o = I_o (1 + 2gI_c) \qquad \ldots\ldots (1.18)$$

Nowadays, it is common practice to include the extinction constant as a parameter in the least-squares refinement. Correction for secondary extinction was applied in two of the structural analyses described in this thesis. The procedure adopted was that of Larson[14] in which the correction is incorporated in the calculated structure amplitudes; the corrected amplitude, $|F_c^*|$, is given by:

$$|F_c^*| = |kF_c| (1 + 2r^* |F_c|^2 \delta)^{-1/4} \qquad \ldots\ldots (1.19)$$

Here, r^* is an extinction constant; δ is given by:

$$\delta = \lambda^3 (e^2/mc^2 V)^2 (p_2/p_1) \bar{T} / \sin 2\theta \qquad \ldots\ldots (1.20)$$

where λ is the X-ray wavelength; e^2/mc^2 consists of universal constants; V is the crystal volume; $\bar{T}$ is the mean path length in the crystal; and p_n is given[15] by:

$$p_n = 1 + \cos^{2n} 2\theta \qquad \ldots\ldots (1.21)$$

Another source of systematic error is multiple reflexion which is expected especially when a crystal is aligned about a symmetry axis.[16] To minimise its effect on diffractometer data, the crystal should be offset so that its axes are not coincident with those of the diffractometer.

1.6. THE STRUCTURE FACTOR AND ELECTRON DENSITY

The structure factor of a reflexion, $F(hkl)$, which results from the scattering of the atoms in the unit cell, is given by:

$$F(hkl) = \sum_j f_j \exp\left[2\pi i\,(hx_j + ky_j + lz_j)\right] \quad \dots \quad (1.22)$$

where f_j and (x_j, y_j, z_j) are, respectively, the scattering factor and fractional co-ordinates of the jth atom. If anomalous scatterers are present in the crystal, a modified scattering factor, $\hat{f}_j$, is appropriate:

$$\hat{f}_j = f_j + \Delta f_j' + i\,\Delta f_j'' \quad\quad \dots\dots \quad (1.23)$$

Values of the primed quantities in the above expression are available for common X-ray wavelengths.[6]

The structure factor is characterised by an amplitude, $|F_c|$, and a phase angle, $\alpha(hkl)$:

$$|F_c| = (A^2 + B^2)^{1/2} \quad\quad \dots\dots \quad (1.24)$$

and

$$\alpha(hkl) = \tan^{-1}(B/A) \quad\quad \dots\dots \quad (1.25)$$

where

$$A = \sum_j f_j \cos 2\pi(hx_j + ky_j + lz_j) \quad \dots\dots \quad (1.26)$$

and

$$B = \sum_j f_j \sin 2\pi(hx_j + ky_j + lz_j) \quad \dots\dots \quad (1.27)$$

The scattering factors, f_j, have been computed, from various atomic wave-functions, for atoms at rest.[6] In a crystal, each atom is vibrating about its mean position: the appropriate scattering factor

is the product of f_j and q(hkl), where q is the Fourier transform of the smearing function.[17] For isotropic vibration,

$$q(hkl) = exp (-B\lambda^{-2} sin^2\theta) \qquad ..... (1.28)$$

where the Debye factor, B, is related to the mean-square amplitude of vibration, $\overline{u^2}$, by:

$$B = 8\pi^2 \overline{u^2} \qquad ..... (1.29)$$

For anisotropic vibration, a number of equivalent expressions are in common use. Perhaps the most useful is:

$$q(hkl) = exp \left[-2\pi^2 \sum_i \sum_j U_{ij}a_i^*a_j^*h_ih_j\right] \qquad ...(1.30)$$

where a_i^* and h_i represent, respectively, the reciprocal cell constants and the Miller indices h, k and l. It is customary to include the B or U_{ij} parameters in the least-squares refinement.

The atomic arrangement in a crystal is triperiodic and, as first suggested by W.H. Bragg,[18] the electron density distribution, $\rho(x,y,z)$ can be represented by a Fourier series:

$$\rho(x,y,z) = V^{-1} \sum_h \sum_k \sum_l |F| cos\left[2\pi(hx+ky+lz)-\alpha(hkl)\right]$$

$$..... (1.31)$$

Hence, all that is required for the calculation of the electron density distribution, from which atomic positions can be obtained, is a comprehensive set of structure amplitudes and corresponding phases. However, the diffraction experiment yields only structure amplitudes. Thus, the main problem encountered in structure analysis is the derivation of a set of correct or nearly correct phases. There is a variety of methods available which can be employed in an

attempted solution of the phase problem; one such technique is the

use of the Patterson function in conjunction with the heavy-atom

method, and this is outlined in the next section. However, once an

approximate structural model has been found a set of phases can be

derived. If these calculated phases and associated structure ampli-

tudes were incorporated in equation (1.31),the electron density

distribution of the original model would be reproduced. When the

calculated phases are combined with the observed structure factors,

the resulting electron distribution should resemble that of the crystal

more closely than did the original model.

1.7. THE PHASE PROBLEM: THE PATTERSON FUNCTION AND THE HEAVY ATOM METHOD

Although there is no general solution to the phase problem, the

Patterson function is a particularly useful tool for the solution of

heavy-atom structures. Thus, in 1934 Patterson[19] derived a function

which yields information on interatomic vectors:

$$P(u,v,w) = \sum_h \sum_k \sum_l |F_o|^2 \cos 2\pi(hu + kv + lw) \quad ....(1.32)$$

A peak in the Patterson synthesis at the position (u,v,w) results

from atoms with fractional co-ordinates (x_1, y_1, z_1) and (x_2, y_2, z_2)

such that

$$u = x_1 - x_2 \qquad\qquad ..... (1.33)$$

$$v = y_1 - y_2 \qquad\qquad ..... (1.34)$$

$$w = z_1 - z_2 \qquad\qquad ..... (1.35)$$

In general, for a cell with N atoms, there are $N(N-1)/2$ distinct

non-origin vector peaks. However, it is usually impossible to derive

atomic co-ordinates from this function unless at least one atom has

a relatively high atomic number so that its vectors are easily

resolvable from all the others. Furthermore, when the crystal possesses

symmetry elements (other than a centre) particular concentrations of

vector density arise, known as Harker lines and planes,[20] and these

have at least one specialised co-ordinate: this can aid the identifi-

cation of the heavy-atom peaks.

The heavy-atom thus located can be used to calculate an approximate

set of phases which are then used in a Fourier synthesis, commonly

employing $|F_o|$ - $|F_c|$ as coefficients, and this should reveal positions

of some of the lighter atoms.

1.8. REFINEMENT OF THE STRUCTURAL MODEL

The structural model is refined by an iterative process which involves

locating some atoms, refining the structural parameters by a least-

squares method, using the refined parameters to calculate a Fourier

synthesis, and repeating the process until all the atoms have been

located and the parameters have been refined. However, some or,

indeed, all of the hydrogen atoms may not be located, particularly

in a heavy-atom structure. In such a case, one can readily calculate

positions for the hydrogen atoms in groups of known chemical structure,

and include them in structure factor calculations.

The least-squares process involves minimising some function of the

differences between the observed and calculated intensities with

respect to the structural parameters p_1, ..., p_n.[6,14] The function

most commonly used is:

$$M = \sum_{r=1}^{m} w_r (|F_o| - |kF_c|)^2 = \sum_{r} w_r \Delta_r^2 \quad \cdots\cdots \quad (1.36)$$

where the summation is over the set of m crystallographically-independent reflexions, w_r is a weight for each term, and k is a scaling parameter applied to $|F_c|$ (rather than $|F_o|$) for any single refinement cycle. For M to be a minimum,

$$\partial M / \partial p_j = \sum_{r} w_r \Delta_r \partial |kF_c| / \partial p_j = 0 \quad (j = 1, \cdots, n)$$

$$\cdots\cdots \quad (1.37)$$

For an initial set of parameters, a_j, close to the correct values, p_j, to a good approximation, we have:

$$|kF_c(p_1, \ldots, p_n)| = |kF_c(a_1, \ldots, a_n)| + \Delta p_1 \partial |kF_c| / \partial p_1 +$$

$$\ldots + \Delta p_n \partial |kF_c| / \partial p_n \quad \cdots\cdots \quad (1.38)$$

where

$$\Delta p_j = p_j - a_j \quad \cdots\cdots \quad (1.39)$$

Substitution of (1.38) into (1.37) yields n equations in n unknowns, termed the normal equations:

$$\sum_{i=1}^{n} \sum_{r=1}^{m} w_r \frac{\partial |kF_c|}{\partial p_i} \cdot \frac{\partial |kF_c|}{\partial p_j} \Delta p_i = \sum_{r=1}^{m} w_r \Delta_r \frac{\partial |kF_c|}{\partial p_j}$$

$$(j = 1, \ldots, n) \quad \cdots\cdots \quad (1.40)$$

Analytical expressions for the derivatives are available.[6]

Solution of (1.40) by a numerical method provides values of Δp_i.[21] From these values one can determine better approximations, $\hat{a}_j$, to the correct values:

$$\hat{a}_j = a_j + \Delta p_j \quad \cdots\cdots \quad (1.41)$$

However, since a truncated Taylor series was used, it is necessary
to repeat the least-squares calculations until the shift in any
parameter is small by comparison with its estimated standard deviation,
$\sigma(p_i)$.

If the weights are on an absolute scale, $\sigma(p_i)$ is given by:

$$\sigma^2(p_i) = b_{ii} \qquad\qquad \ldots\ldots (1.42)$$

or, when the weights are relative,

$$\sigma^2(p_i) = (m - n)^{-1} b_{ii} \sum_r w_r \Delta_r^2 \qquad \ldots\ldots (1.43)$$

where b_{ii} is the ith diagonal element of the inverse matrix obtained
in the numerical solution of the normal equations. Weights on an
approximately absolute scale can often be obtained from:

$$w_r = 1/\sigma^2(F_o) \qquad\qquad \ldots\ldots (1.44)$$

This weighting scheme is only formally valid if $\sum_r w_r \Delta_r^2/(m-n)$ is
close to unity, indicating that the only significant errors are random
experimental ones. In other cases, some function of $|F_o|$ or Δ is
employed. For a weighting scheme to be satisfactory, mean values of
$w \Delta^2$ must be approximately constant when analysed in ranges of $|F_o|$
or $\sin\theta$.

A useful indication of the course of the refinement is given by the
residuals:

$$R = \sum_r |\Delta_r| / \sum_r |F_o| \qquad\qquad \ldots\ldots (1.45)$$

and

$$R' = \left\{ \sum_r w_r \Delta_r^2 / \sum_r w_r |F_o|^2 \right\}^{1/2} \qquad \ldots\ldots (1.46)$$

For the most accurate analyses, typically the residuals have magnitudes of $\underline{ca}$. 0.05 at the end of the refinement.

1.9. ANALYSIS OF RESULTS

From the refined structural parameters and their estimated errors values of functions such as bond lengths, bond angles and mean planes can be derived together with their standard deviations.[22] To interpret these values in a consistent way a variety of statistical significance tests can be employed. Consider, for example, bond length measurements. The probability, p, that a measured difference in bond length, Δ , arises only from random error can be related to the standard deviation, σ , through Student's t-distribution:

$$p \geq 0.05 \qquad \Delta \leq 1.645 \, \sigma$$

$$p \geq 0.01 \qquad \Delta \leq 2.327 \, \sigma$$

$$p \geq 0.001 \qquad \Delta \leq 3.090 \, \sigma$$

The criteria most commonly employed are:

(i)   If $p > 0.05$, the difference is insignificant.

(ii) If $0.05 > p > 0.01$, the difference may be significant.

(iii) If $0.01 > p$, the difference is highly significant.

A fuller account of statistical methods is presented in Vol.II of 'International Tables for X-ray Crystallography.'[6]

1.10. REFERENCES

1. See, e.g. J.M. Robertson, 'Organic Crystals and Molecules,'
   Cornell University Press, Ithaca, New York, 1953.

2. W. Friedrich, P. Knipping, and M. von Laue, Sitzber. Math. Physik.
   Kl. Bayer. Akad. Wiss., Muenchen, 1912, 308.

3. W.L. Bragg, Proc. Cambridge Phil. Soc., 1913, 17, 43.

4. M.J. Buerger, 'X-ray Crystallography,' Wiley, New York, 1942;
   'The Precession Method,' Wiley, New York, 1964.

5. W.R. Busing and H.A. Levy, Acta Cryst., 1967, 22, 457.

6. 'International Tables for X-Ray Crystallography,' Kynoch Press,
   Birmingham, Vols. I-III, 1962; ibid., Vol.IV, 1974, and
   refs. therein.

7. U.W. Arndt and B.T. Willis, 'Single Crystal Diffractometry,'
   Cambridge University Press, Cambridge, 1966.

8. P.W.R. Corfield, R.J. Doedens, and J.A. Ibers, Inorg. Chem.,
   1967, 6, 197; W.R. Busing and H.A. Levy, J. Chem. Phys., 1957,
   26, 563.

9. A.J.C. Wilson, Nature, 1942, 150, 151.

10. L.V. Azaroff, Acta Cryst., 1955, 8, 701.

11. W.R. Busing and H.A. Levy, ibid., 1957, 10, 180.

12. J. de Meulenaer and H. Tompa, ibid., 1965, 19, 1014.

13. C.G. Darwin, Phil. Mag., 1922, 43, 800.

14. A.C. Larson, in 'Crystallographic Computing,' ed. F.R. Ahmed,
    Munksgaard, Copenhagen, 1970, p. 291, and refs. therein.

15. W.H. Zacharaisen, Acta Cryst., 1963, 16, 1139; ibid., 1967,
    23, 558.

16. See, e.g., L.V. Azaroff, R. Kaplow, N. Kato, R.J. Weiss, A.J.C.
    Wilson, and R.A. Young, 'X-Ray Diffraction,' McGraw-Hill,
    New York, 1974, pp. 569-573, and refs. therein.

17. F. Bloch, Z. Phys., 1932, 74, 295.

18. W.H. Bragg, Trans. Roy. Soc. (London), 1915, A215, 253.

19. A.L. Patterson, Phys. Rev., 1934, 46, 372; Z. Krist., 1935, A 90, 517.

20. D. Harker, J. Chem. Phys., 1936, 4, 381.

21. 'Computing Methods in Crystallography,' ed. J.S. Rollet, Pergamon Press, Oxford, 1965, pp.20-21, and refs. therein.

22. See, e.g., G.H. Stout and L.H. Jensen, 'X-ray Structure Determination: A Practical Guide,' Collier-Macmillan, London, 1972, Ch.18, and refs. therein.

CHAPTER TWO

The Crystal and Molecular Structures of Five

Platinum Compexes: Platinum-Ligand Bonding

involving Carbon-Donor and Phosphine Ligands;

the Relative trans-Influence of Ligands and

the Possibility of a cis-Influence of

Carbon Monoxide.

2.1. THE TRANS-INFLUENCE OF LIGANDS

2.1.1. INTRODUCTION

The trans-effect in square-planar and octahedral complexes is defined as the effect of a co-ordinated group A upon the rate of substitution reactions of the group opposite to A. A wealth of kinetic data is available, particularly for platinum (II) derivatives. From this data, a trans-effect series has been derived which has proved very useful for rationalising known synthetic reactions and in devising new ones.[1]

In 1966, Pidcock, Richards, and Venanzi defined the trans-influence of a ligand in a metal complex as the extent to which it weakens the trans-metal-ligand bond in the equilibrium state of the complex.[2] Thus, they distinguished it clearly, for the first time, from the trans-effect, a kinetic phenomenon which may or may not be related to the trans-influence.

Many studies of the trans-influence phenomenon have now been carried out with the use of a variety of analytical techniques such as X-ray crystallography and vibrational, nuclear magnetic resonance, nuclear quadrupole resonance and photoelectron spectroscopy. The trans-influence has been observed in a host of square-planar and octahedral complexes and also in a few square-pyramidal complexes of transition metals.[3] It is the subject of a recent review.[4]

A brief account of experimental techniques and results, and theoretical treatments is presented in the following sections.

2.1.2. THEORETICAL TREATMENTS OF TRANS-INFLUENCE

The first theoretical rationalisation was the electrostatic theory

of Grinberg[5] which relates <u>trans-</u> influence to ligand polarisability.

However, this electrostatic model is now generally considered

implausible since in many complexes, such as those of platinum(II),

the metal-ligand bonding has a high degree of covalency.[6]

A model involving the hybridisation of the metal ion was proposed

by Syrkin.[7] In square-planar complexes of the third transition

series, a metal ion uses hybrid orbitals composed of the $5d_{x^2-y^2}$,

$6s$, $6p_x$ and $6p_y$ orbitals. The relative order of the orbital energies

is $5d \sim 6s < 6p$. It was considered that, if a ligand L forms a strong

covalent bond with a metal ion, the M-L bond has a higher proportion

of metal 5d and 6s orbitals. Since L and the <u>trans</u>-ligand A share

the same 's+d' hybrid orbital (Figure 2.1), the weakening of the M-A

bond is attributed to a decreased involvement of the metal 5d and 6s

orbitals in that bond. The <u>cis</u>-ligands use a nearly independent 's-d'

hybrid orbital and are affected only slightly.
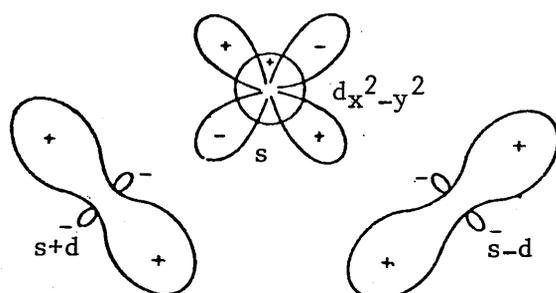
Figure 2.1. Syrkin's s±d hybrid orbitals

In the 1950's and early 1960's emphasis was placed on metal-ligand

π-backbonding when considering the stability of metal complexes with

ligands such as ethylene, carbon monoxide and phosphine. In addition,

the high <u>trans</u>-effect of π-acid ligands was attributed to stabilisation

of the transition state by π-backbonding. It was noted that a metal-

phosphorus bond is weaker when <u>trans</u> to a phosphine than when <u>trans</u>

to chloride: this was attributed to competition between the phosphines

for metal d_{π} electrons. However, in 1966 Pidcock, Richards and

Venanzi[2] asserted that a rationalisation of Pt-P bond strengths in

terms of σ-bonding was more appropriate. Thus, they considered that

trialkyl-phosphine has a strong σ-inductive effect which leads to

<u>trans</u>-bond weakening and that the effect of Pt-P π-bonding on the

Pt-P σ-bonds is insignificant. They supported their conclusions

with coupling constant data for related platinum(II) and platinum(IV)

complexes (Sec. 2.1.3.(b)).

In recent years, theoretical treatments of metal-ligand bonding have

emphasised the maximising of metal-ligand overlap. Thus, Randić

examined the bonding in square-planar complexes using hybrid orbitals

composed of the $3s$, $3p_x$, $3p_y$, $3d_{x2-y2}$ and $3d_{z2}$ metal orbitals.[8] He

showed that the $3d_{z2}$ orbital has only a very small contribution to

the metal-ligand overlap. Furthermore, when $\mu\rho$ is large, μ being the

effective metal atomic charge and ρ the internuclear distance, the

contribution to the total overlap is in the order $p_{\sigma} > s > d_{x2-y2}$.

If a strong covalent metal-ligand bond is formed such that $\mu\rho$ is

large, the M-L bond contains a higher proportion of p_{σ} character than

the <u>trans</u>-M-A bond, whereas if $\mu\rho$ is small, s-character is increased

in the M-L bond at the expense of that in the M-A bond. Unfortunately,

these results cannot be extrapolated reliably to platinum(II)

complexes where $5d_{x2-y2}$, $6s$ and $6p$ metal hybrid orbitals are involved.

Mason and co-workers[9] considered that the magnitude of the quantity

$S^2/\Delta E$ could be used as a measure of the <u>trans</u>-influencing ability

of a ligand L; S is the overlap integral between the metal p_σ orbital and the appropriate ligand orbital, and ΔE is the difference in energy of these orbitals, which is related to the Pauling electro-negativity of the donor atom of L. They showed that both the relative metal-ligand σ-overlap integrals and the relative ligand σ-orbital energies reproduce the trends of the <u>trans</u>-influencing ability of ligands deduced from observed bond lengths in square-planar platinum(II) complexes in which the <u>trans</u> ligand (chloride) has negligible π-acidity. A corresponding, though less satisfactory, ordering of <u>trans</u>-influencing ability for ligands in a variety of octahedral d^6 metal complexes confirmed the usefulness of this view. The conclusion that platinum $6p_\sigma$ character is enhanced in the platinum-ligand bond for ligands of high <u>trans</u>-influence is the reverse of that of Syrkin.

In the above study relatively high <u>trans</u>-influence was predicted for π-acceptor ligands such as ethylene and carbon monoxide which are found to have low <u>trans</u>-influence. This led to the suggestion that for such ligands the σ-inductive effect is partially cancelled by competition between the Lewis acid and the <u>trans</u> ligand for excess charge in the metal.[9]

Zumdahl and Drago[10] made a detailed study, using an extended Hückel molecular orbital method, of the <u>trans</u>-influence of the ligands L in the series <u>trans</u>-$[PtCl_2(L)NH_3]$, where L is H_2O, NH_3, Cl^-, H_2S, PH_3, H^- and CH_3^-. They concluded that the weakening of the Pt-N bond is due to diminished interaction of the nitrogen atom with the platinum 6s and $5d_{x^2-y^2}$ orbitals (as in Syrkin's theory). The changes they observed in the energy and population of the Pt-N bond are consistent with the experimental order of <u>trans</u>-influence

for ligands similar to L. In addition, they concluded that Pt-P

π-backbonding is energetically insignificant for the PH_3 ligand,

and they predicted that in the series of complexes the cis-Pt-Cl

bonds would be weakened in the same manner as and to an extent

comparable with that of the Pt-N bond weakening. However, most

studies have indicated that the trans-influence of a ligand is, in

general, much greater than any cis-influence it may possess.[4]

In conclusion, it is clear that a metal ion undergoes a rehybrid-

isation of its orbitals when it forms a strong covalent bond with a

ligand. However, the various theoretical treatments outlined above

do not present a consistent account of the type of metal orbital

which participates in the M-L bond at the expense of the M-A (trans

to L) bond.

2.1.3. EXPERIMENTAL TECHNIQUES

(a)   Vibrational Spectroscopy

The relative trans-influence of a ligand can be inferred from

vibrational stretching frequencies: a decrease in a force constant

is attributed to a weakening of the bond involved. However, force

constants are often not available and vibrational stretching

frequencies are used instead.

A number of complicating factors must be considered in the inter-

pretation of this data:

(i)   as the mass of L increases the effective mass of the ML_n

       grouping increases and ν(M-A) decreases;

(ii)   coupling can occur between molecular vibrations;

(iii)   lattice effects can produce band splitting and give rise

to frequencies not observed in solution;

(iv)   for a charged metal complex, frequencies can be influenced

by the nature of the counter-ion;   and

(v)   hydrogen bonding can affect the stretching frequencies.

Despite these complexities, numerous studies have been made of trans-influence using infra-red data. In particular, attention has centred on platinum(II) and platinum(IV) complexes using, for the most part, platinum-chlorine and -bromine stretching frequencies. Other indicators that have been employed include $M-CH_3$, M-H and M-P stretching frequencies, and internal ligand vibrations of groupings such as N-H(amine), CO, CN and CH_3.[4]

From the vibrational frequencies, orders of relative trans-influence for a variety of ligands and metal ions have been derived. For example, ν(Pt-Cl) data for the series trans-$[Pt\,XClL_2]$ (L = PEt_3 or PMe_2Ph) lead to the trans-influence order for ligands X: CO $\lesssim$ t-BuNC $\lesssim$ Cl$^-$ $\lesssim$ p-MeOC$_6$H$_4$NC $\lesssim$ P(OPh)$_3$ $\approx$ P(OMe)$_3$ $\ll$ PPh$_3$ $\lesssim$ PEt$_3$ $\ll$ CH$_3^-$ $\lesssim$ Ph$^-$ $\lesssim$ H$^-$ $\ll$ SiMe$_2$Ph$^-$.[11] Some idea of the physical significance of trans-influence can be drawn from the wide range of the stretching frequencies for these ligands, namely 242 to 344 cm^{-1}; the order of increasing trans-influence is that of decreasing frequency.

(b)   Nuclear Magnetic Resonance Spectroscopy.

Pidcock, Richards, and Venanzi[2] related the variation of ^1J(Pt-P) coupling constants to the Fermi contact term which is believed to be predominant in such couplings.[2,12] To a good approximation, for

the covalent component of a Pt-P bond, the coupling constant is given by:

$$J(Pt\text{-}P) \propto \gamma_{Pt} \, \gamma_P \, \alpha_{Pt}^2 \, \alpha_P^2 |\psi_{Pt}(6s)(0)|^2 |\psi_P(3s)(0)|^2 ({}^3\Delta E)^{-1}$$

$$\ldots\ldots(2.1)$$

where γ_i is the magnetogyric ratio for nucleus i, α_i^2 is the s-character of the bonding hybrid orbital used by atom i in the Pt-P bond, $|\psi_i(ns)(0)|^2$ is the electron density of the ns valence orbital at nucleus i, and ${}^3\Delta E$ is a mean singlet-triplet excitation energy.

From the Pt-P couplings in the cis- and trans-isomers of the $[PtCl_2(Bu_3^n P)_2]$ and $[PtCl_4(Bu_3^n P)_2]$ complexes, Pidcock et al.[2] inferred that any synergic effect of Pt-P d_π—d_π bonding on the Pt(II)-P σ-bonding is insignificant. Thus, the ratio J(Pt-P) (cis isomer)/ J(Pt-P) (trans isomer) is very similar for the platinum(II) and platinum(IV) derivatives although platinum →ligand π-bonding is expected to be of lesser importance in the higher oxidation state. In addition, from the Pt(II)-Cl bond lengths, they deduced that trialkylphosphine and hydride ligands have greater trans-influence than chloride and they attributed this to an inductive effect operating through the σ-molecular framework.

Later studies of, for example, trialkylphosphine,[13] phosphite and phosphonate[14] derivatives strengthened the belief that Pt-P coupling constants are determined mainly by the covalency and the s-character of the Pt-P bonds, and that the couplings are more sensitive to changes in the trans than the cis ligand; a few cases were found, however, of significant variations in the coupling constants upon

change of cis-ligands.[15]

From this spectroscopic data, orders of relative trans-influence have
been derived; to this end, it is assumed that a reduction of $^1J(Pt-P)$
coupling constants indicates Pt-P bond weakening. Thus, for example,
Allen and Sze combined several sets of results to obtain the trans-
influence series $SiMePh_2^- > Ph^- > Me^- \gg PEt_3$, $PBu_3^n > PMe_2Ph > PPh_3 >$
$P(OPh)_3$, $CN^- > AsEt_3 > NO_2^- >$ p-toluidine $> EtNH_2 > Et_2NH >$ pyridine,
N_3^-, NCO^-, $NCS^- > Cl^-$, Br^-, $I^- > NO_3^-$.[16]

Of especial interest are the correlations found in related complexes
in which phosphonate, methyl and hydride ligands are, in turn, trans
to a variety of anionic ligands. Thus, Allen et al.[14] observed a
dependence of $^1J(Pt-P)$(phosphonato) on the trans ligand X^- in the
complexes trans-$[PtX\{(PhO)_2PO\}(PBu_3^n)_2]$ and noted a linear corre-
lation between these coupling constants and $^2J(Pt-Me)$ constants in
related trans-$[PtXMe(PEt_3)_2]$ complexes. Church and Mays observed
that the variations in $^1J(Pt-H)$ constants with the trans-ligand in the
cations trans-$[PtHL(PEt_3)_2]^+$ paralleled those in $^1J(Pt-P)$ coupling
constants.[17] In addition, various authors have noted essentially
linear correlations between $^2J(Pt-Me)$ and $^1J(Pt-H)$ constants within
related series of complexes.[18] The above correlations may be taken
as evidence that the variations in $^1J(Pt-H)$, $^2J(Pt-Me)$ and $^1J(Pt-P)$
couplings are dominated by changes in the metal-ligand s-orbital bond
order.

Another correlation that is of considerable import is that suggested
between $^1J(Pt-P)$ constants and Pt-P bond lengths in square-planar
platinum(II) complexes containing monotertiary phosphine ligands.[19]
This relationship is expected to be valid if variations other than in

the total molecular orbital bond order between the platinum and

phosphorus valence state s-orbitals are insignificant. However,

the correlation curve is not accurately defined and, in particular,

the shorter Pt-P bonds display marked deviations from the general

trend. This suggests that factors other than the s-orbital bond

order may determine the Fermi contact term (equation 2.1) in some

cases. Alternatively, electronic effects (such as $M \rightarrow P$ π-bonding)

or steric influences may be present; unfortunately, the n.m.r. method

does not monitor these directly.

(c) X-Ray Crystallography

The most straightforward measure of bond strength and, hence, of

trans-influence appears to be the length of a given metal-ligand

bond. Measurement of a bond length can, of course, be achieved in a

single-crystal X-ray study. However, there has been much less

recourse to this method than to the spectroscopic techniques, largely

because of the often considerable experimental and computational

effort that is required.

X-ray studies of trans-influence have dealt largely with metal complexes

containing σ-donor ligands. Thus, for example, McWeeny et al.[9]

examined the molecular structures of a number of square-planar

platinum (II) complexes in which the ligands trans to chloride have

negligible π-acidity. From Pt (II)-Cl bond lengths, they derived

the order of trans-influence $R_3Si^- > H^- > R_3P > R_2C{=}CR_2, Cl^- > O(acac)$.

Mason and Towl, in a study of trans-influence in octahedral d^6

metal complexes (including some of platinum (IV)), noted a lack of

adequate structural data.[9] To circumvent this problem they proposed

that the relative lengthening of a given M-A bond, expressed as a

fraction of the bond length when trans to A itself (or as a fraction

of the sum of the covalent radii of M and A), be used as a measure

of the trans-influence of a ligand trans to A. They found a high

degree of correlation between the trans-influence order obtained

from bond length data and that obtained from metal-ligand $s^2/\Delta E$

ratios. Nevertheless, there are drawbacks to the use of indicator

groups: it has been remarked that some caution is required in the

application of this method if the ligands A have relatively high

trans-influence or can exhibit π-bonding properties.[4]

The present author has contributed significantly to a recently

undertaken and continuing research project.[3] A Departmental group has

set out to obtain, by single-crystal X-ray methods, accurate

structural information on closely related complexes which is

relevant to the following topics:

(i)   the bonding of carbon-donor ligands to platinum ions;

(ii)   the relative trans-influence of such ligands; and

(iii)   the relative importance of inductive and mesomeric

        mechanisms of trans-influence.

Prior to this work, it was not possible to assess with any confidence

the relative contributions of these mechanisms, for ligands capable

of π-bonding to a metal, due to lack of adequate structural data.

To date, effort has been concentrated on monomeric, electroneutral,

square-planar complexes of platinum (II); these derivatives contain

a linear C-Pt-Cl arrangement and unidentate ligands.[3] Moreover,

the ligands that have been examined are such that a wide variety

of σ -donor-π -acceptor properties is displayed.

More recently, attention has been directed at platinum (II) complexes

containing phosphine ligands which have a variety of electronegative

substituents.[20] Interest lies in the nature of the Pt-P bonding

(σ - and π -interactions), the proposed relationship[19] between Pt-P

bond lengths and ^1J(Pt-P) coupling constants, and the relative trans-

influence of substituted phosphine ligands.

An account of this work detailing, in particular, the present author's

contribution is presented in the ensuing sections.

2.2 THE cis-INFLUENCE OF LIGANDS

There are relatively few studies reported of cis-influence. The most important works appear to be as follows.[21]

(i) In a Raman study of the anions $[PtCl_3(NH_3)]^-$ and $[PtCl_3(CO)]^-$, Denning and Ware deduced that in the carbonyl derivative strengthening of the Pt-Cl(cis to CO) bond is as important as the weakening of the Pt-Cl(trans to CO) bond. They attributed this cis-influence to an increased positive charge on the platinum atom due to electron withdrawal via π-bonding to carbon monoxide.

(ii) Allen and Sze obtained the order of cis-influence CN^- , I^- > NCS^-, Br^- > NCO^-, Cl^- > N_3^- > NO_2^- > NO_3^- from $^1J(Pt-P)$ coupling constants in the series trans-$[PtHX(PEt_3)_2]$, trans-$[PtMeX(PEt_3)_2]$ and trans-$[Pt\{(PhO)_2PO\}X(PEt_3)_2]$ (X = CN^-, ..., NO_3^-]. In addition, from $^1J(Pt-P)$ values in the series cis-$[PtCl_2L(PBu_3^n)]$, they derived the cis-influence order $(PhO)_3P$ > $(MeO)_3P$ > PPh_3 > $PMePh_2$ > PBu_3^n, PEt_3.

(iii) An inverse correlation was found in platinum(II) complexes between ^{35}Cl nuclear quadrupole resonance frequencies and the lengths of the Pt-Cl bonds. Although the frequency is observed to be more sensitive to variation of the trans-ligand, a small dependence on the cis-ligand was noted. Furthermore, from ^{35}Cl n.q.r. frequencies in trans-$[PdCl_2L_2]$ derivatives a cis-influence series was obtained: piperidine < pyridine < $AsBu_3^n$ < PBu_3^n < dimethyl sulphoxide < EtCN < PhCN. For the analogous platinum(II) complexes the corresponding order obtained was NH_3 < Me_2NH < pyridine < PEt_3 < PBu_3^n < PBu_2^nPh.

(iv) There are few pertinent crystallographic results. However, in Sec. 2.3.3 structural data are presented on two platinum(II) complexes:

these are related to a cis-influence of carbon monoxide.

After the completion of the experimental work detailed in this thesis, Manojlović-Muir, Muir and Solomun extended the crystallographic study of cis-influence with additional data on complexes of the type cis-$[PtCl_2(PEt_3)L]$.[22] They derived the order of cis-influence of the ligands L : $Cl^- <$ $C(NPhCH_2)_2 \sim$ CNPh $\sim$ C(OEt)(NHPh)< $PEt_3 \sim$ CO $\sim$ $P(OPh)_3 \sim PF_3$; this order is that of increasing Pt-P distances.

2.3. THE CRYSTAL AND MOLECULAR STRUCTURES OF THE PLATINUM(II) CARBONYL COMPLEXES cis -[PtCl$_2$(CO)L], L = PPh$_3$ (I) AND PMe$_2$Ph (II).

2.3.1. INTRODUCTION

The chemistry and spectroscopic properties of platinum(II) carbonyl complexes have been investigated at length.[23] However, only a few X-ray structural analyses of mononuclear platinum(II)-carbonyl derivatives have been reported and the results are of low or unstated accuracy.[24-27] To obtain detailed information on the nature of the platinum(II) carbonyl bonding and on the relative trans-influence of carbon monoxide, an accurate structural analysis of the complex cis-[PtCl$_2$(CO)(PPh$_3$)],(I), was undertaken. Prior to this work Muir and Manojlović-Muir, from structural studies of platinum(II) complexes, derived the π-acidity series σ-carbyl < carbene < isocyanide and noted that this was an exact reversal of the corresponding trans-influence order.[3] The opportunity of studying the relatively stronger π-acid ligand carbon monoxide was, therefore, welcomed.

It was also anticipated that the structural data would permit an assessment of the cis-influence, if any, of carbon monoxide. In this connection structural and spectroscopic data are of especial interest. Thus, the Pt-P distances (2.34 and 2.35 Å) in trans-[PtCl(CO)-(PEt$_3$)$_2$]$^+$ are slightly longer than the usual values (2.27 - 2.32 Å) for Pt(II)-P(trans to P) bonds.[28] Moreover, Pt(II)-Cl(trans to Cl) distances are normally close to 2.31 Å but in trans-[PtCl$_2$(CO)-(ONC$_5$H$_4$OMe)] the Pt-Cl bond lengths are 2.25(3) and 2.26(3) Å.[28, 25] Furthermore, spectroscopic data for cis-[PtCl$_2$L(PEt$_3$)] complexes, where L is a neutral ligand, indicate that the Pt-P bond is weakest and the Pt-Cl bonds are strongest when L is carbon monoxide.

The ^{1}J(Pt-P) coupling constants (Hz) are: 2754, L = CO; 3049,

L = CNPh; and 3520, L = PEt$_3$.[29,30] The mean ν(Pt-Cl) stretch-

ing frequencies (cm^{-1}) are: 330, L = CO; 307, L = CNPh; and

294, L = PEt$_3$.[29,31]

The X-ray analysis of (I) confirmed the conclusions drawn from the

spectroscopic and structural data given above. However, it was not

possible to distinguish unambiguously between alternative rational-

isations of the metal-ligand bond lengths: one involving steric and

electronic properties of the triphenylphosphine, the other stipu-

lating a cis-influence of carbon monoxide. With the aim of resolving

this ambiguity, the accurate X-ray analysis of cis-[PtCl$_2$(CO)(PMe$_2$Ph)]

(II) was undertaken.

A full account of the analysis of (I) has been published[32] and a

report of the structural analysis of the analogous complex cis-

[PtCl$_2$(CO)(PEt$_3$)], (III), has appeared recently.[22]

2.3.2. EXPERIMENTAL

Crystal Data

Molecule		(I)	(II)
Formula		$C_{19}H_{15}Cl_2OPPt$	$C_9H_{11}Cl_2OPPt$
Molecular weight	M (a.m.u.)	556.3	432.2
Crystal system	-	Triclinic	Orthorhombic
Unit-cell constants	a (Å)	10.4822(9)	15.8515(12)
	b (Å)	9.5929(7)	7.5296(8)
	c (Å)	11.0065(8)	10.6843(11)
	α (°)	97.57(1)	--
	β (°)	117.96(1)	--
	γ (°)	93.80(1)	--
Temperature	T (°C)	20	20
Unit-cell volume	U (Å^3)	958.6	1275.2
Number of formula units per cell	Z	2	4
Calculated density	D_c (gm cm^{-3})	1.927	2.251
Number of electrons per unit-cell	F(000)	528	800
Wavelength of X-radiation	λ (Mo-K$_\alpha$)(Å)	0.71069	0.71069
Linear absorption coefficient	μ(Mo-K$_\alpha$)(cm^{-1})	80.6	120.8
Space group	--	P$\bar{1}$	$P2_12_12_1$

Crystallographic Measurements. - Complex (I). The crystals are air-stable, transparent plates. The specimen chosen for the analysis displayed all members of the {100}, {010}, and {001} forms, and the perpendicular distances between parallel faces were 0.40, 0.24 and 0.09 mm.

The crystal system and some of the unit-cell parameters were obtained from rotation and Weissenberg photographs. The crystal specimen was then centred on a Hilger and Watts' Y290 four-circle diffractometer, controlled by a PDP8 computer, and offset to minimise the effects of multiple reflexion.[33] A preliminary orientation matrix was derived from the manually-optimised setting angles of two strong low-angle reflexions. The final values of the dimensions of a triclinic cell and the orientation matrix used for the collection of the intensity data were derived by a least-squares treatment of the setting angles of twelve reflexions having a wide range of χ and ϕ values and suitable Bragg angles (typically, $13^{\circ} \leq \theta \leq 20^{\circ}$).[34a] The space group $P\bar{1}$ led to a satisfactory structural model.

Complex (II). The crystals are white, air-stable needles elongated along the c-axis. The specimen used in the analysis displayed all members of the {001} and {210} forms, and the perpendicular distances between parallel faces were 0.52, 0.11 and 0.08 mm.

The crystal system and unit-cell dimensions were obtained from rotation and Weissenberg photographs. The systematically-absent reflexions, h00 when h = 2n + 1, 0k0 when k = 2n + 1, and 00l when l = 2n + 1, restrict the space group uniquely to $P2_1 2_1 2_1$. The crystal specimen was centred on the Y290 diffractometer and offset to minimise

the effects of multiple reflexion. The final values of the cell
dimensions were obtained by a least-squares method.[34b]

Intensity Measurements. - Complex (I). The intensities of all
independent reflexions with $\theta(\text{Mo} - K_\alpha) \leq 30^\circ$ were measured on the Y290
diffractometer with the use of zirconium-filtered molybdenum radiation
and a pulse-height analyser. The $\theta - 2\theta$ scan technique was employed,
with a scan step in 2θ of 0.04° and a counting time per step of 2.5s.
Each reflexion was scanned from $\widehat{2\theta} - 0.6^\circ$ to $\widehat{2\theta} + 0.6^\circ$, where $\widehat{2\theta}$ is
the calculated Mo-K_α peak position. At each end of the scan range,
the local background was counted for 10s with crystal and counter
stationary. To check crystal and electronic stability, the intensities
of three intense low-angle reflexions from diverse areas of reciprocal
space were remeasured periodically throughout the experiment, but
only random fluctuations of up to $\pm$ 5% of their mean values were
observed.

The integrated intensities, I, and their standard deviations, $\sigma(I)$,
were derived using standard relationships described earlier in the
text;[35] a value of 0.04 was assigned to the empirical factor q. They
were scaled according to the variations in intensity of the three
standard reflexions and corrected for Lorentz, polarisation and counting-
loss effects.[35,36] An absorption correction was also applied using
a Gaussian integration grid of 12 x 12 x 14 points.[37] The transmission
factors on $|F_o|$ ranged from 0.41 to 0.72.

Of 5618 reflexions measured, only 4198 for which $I > 3\sigma(I)$ were used
in subsequent calculations.

Complex (II). The intensities of all independent reflexions with $\theta(\text{Mo-K}_\alpha) \leq 35^\circ$ were measured on the Y290 instrument with the use of graphite-monochromated molybdenum radiation and a pulse-height analyser. The θ-2θ scan technique was employed. Each reflexion was scanned through a 2θ range of 1.2°, with a scan step in 2θ of 0.04°, and a counting time of 2.5s. The local background was counted for 15s at each end of the scan range. The intensities of three strong reflexions, remeasured periodically throughout the experiment, varied by less than $\pm$ 4% of their mean values.

The integrated intensities, I, and their standard deviations, $\sigma(I)$, were obtained using relationships referenced above (q 0.04). They were corrected for Lorentz, polarisation, counting-loss and absorption effects. The transmission factors on $|F_o|$, calculated by Gaussian integration, varied between 0.46 and 0.63.

Of 3172 reflexions measured, only 2390 with $I \geq 3\sigma (I)$ were used in the subsequent calculations.

Structure Analysis. - In both analyses, the position of the platinum atom was derived from a Patterson synthesis and the other non-hydrogen atoms were located in subsequent difference syntheses.
The structural models were refined by the method of full-matrix least-squares. The function minimised was $\sum w \Delta^2$, where $w = 1/\sigma^2(F_o)$ and $\Delta = |F_o| - |F_c|$. Atomic scattering factors were taken from ref. 38 except those of platinum[39] and hydrogen.[40] Allowance was made for the anomalous scattering of the platinum, chlorine and phosphorus atoms using Cromer's values of $\Delta f'$ and $\Delta f''$.[41]

Complex (I). The refinement of the scale factor and of the positional

and isotropic thermal parameters of the platinum atom led to R 0.28.

After the other non-hydrogen atoms were included, oxygen and carbon

atoms with isotropic temperature factors and all the remaining atoms

with anisotropic temperature factors, R decreased to 0.09. The

carbon and oxygen atoms of the carbonyl group were then assigned

anisotropic thermal parameters. The positions of the hydrogen atoms

were determined from those of the phenyl carbon atoms, assuming a

C-H distance of 1.0 $\overset{o}{A}$; the scattering of these atoms was allowed

for in subsequent structure factor calculations but their positions

were not varied. The refinement converged at R 0.037 and R' 0.041.

In the last cycle of refinement all parameters shifted by $< 0.1\sigma$.

The standard deviation of an observation of unit weight, S.D., was

1.3. The mean values of $(|F_o| - |F_c|)^2 / \sigma^2(F_o)$ showed no systematic

trends when analysed as a function of $|F_o|$ or $\sin\theta$, indicating that

the weighting scheme was satisfactory. The extreme function values

in the final difference synthesis (1.7 and -1.1 $e\overset{o}{A}^{-3}$) were associated

with the positions of the platinum and C(24) atoms, respectively.

Extinction corrections did not appear necessary.

Complex (II). The refinement of the scale factor and of the

positional and isotropic vibrational parameters of the platinum atom

led to R 0.19. After the remaining non-hydrogen atoms were included

with isotropic thermal parameters, R decreased to 0.10. The platinum,

chlorine and phosphorus atoms, and the carbon and oxygen atoms of the

carbonyl group were then assigned anisotropic thermal parameters: R

decreased to 0.064. In all subsequent calculations, the data corrected

for absorption effects were employed. In addition, the positions of

all non-methyl hydrogen atoms were inferred and the scattering of

these atoms was allowed for in subsequent structure factor calcu-

lations but the positional parameters were not varied. The refine-

ment of the structural model converged at R 0.037 and R' 0.044.

With no increase in the number of structural parameters, the enantio-

meric model was refined. This refinement converged at R 0.053 and

R' 0.068; Hamilton's R-ratio test indicates that these represent

highly significant increases.[42]   Accordingly, the original structural

model was assumed to represent correctly the absolute configuration

of the molecules in the crystal. Examination of the structure factor

discrepancies of low-angle reflexions indicated that moderate

extinction effects were present. Accordingly, a secondary extinction

parameter, r^*, was included in the refinement;[43]   convergence was

achieved at R 0.036 and R' 0.043.   In the final cycle of least-

squares all parameters shifted by less than 0.3σ . The value of r^*

was $6.8(5) \times 10^{-3}$ deg^{-1} and that of $\underline{S.D.}$ 1.5. The mean values of

$(|F_o| - |F_c|)^2/\sigma^2(F_o)$ showed no systematic trend when analysed as a

function of $|F_o|$ or $\sin\theta$. The extreme function values in the final

difference synthesis ranged from 2.1 to -1.7 $e\text{Å}^{-3}$; all peaks outwith

the range ± 1.1 $e\text{Å}^{-3}$ were associated with the position of the platinum

atom. The methyl hydrogen atoms were not located.

The observed and final calculated structure amplitudes are listed

in the Appendix [pp. 1 to 32,(I), and 33 to 52,(II)]. Final atomic

parameters and a selection of derived functions are presented in

Tables 2.1 - 2.6. Views of the molecular structures are shown and

the atomic numbering schemes are indicated in Figs. 2.2 and 2.3.

The computer programs used were the Hilger and Watts' software

package for the Y290 diffractometer, the cell reduction program of

K.W. Muir, J.G. Sime's data processing program, the counting-loss

correction program of K.W. Muir and R. Walker, J.M. Stewart's

'X-ray '70 System,' the RBLS2 full-matrix least-squares program

of P.K. Gantzel, R.A. Sparks, K.N. Trueblood, D.N.J. White, P.D.Cradwick,

S.E.V. Phillips, and P.R. Mallinson, the ORFFE program of W.R. Busing,

K.O. Martin, and H.A. Levy, and C.K. Johnson's ORTEP.

2.3.3. RESULTS AND DISCUSSION

The crystals of both structures are built of discrete monomeric

molecules. Calculation of all intermolecular distances $\leq 4.0\ \overset{o}{A}$

indicated that the interactions between molecules are of the van der

Waals type (Tables 2.3 and 2.4(d)).[44]

<u>The Co-ordination of the Metal Atoms.</u> - The molecules in both

structures have the expected <u>cis</u>-square-planar configuration.

The orientation of the phosphine ligand is such that an α-carbon atom

[C(31) in (I) and C(11) in (II)] lies close to the co-ordination plane

of the metal atom, near to the carbonyl group: relevant torsion

angles are C(1)-Pt-P-C(31) 2.7(3)^{o} in (I) and C(1)-Pt-P-C(11)

8.2(5)^{o} in (II). Furthermore, there are a number of short

intramolecular contacts involving carbon and chlorine atoms. Thus,

in (I) there is a separation of 3.34 $\overset{o}{A}$ between a β-carbon, C(16), and

a chlorine atom, Cl(2). The resulting Cl(2)···H distance of <u>ca.</u>

2.55 $\overset{o}{A}$ is shorter by 0.45 $\overset{o}{A}$ than the sum of the van der Waals radii

of hydrogen (1.2 $\overset{o}{A}$) and chlorine (1.8 $\overset{o}{A}$),[44] and the C(16)-H···Cl(2)

angle is 147°: a weak hydrogen bond is indicated.[45] In (II) the

methyl carbon···chlorine separations C(2)···Cl(2) 3.42 $\overset{o}{A}$ and C(3)···Cl(2)

3.62 $\overset{o}{A}$ suggest a weak interaction although this conclusion is not

certain since the methyl hydrogen atoms were not located.

The non-bonded intramolecular contacts involving carbonyl and phenyl

atoms, namely, C(1)···C(31) and C(1)···C(32) in (I), and C(1)···C(11)

in (II) [3.06, 3.14 and 3.11 $\overset{o}{A}$, respectively] indicate steric strain

in the molecules of (I) and (II). The distortions of the metal

co-ordination planes from ideal square-planar geometry can best

be attributed to ligand-ligand repulsions, particularly those involving

the carbonyl and bulky phosphine ligands; as expected, the

distortions are greater in (I) where a phosphine of greater steric bulk is present.[46] Thus, the P-Pt-C(1) angle departs from 90° by 4.6° in (I) and 3.9° in (II); the corresponding deviations of the C(1)-Pt-Cl(1) angle are -3.2 and -2.0°, respectively. The C(1)-Pt-Cl(2) angle is only $173.5(2)^\circ$ in (I) but is more nearly regular in (II), being $178.0(3)^\circ$. Similar distortions are found in the complex cis-$[PtCl_2(CNEt)(PEt_2Ph)]$.[47] In addition, as is often found in square-planar platinum(II) complexes, there are small but significant displacements of the platinum and ligand donor atoms from the metal co-ordination plane (Tables 2.5 and 2.6):[47] individual atoms are displaced by up to ± 0.04 Å in (I) and ± 0.02 Å in (II). The carbonyl oxygen atoms have displacements from these planes of -0.16Å and -0.02Å in (I) and (II), respectively.

The Geometry of the Phosphine Ligands. - The phosphine ligands display no unexpected features.[48] Thus, the P-C(phenyl) separations are in excellent agreement: respective values are 1.815(3) Å (mean) in (I) and 1.802(8) Å in (II). In addition, the P-C(methyl) bond lengths do not deviate significantly from their mean value of 1.821(9) Å. These distances are similar to those found in other monotertiary phosphine complexes of platinum(II).[49] Moreover, the Pt-P-C and C-P-C angles display the expected deviations from the regular tetrahedral angle of $109^\circ28'$:[48] they are, respectively, significantly larger and smaller than the latter value. The Pt-P-C angles in (I) and (II) have the respective ranges 110.2(3) - 118.3(2) and 111.2(3) - $113.1(3)^\circ$. The corresponding ranges of the C-P-C angles are 105.4(3) - $107.2(3)^\circ$ (mean $105.8(7)^\circ$) in (I) and 105.6(4) - $107.2(5)^\circ$ in (II).

The carbon-carbon distances in the phenyl groups are normal, with mean values of 1.382(9) and 1.384(4) Å in (I) and (II), respectively; these means are shorter than the spectroscopic value of 1.397(1) Å for benzene:[50] such contractions have been attributed to the effects of thermal motion.[48] The C-C-C angles are normal [means range from 119.9(6) to 120.0(3)°], and the phenyl rings are accurately planar with root mean-square deviations from planarity of $\leq$ 0.03 Å. The deviations of the individual distances and angles from their respective mean values are insignificant, with the exception of the bond lengths involving atoms C(21) - (26) in (I) where the deviations are highly significant (0.1% level, χ^2 = 35.8 on five degrees of freedom). In principle, this may result from neglect of any anisotropic thermal motion of the ring carbon atoms, from underestimation of the errors of the positional parameters derived in the least-squares refinement, or from distortions from regular hexagonal geometry. Similar variations have often been ascribed to a swinging motion of the rings about the P-C bonds.[51] The bond length pattern noted by Churchill, Kalra and Veidis is evident with only minor discrepancies: C(ortho)-C(meta) > C(P-bonded)-C(ortho) > C(meta)-C(para).[51]

In complex (I) the phenyl rings have the usual 'propeller' arrangement at the phosphorus atom with dihedral angles between the planes of 97.5, 109.4 and 81.5°.[51,52] The phosphorus atom is displaced from the phenyl planes by up to 0.20 Å in (I) and by 0.09 Å in (II): distortions of such a magnitude are common in arylphosphine derivatives and have been attributed to repulsions between the phosphine substituents.[48]

The endocyclic angles at the _ipso_-carbon atoms [119.5(4)°(mean),(I); 118(1)°,(II)] are comparable with the values noted by Coulson and co-workers for a phenylphosphine σ-bonded to a transition metal.[53,54]

- 46 -

The Platinum-Carbonyl Bonding. The Pt-C-O fragment is linear in

(II) but slightly bent by 4.4(7)$^{\circ}$ in (I): such distortions can arise

from electronic effects but, in this case, may be simply due to

steric repulsion by the bulky phosphine ligand.[55] The Pt-C(donor)

distances [1.858(7) Å, (I); 1.834(11) Å, (II); 1.855(14) Å, (III)]

are in good agreement and in the range found in other platinum(II)

carbonyl complexes [1.74(4) to 1.97(5) Å].[24-27] However, they are

considerably shorter than the Pt-C(sp) distance[56] of 1.98(2) Å in

trans-[PtCl(C≡CPh)(PEt$_2$Ph)$_2$], and the Pt-C(sp^2) distances[57,58] in

cis-[PtPh$_2$(Ph$_2$PCH$_2$PPh$_2$)] [2.05(1) Å] and cis-[PtPh(GePh$_2$OH)(PEt$_3$)$_2$]

[2.04(1) Å]. When allowance is made for the difference in covalent

radii[59] of sp^2 and sp hybridised carbon atoms (0.74 and 0.70 Å,

respectively), it is clear that the co-ordinated carbonyl groups

exhibit appreciable π-acceptor properties. In addition, the

Pt-C(donor) separations are somewhat shorter than the mean value of

1.896(16) Å in cis-[PtCl$_2$(CNPh)$_2$], suggesting increased Pt ⟶ C

backdonation in the carbonyl complexes.[60]

The C-O bond lengths [1.114(8) and 1.106(13) Å] appear a little

short by comparison with those in other metal carbonyls [typically

ca. 1.15 Å with esd's of ca. 0.02 Å][61] and with the distance[50] of

1.128 Å in free carbon monoxide: these contractions can be

attributed reasonably to the effects of the high thermal motion of

the terminal oxygen atoms.

The Trans-Influence of Carbon Monoxide. - The Pt-Cl(trans to C)

distances in the title complexes [2.276(1) Å,(I);2.291(2) Å, (II)] and

in (III) [2.296(4) $\overset{\text{o}}{\text{A}}$][22] are extremely short by comparison with those in

related complexes[26,29,47, 63] (Table 2.7) and with the mean length [2.303(5) $\overset{\text{o}}{\text{A}}$][3]

of the Pt-Cl(<u>trans</u> to Cl) bonds in five other platinum(II) complexes:

the carbonyl group exerts only a weak <u>trans</u>-influence which is

significantly less than that of CNEt or chloride.   In contrast, the

<u>trans</u>-influence of the σ-bonded carbon-donor ligand in <u>cis</u>-[PtCl-

(C≡CPh)(PEt$_2$Ph)$_2$] is high, the Pt-Cl (<u>trans</u> to C) distance being

2.407(6) $\overset{\text{o}}{\text{A}}$.[56]

The bond length data lead to the π-acidity series σ-carbyl <

carbene < isonitrile < carbon monoxide, which is the exact reversal

of the <u>trans</u>-influence order carbon monoxide < isonitrile < carbene <

σ-carbyl.   Thus, the π-acidity of carbon-donor ligands appears to reduce

their <u>trans</u>-influence on Pt-Cl bonds.

Manojlović-Muir and Muir proposed a model of <u>trans</u>-influence which

takes account of both the σ-donor and the π-acceptor properties

of ligands.[3]   Thus, if a strong covalent Pt-L bond is formed, with

negligible π-component, the bonding electron density will lie mainly

in the L-Pt bond and on the ligand Cl$^-$.   The concentration of electron

density in the L-Pt bond causes repulsion of the metal d_π electrons

in the direction of the chloride ligand and, thereby, weakens the

Pt-Cl bond.   As the electronegativity of the ligands L increases,

the Pt-L covalency decreases and, consequently, the <u>trans</u>-influence

decreases.   Moreover, π-acid ligands can accept charge from the

metal d_π orbital.   Thus, the <u>trans</u>-influence of carbon-donor ligands

is expected to decrease as the π-acidity increases throughout a

series.

The <u>cis</u>-Influence of Carbon Monoxide - The lengths of the metal-
ligand bonds <u>cis</u> to the carbonyl group are of especial interest.
Thus, in (I) the Pt-Cl(<u>trans</u> to P) and Pt-P distances are,
respectively, 0.036(4) $\overset{o}{A}$ (9σ) shorter and 0.045(3) $\overset{o}{A}$ (15σ) longer
than the weighted mean values [2.379(3) and 2.237(2) $\overset{o}{A}$, respectively]
of corresponding distances in five other <u>cis</u>-[$PtCl_2(L)(PR_3)$]
complexes (Table 2.7).   These differences, although small, are
statistically highly significant and are consistent with the trends
in the structural and spectroscopic data noted in Sec. 2.3.1.
They lead to two rationalisations (not necessarily mutually exclusive):
(a) that carbon monoxide exerts a <u>cis</u>-influence which weakens the
Pt-P bond and strengthens the Pt-Cl(<u>trans</u> to P) bond, or (b) that
PPh_3 forms a weaker bond to platinum and has a lower <u>trans</u>-influence
than PEt_3, PMe_3 or $PPhEt_2$.

Consider, for the moment, the electronic and steric properties of the
substituents of phosphine ligands.   These have been examined by
Tolman[46] who used the perturbation of the A_1 carbonyl stretching
frequency in $Ni(CO)_3PR_3$ complexes as a measure of the electron-
withdrawal by individual substituents on the phosphorus atom.   He
assigned, for example, the values of χ_i [a measure of electron-
withdrawal] 2.6, 1.8 and 4.3 cm^{-1} to the Me, Et and Ph groups,
respectively [<u>cf</u>., <u>e.g</u>., 19.6, CF_3;   11.2, C_6F_5; and 0, t-Bu
(internal standard)].   Moreover, he defined a steric parameter as
the angle θ of a cylindrically symmetrical cone which has its apex
at the metal and which just encloses the van der Waals envelope of
the ligand.   The θ values were obtained from models, assuming a M-P
distance of 2.28 $\overset{o}{A}$.   For unsymmetrical $PR^1R^2R^3$ ligands, an effective

cone angle is given by:

$$\theta = 2/3 \ (\theta_1/2 + \theta_2/2 + \theta_3/2) \qquad\qquad .....(2.1)$$

Thus, for example, θ has the values: 143, PPh_3; 122, PMe_2Ph; and

132°, PEt_3. The above parameters are useful, although crude, measures

of steric and electronic properties of substituents.

Let us now return to the problem concerning the metal-ligand bond

lengths cis to carbon monoxide. If the steric mechanism is predomin-

ant, change of phosphine from PPh_3 to the less bulky PMe_2Ph or PEt_3

ligands (smaller in cone angles by 21 and 11°, respectively) should

produce Pt-P and Pt-Cl bond lengths that resemble more closely

the corresponding mean values in Table 2.7. However, the Pt -Cl

(trans to P) and Pt -P bond lengths in the PMe_2Ph (II) and PEt_3

(III) analogues of (I) are 2.362(3) and 2.264(2) $\overset{o}{A}$, respectively,

in (II) and 2.368(3) and 2.265(3) $\overset{o}{A}$, respectively, in (III). Thus,

it can be seen that the trends observed in (I) are present also in

(II) and (III), although they are not as pronounced. They are

consistent with carbon monoxide exerting a small cis-influence of

ca. +0.03 $\overset{o}{A}$ on a Pt-P bond and ca. -0.02 $\overset{o}{A}$ on a Pt-Cl bond.

A cis-influence also provides a satisfactory rationalisation of the

bond lengths in cis -$[PtCl_2(L)(PR_3)]$ complexes in general. In

this series, one of the ligands cis to phosphine and the ligand trans

to phosphine are always the same. The Pt-P bond lengths cover a

large range $[2.215(4)$ to $2.282(2)$ $\overset{o}{A}]$ and can be divided into three

groups: (i) 2.215(4) $\overset{o}{A}$ when L = Cl^- (in the anion of $[Et_4N][PtCl_3-$

$(PEt_3)])$;[64] (ii) 2.242(2) $\overset{o}{A}$, the mean for seven complexes in which

L is a weak π-acid such as carbenoid, isocyanide or phosphine;[65]

and (iii) 2.280(5) $\overset{o}{A}$, the mean for the three carbonyl complexes

(I) - (III).   The variations in bond distance do not appear to be
of steric origin since such a rationalisation implies that the Pt-Cl
and Pt-P bond lengths cis to L should vary in the same manner: a
slight trend in the opposite sense is indicated, the mean Pt-Cl
(cis to L) distances being 2.382(4), 2.375(3) and 2.353(8) Å,
respectively, for groups (i), (ii) and (iii).   Differences in the
electronic properties of the phosphine substituents are also unlikely
to be a major factor in these variations: the Pt-P distances in
the complexes (I) - (III) differ by at most 0.018(3) Å; Pt-P(trans to P)
distances in monomeric, square-planar complexes (Table 2.8) show no
consistent variation with the electron-withdrawing ability of the
phosphine substituents.   Thus, an electronic mechanism operating
through the cis-ligand is strongly indicated.   By analogy with
the trans-influence of π-acceptor ligands, it is suggested that the
cis-influence of a ligand L may result from its π-acceptor ability.
Thus, the weakening of the Pt-P bond may be ascribed to competition
between L and PR_3 ligands for metal d_{π} electrons.   In addition,
significant Pt $\longrightarrow$ L backdonation will lead to an increased
electrostatic attraction between platinum and chloride ligands, thus
shortening the Pt-Cl bond cis to L (as well as that trans to L).
Alternatively, the cis-Pt-Cl bond may shorten because of a diminution
of the trans-influence of the phosphine that is effected by the cis-
influence of L.

TABLE 2.1

(a) Fractional atomic co-cordinates ($\times 10^4$) and vibrational parameters for <u>cis</u>-[$PtCl_2(CO)(PPh_3)$] (I); standard deviations are given in parentheses.*

Atom	x	y	z	$B \times 10 \text{Å}^2$
Pt	2422.6(3)	2223.8(2)	832.6(3)	*
P	1393(2)	1363(1)	-1510(2)	*
Cl(1)	3496(2)	3174(2)	3227(2)	*
Cl(2)	1798(2)	4399(2)	382(2)	*
C(1)	3136(8)	556(7)	1359(7)	*
O	3648(8)	-395(6)	1723(7)	*
C(11)	-549(6)	1389(5)	-2598(6)	31(1)
C(12)	-1416(7)	236(6)	-3643(7)	39(1)
C(13)	-2857(8)	300(7)	-4570(8)	47(1)
C(14)	-3434(8)	1512(7)	-4459(8)	49(1)
C(15)	-2611(9)	2664(8)	-3441(9)	54(2)
C(16)	-1157(8)	2606(7)	-2470(8)	47(1)
C(21)	2285(6)	2341(6)	-2275(6)	32(1)
C(22)	1524(7)	2602(6)	-3597(7)	40(1)
C(23)	2258(9)	3349(8)	-4161(8)	52(1)
C(24)	3697(9)	3813(8)	-3379(9)	54(2)
C(25)	4467(10)	3567(9)	-2068(10)	62(2)
C(26)	3764(8)	2825(7)	-1482(8)	49(1)
C(31)	1629(6)	-483(6)	-1811(6)	33(1)
C(32)	909(7)	-1476(6)	-1444(7)	40(1)
C(33)	1066(8)	-2899(7)	-1625(8)	50(1)
C(34)	1985(10)	-3314(9)	-2113(10)	61(2)
C(35)	2705(10)	-2344(9)	-2502(10)	61(2)
C(36)	2513(8)	-929(7)	-2358(8)	46(1)

TABLE 2.1 (Cont'd)

* These atoms were assigned anisotropic temperature factors

of the form $\exp\left[-(B_{11}h^2+B_{22}k^2+B_{33}l^2+2B_{12}hk+2B_{13}hl+2B_{23}kl)\right]$.

The final values of the B_{ij} parameters $(\times 10^4)$ are:

Atom	B_{11}	B_{22}	B_{33}	B_{12}	B_{13}	B_{23}
Pt	95.0(3)	84.7(2)	88.9(3)	23.7(2)	46.1(2)	23.9(2)
P	93(2)	70(1)	95(2)	20(1)	49(1)	22(1)
Cl(1)	197(3)	154(2)	91(2)	36(2)	52(2)	22(2)
Cl(2)	154(2)	83(1)	128(2)	33(2)	31(2)	14(1)
C(1)	164(11)	134(9)	106(9)	40(8)	59(8)	33(7)
O	281(12)	162(8)	188(10)	108(8)	103(9)	91(7)

* Throughout this thesis, the limits of error have been derived from the appropriate least-squares matrix and are given in units of the least significant digit of the quantities to which they refer.

TABLE 2.1 (Cont'd)

(b) Calculated fractional co-ordinates $(\times 10^3)$ and assumed isotropic

vibrational parameters for hydrogen atoms; each hydrogen atom is

numbered according to the carbon atom to which it is attached.

Atom	x	y	z	$B \times 10 Å^{2*}$
H(12)	-106	-58	-373	49
H(13)	-339	-46	-528	55
H(14)	-439	155	-508	58
H(15)	-301	345	-336	62
H(16)	-64	337	-178	57
H(22)	54	229	-408	49
H(23)	175	353	-508	62
H(24)	419	429	-373	62
H(25)	544	393	-150	73
H(26)	427	263	-60	58
H(32)	27	-121	-114	51
H(33)	56	-358	-145	59
H(34)	214	-424	-222	68
H(35)	335	-264	-281	70
H(36)	301	-26	-261	54

* B of adjacent carbon atom multiplied by 1.25.

TABLE 2.2 :

(a) Fractional co-ordinates $(\times 10^4)$ and vibrational parameters for

$$\underline{cis}\text{-}[PtCl_2(CO)(PMe_2Ph)] \quad (II)$$
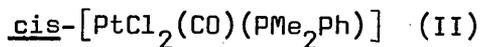
Atom	x	y	z	$B \times 10^2 \AA^2$
Pt	1269.4(2)	-1398.5(4)	2224.4(3)	*
P	180(1)	-3440(3)	883(2)	*
Cl(1)	759(2)	719(4)	3668(2)	*
Cl(2)	2110(2)	-2606(4)	3748(2)	*
C(1)	571(7)	-407(15)	1048(10)	*
O	153(7)	195(16)	337(9)	*
C(11)	1475(5)	-3088(11)	-714(8)	33(1)
C(12)	1903(7)	-1907(14)	-1468(10)	44(2)
C(13)	1647(7)	-1568(14)	-2704(11)	48(2)
C(14)	929(7)	-2420(14)	-3147(10)	44(2)
C(15)	494(8)	-3555(17)	-2421(13)	59(2)
C(16)	782(7)	-3941(15)	-1200(11)	49(2)
C(21)	2955(6)	-3414(14)	855(10)	44(2)
C(31)	1479(6)	-5664(14)	1313(10)	43(2)

* These atoms were assigned anisotropic temperature factors of the

form $\exp\left[-\sum_{ij}\sum B_{ij}h_ih_j\right]$. The final values of the B_{ij} parameters $(\times 10^4)$

are:

TABLE 2.2 (Cont'd)

Atom	B_{11}	B_{22}	B_{33}	B_{12}	B_{13}	B_{23}
Pt	32.6(1)	146.3(5)	54.7(2)	-0.6(2)	0.9(1)	0.2(3)
P	35(1)	138(3)	63(1)	3(1)	4(1)	0(2)
Cl(1)	46(1)	232(5)	98(2)	0(2)	9(1)	-56(3)
Cl(2)	70(2)	270(6)	67(2)	27(3)	-17(1)	24(3)
C(1)	56(5)	227(22)	89(8)	42(9)	-2(6)	-29(12)
O	104(7)	415(30)	128(10)	88(13)	-56(8)	-6(15)

(b) Calculated fractional co-ordinates $(\times 10^{3})$ and assumed isotropic vibrational parameters for hydrogen atoms; each hydrogen atom is numbered according to the carbon atom to which it is attached.

Atom	x	y	z	$B \times 10 \ \AA^{2*}$
H(12)	241	-128	-113	53
H(13)	196	-72	-324	56
H(14)	76	-222	-403	51
H(15)	-4	-409	-274	67
H(16)	50	-488	-68	57

* See footnote, Table 2.1 (b)

TABLE 2.3

Selected interatomic distances (Å) and angles (°) in (I)

(a) <u>Bond lengths with standard deviations in parentheses</u>

Pt-Cl(1)	2.343(2)	C(21)-C(22)	1.360(8)
Pt-Cl(2)	2.276(1)	C(22)-C(23)	1.408(10)
Pt-P	2.282(2)	C(23)-C(24)	1.344(11)
Pt-C(1)	1.858(7)	C(24)-C(25)	1.346(11)
C(1)-O	1.114(8)	C(25)-C(26)	1.402(11)
		C(26)-C(21)	1.382(9)
P-C(11)	1.819(6)	Mean	1.374(11)
P-C(21)	1.815(6)	C(31)-C(32)	1.390(8)
P-C(31)	1.813(5)	C(32)-C(33)	1.385(9)
Mean*	1.815(3)	C(33)-C(34)	1.362(11)
		C(34)-C(35)	1.390(12)
C(11)-C(12)	1.387(8)	C(35)-C(36)	1.386(10)
C(12)-C(13)	1.382(10)	C(36)-C(31)	1.384(9)
C(13)-C(14)	1.363(9)	Mean	1.384(4)
C(14)-C(15)	1.365(11)		
C(15)-C(16)	1.403(11)		
C(16)-C(11)	1.389(8)		
Mean	1.382(6)		

* Throughout this thesis, each mean value, $\bar{x}$, is derived from the relation $\bar{x} = \sum_j w_j x_j / \sum_j w_j$, where the summations are over the set of n individual measurements, x_j, and the weights, w_j, are equated with the reciprocal of the variance of x_j. The standard deviation of each weighted mean is the larger of σ_A and σ_B. σ_A is calculated from the individual standard deviations, σ_j, by the relation $\sigma_A = (\sum_j 1/\sigma_j^2)^{-\frac{1}{2}}$; σ_B is derived from the deviations of the individual values from their mean by the relation $\sigma_B = [\sum_j w_j (x_j - \bar{x})^2 / \{(n-1) \sum_j w_j\}]^{\frac{1}{2}}$.

TABLE 2.3(Cont'd)

(b) Interbond angles with standard deviations in parentheses

Cl(1)-Pt-Cl(2)	88.4(1)	C(21)-C(22)-C(23)	119.6(6)
Cl(1)-Pt-C(1)	86.8(2)	C(22)-C(23)-C(24)	119.6(7)
Cl(2)-Pt-P	90.1(1)	C(23)-C(24)-C(25)	121.7(8)
P-Pt-C(1)	94.6(2)	C(24)-C(25)-C(26)	119.9(8)
Cl(1)-Pt-P	178.3(2)	C(25)-C(26)-C(21)	119.0(7)
Cl(2)-Pt-C(1)	173.5(2)	C(26)-C(21)-C(22)	120.3(6)
		Mean	120.0(3)
Pt-C(1)-O	175.6(7)	C(31)-C(32)-C(33)	120.8(6)
		C(32)-C(33)-C(34)	119.3(7)
Pt-P-C(11)	118.3(2)	C(33)-C(34)-C(35)	121.0(8)
Pt-P-C(21)	110.3(2)	C(34)-C(35)-C(36)	119.5(8)
Pt-P-C(31)	110.2(2)	C(35)-C(36)-C(31)	120.1(7)
		C(36)-C(31)-C(32)	119.3(5)
C(11)-P-C(21)	105.4(3)	Mean	119.9(3)
C(11)-P-C(31)	104.9(3)		
C(21)-P-C(31)	107.2(3)	P-C(11)-C(12)	120.3(4)
Mean	105.8(7)	P-C(11)-C(16)	120.3(5)
		P-C(21)-C(22)	121.2(5)
		P-C(21)-C(26)	118.6(5)
C(11)-C(12)-C(13)	120.8(6)	P-C(31)-C(32)	118.0(4)
C(12)-C(13)-C(14)	119.7(7)	P-C(31)-C(36)	122.7(5)
C(13)-C(14)-C(15)	121.0(7)	Mean	120.2(7)
C(14)-C(15)-C(16)	120.1(7)		
C(15)-C(16)-C(11)	119.2(7)		
C(16)-C(11)-C(12)	119.1(6)		
Mean	120.0(3)		

TABLE 2.3 (Cont'd)

(c) Intramolecular non-bonded distances* within the limits of the

van der Waals radii ($\overset{o}{A}$): C($\underline{sp}$), 1.7; C($\underline{sp}^2$), 1.85; C($\underline{sp}^3$), 2.0;

Cl, 1.8; O, 1.4; P, 1.9. **

Cl(2)···C(16)	3.34	C(12)···C(31)	3.06
Cl(2)···C(21)	3.57	C(12)···C(32)	3.25
C(1)···C(31)	3.06	C(16)···C(21)	3.54
C(1)···C(32)	3.14	C(16)···C(22)	3.56
C(11)···C(22)	3.09	C(21)···C(36)	3.15
C(11)···C(32)	3.34	C(26)···C(31)	3.63
C(12)···C(22)	3.68	C(26)···C(36)	3.59

* Values for atoms bonded to a common atom have been omitted from
such lists.

** Here, and throughout, the labels refer to formal hybridisation
states.

TABLE 2.3 (Cont'd)

(d) Intermolecular non-bonded distances within the limits of the van der Waals radii

$Cl(1) \cdots C(24^{I})$*   3.61 $C(13) \cdots C(36^{III})$ 3.68

$Cl(2) \cdots C(33^{II})$ 3.52

* The Roman numeral superscripts refer to the equivalent positions relative to the reference molecule at x, y, z:

I   x,   y, 1 + z   III   -x, -y, -1-z

II   x, 1 + y,   z

TABLE 2.4

Selected interatomic distances (Å) and angles (°) in (II)

(a) Bond lengths

Pt-Cl(1)	2.362(3)	C(1)-O	1.106(13)
Pt-Cl(2)	2.291(2)		
Pt-P	2.264(2)	C(11)-C(12)	1.378(13)
Pt-C(1)	1.834(11)	C(12)-C(13)	1.404(16)
		C(13)-C(14)	1.390(15)
P-C(11)	1.802(8)	C(14)-C(15)	1.345(16)
		C(15)-C(16)	1.412(18)
P-C(21)	1.830(10)	C(16)-C(11)	1.374(14)
P-C(31)	1.811(11)	Mean	1.382(9)
Mean	1.821(9)		

<u>TABLE 2.4 (Cont'd)</u>

(b) <u>Interbond angles</u>

Cl(1)-Pt-Cl(2)	90.2(1)	C(21)-P-C(31)	107.2(5)
Cl(1)-Pt-C(1)	88.0(3)		
Cl(2)-Pt-P	88.0(1)	P-C(11)-C(12)	120.5(7)
P-Pt-C(1)	93.9(3)	P-C(11)-C(16)	121.2(7)
Cl(1)-Pt-P	178.0(1)	Mean	120.9(5)
Cl(2)-Pt-C(1)	178.0(3)		
		C(11)-C(12)-C(13)	121.7(10)
Pt-P-C(11)	113.1(3)	C(12)-C(13)-C(14)	118.2(10)
		C(13)-C(14)-C(15)	121.1(11)
Pt-P-C(21)	112.0(4)	C(14)-C(15)-C(16)	119.9(12)
Pt-P-C(31)	111.2(3)	C(15)-C(16)-C(11)	120.7(11)
Mean	111.5(4)	C(16)-C(11)-C(12)	118.3(9)
		Mean	119.9(6)
Pt-C(1)-O	179.7(19)		
C(11)-P-C(21)	105.6(4)		
C(11)-P-C(31)	107.2(4)		
Mean	106.4(8)		

<u>TABLE 2.4 (Cont'd)</u>

(c) <u>Intramolecular non-bonded distances</u>

Cl(2)···C(21)	3.42	C(12)···C(21)	3.20
Cl(2)···C(31)	3.62	C(16)···C(31)	3.18
C(1)···C(11)	3.11		

TABLE 2.4 (Cont'd)

(d) Intermolecular non-bonded distances

$Cl(1)\cdots C(16^{I})$*	3.65	$Cl(2)\cdots C(31^{III})$	3.77
$Cl(1)\cdots C(21^{II})$	3.71	$C(13)\cdots C(31^{IV})$	3.78
$Cl(1)\cdots C(31^{I})$	3.70	$C(14)\cdots C(21^{IV})$	3.76
$Cl(2)\cdots C(21^{III})$	3.75	$C(15)\cdots C(21^{IV})$	3.83

* The Roman numeral superscripts refer to the following co-ordinate

transformations:

I	$- x, 1/2 + y, 1/2 - z$	III	$1/2 - x, - 1 - y, 1/2 + z$
II	$1/2 - x, \quad - y, 1/2 + z$	IV	$1/2 - x, - 1 - y, -1/2 + z$

TABLE 2.5

Equations of least-squares planes of (I) in which X, Y, Z refer
to orthogonal co-ordinates in Å. Deviations of selected atoms
from the plane are given in square brackets.

Plane 1: Pt, P, Cl(1), Cl(2), C(1)

$$0.958X + 0.287Y + 0.019Z - 2.506 = 0$$

[Pt 0.039, P 0.020, Cl(1) 0.022, Cl(2) -0.036, C(1) -0.044,
 O -0.163]

Plane 2: C(11) - (16)

$$-0.634X - 0.474Y + 0.611Z + 2.786 = 0$$

[P -0.207, C(11) -0.011, C(12) 0.000, C(13) 0.007, C(14) -0.002,
 C(15) -0.010, C(16) 0.016]

Plane 3: C(21) - (26)

$$0.470X - 0.808Y - 0.355Z - 0.233 = 0$$

[P 0.017, C(21) 0.004, C(22) -0.004, C(23) 0.003, C(24) -0.003,
 C(25) 0.002, C(26) -0.003]

Plane 4: C(31) - (36)

$$-0.374X + 0.003Y - 0.927Z - 0.613 = 0$$

[P -0.075, C(31) -0.009, C(32) -0.007, C(33) 0.019, C(34) -0.015,
 C(35) -0.001, C(36) 0.013]

Angles (°) between planes:

(2) - (3)   97.6   (3) - (4)   81.3

(2) - (4)   109.4

TABLE 2.6

Least-squares planes of (II)

Plane 1: Pt, P, Cl(1), Cl(2), C(1)

$$0.733X + 0.630Y - 0.257Z - 0.200 = 0$$

[Pt 0.000, P 0.016, Cl(1) 0.016, Cl(2) -0.015, C(1) -0.018,

O -0.023]

Plane 2: C(11) - (16)

$$-0.572X + 0.747Y + 0.338Z + 3.339 = 0$$

[P 0.088, C(11) 0.006, C(12) 0.010, C(13) -0.013, C(14) -0.001,

C(15) 0.017, C(16) -0.020]

TABLE 2.7

Bond lengths (Å) in cis-[PtCl$_2$(L)(R$_3$P)] complexes

L	R$_3$P	Pt-Cl (trans to L)	Pt-Cl (trans to P)	Pt-P	Ref.
PMe$_3$	PMe$_3$	2.376(12)*	2.376(12)*	2.248(9)*	62
C(OEt)NHPh	PEt$_3$	2.365(5)	2.368(7)	2.240(8)	26
C(NPhCH$_2$)$_2$	PEt$_3$	2.362(3)	2.381(3)	2.234(3)	63
CNPh	PEt$_3$	2.333(12)	2.365(11)	2.238(8)	26,29
CNEt	PEt$_2$Ph	2.314(10)	2.390(8)	2.244(8)	47
Weighted means	——	——	2.379(3)	2.237(2)	
CO	PPh$_3$	2.276(1)	2.343(2)	2.282(2)	Present work
CO	PMe$_2$Ph	2.291(2)	2.362(3)	2.264(2)	" "
CO	PEt$_3$	2.296(4)	2.368(3)	2.265(3)	22

* Mean values

TABLE 2.8

Mean Pt-P(trans to P) bond lengths (Å) in various types of

platinum (II) complexes[a]

Phosphine[b]	PR_3	PR_2Ph	PMe_2Ph	PPh_3
Electroneutral complexes	2.312(5)	2.299(8)	2.294(3)	2.304(2)
Monocationic complexes	2.330(12)	--	2.295(5)	--
Tolman's $\sum \chi_i$ parameter[c]	5.4	7.9	9.5	12.9

[a] K.W. Muir, personal communication.

[b] R = Et or n-Bu

[c] A measure of the total electron-withdrawing ability of the substituents on phosphorus (see ref. 46).

Figure 2.2 : A view of the cis-$[PtCl_2(CO)(PPh_3)]$

molecule; thermal vibration ellipsoids

enclose 50% of probability. Hydrogen

atoms are omitted for clarity.
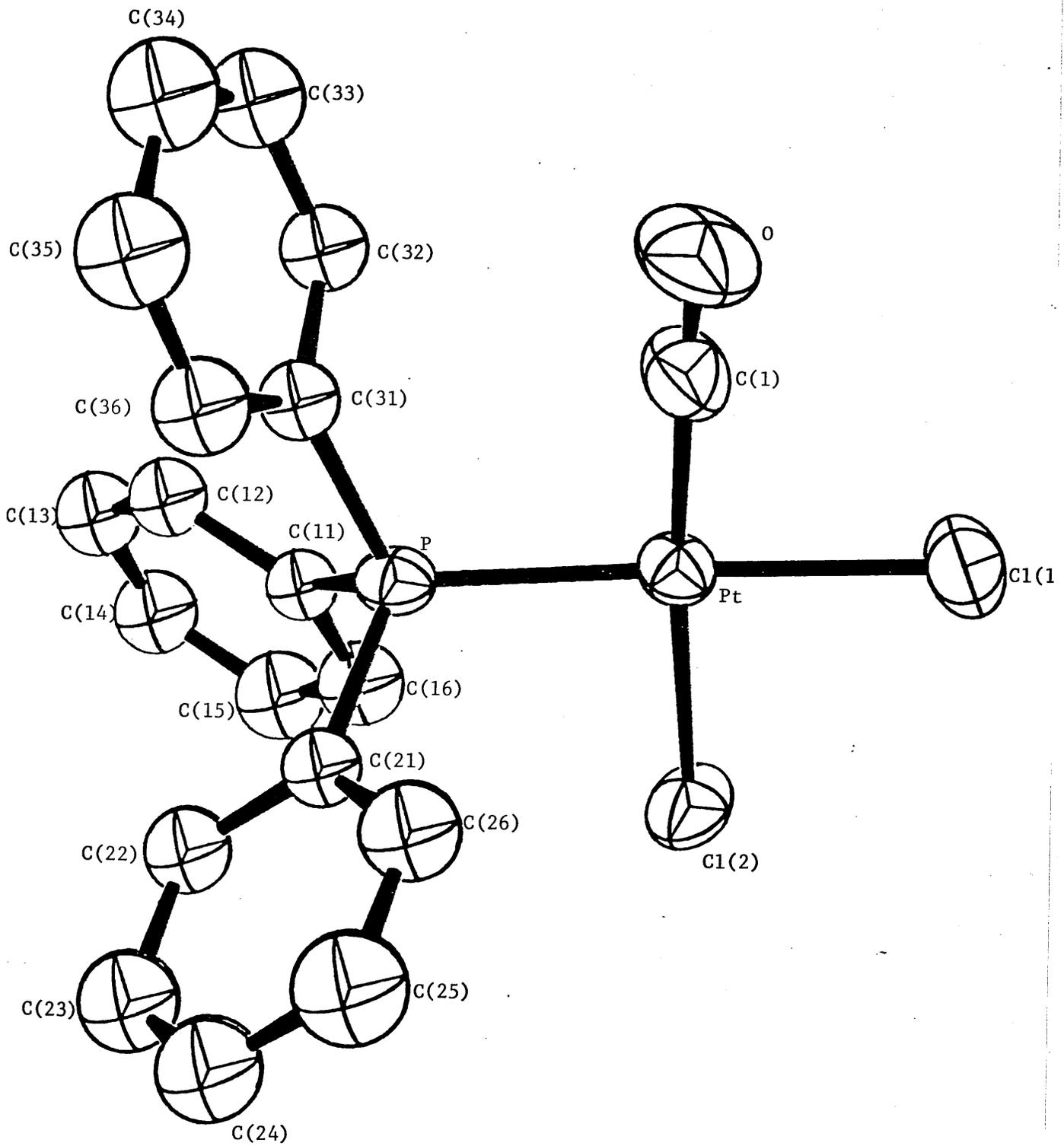
Figure 2.3: A view of the cis-$[PtCl_2(CO)(PMe_2Ph)]$

molecule; thermal ellipsoids enclose

50% of probability.
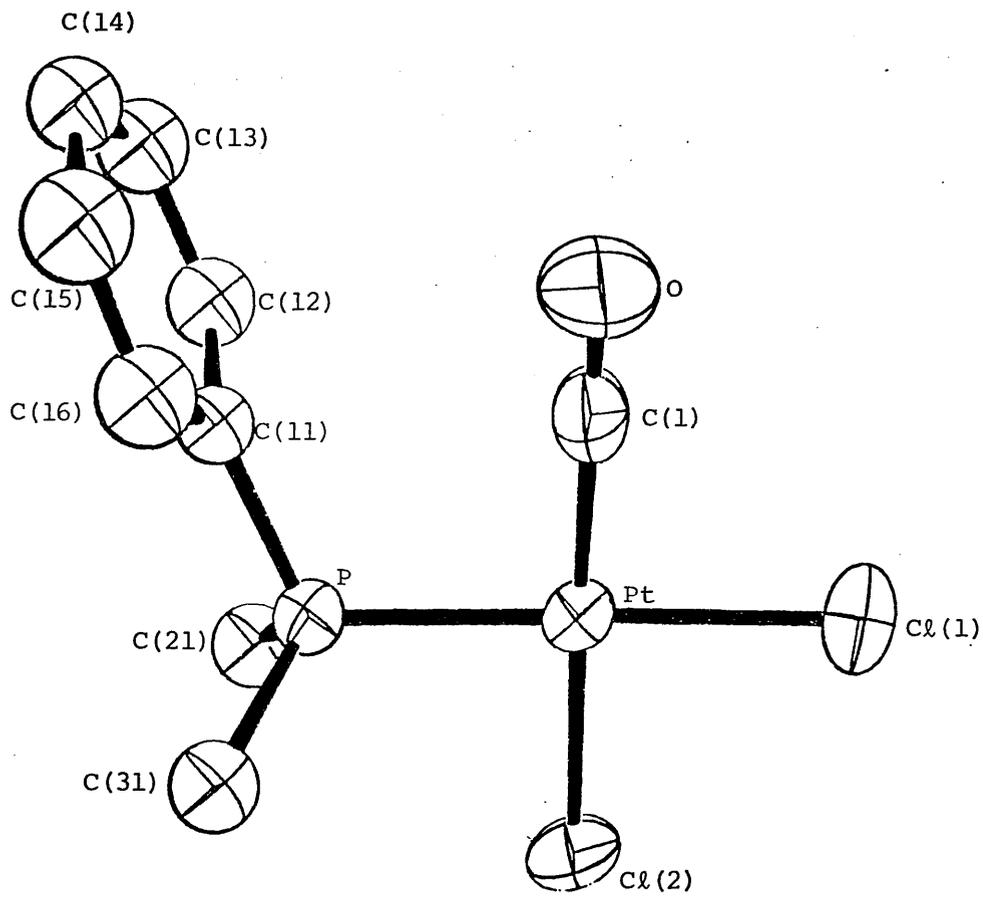
2.4   THE CRYSTAL AND MOLECULAR STRUCTURE OF THE PLATINUM (II)

PHOSPHINE COMPLEX cis-[PtCl$_2${Ph$_2$PCH$_2$CH$_2$P(CF$_3$)$_2$}]

2.4.1.   INTRODUCTION

Recently, the novel unsymmetrical ditertiary phosphine Ph$_2$PCH$_2$CH$_2$P-(CF$_3$)$_2$, L, and its chelate complexes cis-[MCl$_2$L], M = palladium or platinum, were synthesised.[66] An X-ray structure determination of the palladium complex showed that the electronic properties of the substituents on the phosphorus atoms have a pronounced effect on the palladium-ligand bonding.[66]   Thus, the Pd-P distance involving the trifluoromethylphosphine ligand is extremely short and, furthermore, this phosphine exerts a considerably smaller trans-influence on a Pd-Cl bond than does the phenyl-substituted phosphorus donor atom.

An account is now given of the accurate X-ray analysis of the platinum analogue cis-[PtCl$_2$L]. This work was undertaken for the following reasons.

(i)   It extends the study[3] of the bonding and trans-influence of
       carbon-donor ligands in monomeric square-planar platinum(II)
       complexes (Sec. 2.3):   an analogy can be drawn in that one of
       the phosphorus atoms (namely, that of the P(CF$_3$)$_2$ group) is
       believed to receive significant π-backdonation from the metal
       atom.

(ii)   Platinum, unlike palladium, has an isotope (^{195}Pt) with nuclear
       spin angular momentum and, consequently, ^{1}J(Pt-P)   coupling
       constants can be obtained. In the present complex, the two
       metal-phosphorus bonds have appreciably different ^{1}J(Pt-P)
       coupling constants. This result is significant in view of the
       proposed correlation between ^{1}J(Pt-P)   coupling constants and
       Pt-P   bond lengths in platinum(II) complexes containing
       monotertiary phosphine ligands.[19]

(iii) There is an extensive structural literature on platinum(II) phosphine complexes:[67] accordingly, a more critical evaluation of the metal-phosphorus bonding should be possible for the platinum complex.

(iv) The bonding in analogous second and third row transition metal complexes can show marked differences, especially when π-acid ligands are involved.[68]

A preliminary account of this work is available.[69]

2.4.2. EXPERIMENTAL

Crystal Data. - $C_{16}H_{14}Cl_2F_6P_2Pt$, M = 648.2. Monoclinic, a = 10.062(1), b = 13.690(1), c = 15.930(1) Å, β = 108.66(1)^{o}, T = 19°C, U = 2078.9 Å^3, Z = 4, D_c = 2.071 gm cm^{-3}, F(000) = 1224. Mo-K$_\alpha$ radiation, λ = 0.71069 Å, μ(Mo-K$_\alpha$) = 75.6 cm^{-1}. Space group P2$_1$/c.

Crystallographic Measurements. - The crystals are white, air-stable plates. The specimen chosen for the analysis displayed all members of the {100}, {010} and {001} forms, and the (110) and (1$\bar{1}$0) faces; the perpendicular distances between the parallel faces were 0.17, 0.32 and 0.09 mm.

The crystal system and unit-cell dimensions were derived from rotation and Weissenberg photographs. Final values of the cell dimensions were obtained by a least-squares treatment of the setting angles of 12 reflexions centred on a Hilger and Watts' Y290 diffractometer controlled by a PDP8 computer.[34b] The crystals are nearly isomorphous with those of the palladium analogue.[68]

Intensity Measurements. - The intensities of all independent reflexions with θ(Mo-K$_\alpha$) ≲ 28° were measured on the Y290 instrument with the use of graphite-monochromated molybdenum radiation and a pulse-height analyser. A symmetrical θ - 2θ scan was employed: 2.5s counts were taken at 0.02^{o} intervals over a range of 0.60^{o} in θ, and stationary crystal-stationary counter backgrounds were measured for 15s at each end of the scan. The intensities of three strong low-angle reflexions, remeasured periodically during the experiment, varied by less than 6% of their mean values.

Structure amplitudes and their standard deviations were derived in the usual way (q 0.04).[35] A correction was made for absorption effects; the transmission factors on $|F_o|$, calculated by Gaussian integration over a grid of 14 x 14 x 14 points, ranged from 0.41 to 0.70.[37]

Of 3531 intensities measured, only 3364 for which $I \geqslant 3\sigma(I)$ were used in the subsequent calculations.

Structure Analysis - The fractional atomic co-ordinates of the palladium analogue were employed in a trial solution: this led to a satisfactory structural model. This model was refined by the method of full-matrix least-squares. The function minimised was $\Sigma w \Delta^2$, where $w = 1/\sigma^2(F_o)$ and $\Delta = |F_o| - |F_c|$. Atomic scattering factors were taken from ref.38, except those for the hydrogen atoms.[40] Allowance was made for the anomalous scattering of the platinum, phosphorus and chlorine atoms with values of $\Delta f'$ and $\Delta f''$ from ref. 41.

Refinement of the scale factor and of the positional and isotropic thermal parameters of all non-hydrogen atoms led to R 0.099 and R 0.120. When the data were corrected for absorption effects and anisotropic temperature factors were assigned to the platinum, phosphorus and chlorine atoms, R and R' decreased, respectively, to 0.041 and 0.054. Hydrogen atom positions were inferred and their contributions to the scattering were included in all subsequent structure factor calculations but their positional and thermal parameters were not refined. In addition, anisotropic temperature factors were assigned to the fluorine atoms. It then became evident that extinction effects were present. Accordingly, a secondary extinction parameter, r^*,[43] was included in the refinement: convergence was achieved at R 0.029 and R' 0.036.

In the final cycle of least-squares refinement all parameters shifted by less than 0.2σ. The standard deviation of an observation of unit weight was 1.3 and r^* was $2.9(1) \times 10^{-3}$ deg^{-1}. Mean values of $w\Delta^2$ showed no apparent trend when analysed as a function of $|F_o|$ or $\sin\theta$, indicating that the weighting scheme was satisfactory. The extreme function values (1.1 and -0.5 e$\mathring{A}^{-3}$) in the final difference synthesis occurred in regions close to the platinum atom.

The observed and calculated structure amplitudes are listed in the Appendix (pp. 53 to 77). Final atomic parameters and a selection of derived functions are presented in Tables 2.9 - 2.11. A view of the molecular structure is shown and the atomic numbering scheme is indicated in Fig. 2.4.

The computer programs employed have been described in Sec. 2.3.2.

2.4.3. RESULTS AND DISCUSSION.

The crystals are built of discrete <u>cis</u>-$[PtCl_2\{Ph_2PCH_2CH_2P(CF_3)_2\}]$
molecules.   A calculation of all intermolecular distances $\leq$ 4.0 Å
indicated that the interactions between molecules are of the van der
Waals type.[44] Of the contact distances shown (Table 2.10(e)),
the only one of interest is that of 3.59 Å between C(13) and Cl(1):
the resultant H(13)···Cl(1) distance of 2.81 Å and the C(13)-H···Cl(1)
angle of 136° may indicate a weak hydrogen bond.[45]

<u>The Co-ordination of the Metal Atom.</u> - The molecules have the expected
<u>cis</u>-square-planar configuration at the platinum atom with the
ditertiary phosphine acting as a chelating bidentate ligand;   the
remaining co-ordination sites are occupied by chlorine atoms.   There
are small but significant distortions of the metal co-ordination from
ideal square-planar geometry.   Thus, the P(1)-Pt-P(2) angle is
only 86.0(1)°:   this may be attributed to a constraint of chelation.
There is also a slight opening of the P(2)-Pt-Cl(2) angle to 94.1(1)°
and the P(2)-Pt-Cl(1) angle is only 175.2(1)°.   In addition, the
platinum, phosphorus and chlorine atoms deviate significantly by
up to $\pm$ 0.02 Å from the metal co-ordination plane: similar distor-
tions have been observed in a number of monomeric, square-planar
complexes of platinum(II) and have been attributed to ligand-ligand
repulsions.[47] That the molecule is subject to steric strain is
shown by a number of short intramolecular contacts (Table 2.10(d)).
Thus, the shortest contact involving the phenyl carbon atoms is 3.14 Å
between C(16) and C(21);   contacts of a similar magnitude have been
observed in other arylphosphine derivatives[48] and in the triphenyl-
phosphine molecule.[52] The C···Cl and C(methylene)···F contacts may

also indicate strain; the C···F distances do not result from

hydrogen bonding since the shortest H···F contact is 2.70 $\overset{o}{A}$ involving

H(3a) and F(21) and this is $\underline{ca}$. 0.15 $\overset{o}{A}$ longer than the sum of the van

der Waals radii of hydrogen (1.2 $\overset{o}{A}$) and fluorine (1.35 $\overset{o}{A}$) atoms.[44]

The CF_3···CF_3 intramolecular distances are unexceptional, the shortest

distance being 3.07 $\overset{o}{A}$ involving C(2) and F(12); they lead to a contact

radius of $\underline{ca}$. 1.8 $\overset{o}{A}$ for the trifluoromethyl carbon atom and this is

not unduly short.

The five-membered chelate ring is puckered with the methylene atoms

C(3) and C(4) displaced by -0.24 and +0.37 $\overset{o}{A}$, respectively, from the

platinum co-ordination plane. Bidentate chelating ligands, such as

diphosphines, are expected to display a variety of conformations

(symmetrical and unsymmetrical) of nearly equivalent energy.[70] In

the title complex the conformation exhibited is intermediate between

those of the envelope (C_s) and half-chair (C_2) forms, being closer to

the latter type: of the torsion angles given in Table 2.10(c), the

ones of primary interest are those about the Pt-P bonds, P(1)-Pt-P(2)-C(3)

-7.4(3) and P(2)-Pt-P(1)-C(4) -13.5(3)^o, and that about the central

C-C bond, P(2)-C(3)-C(4)-P(1) -42.0(6)^o. These values are normal,

being in the range found in a number of other metal-diphosphine systems.[71]

The Geometry of the Phosphine Ligands - The geometry of the phenyl-

substituted phosphine is normal.[48] Thus, the P-C($\underline{sp}^2$) distances

(mean value 1.812(6) $\overset{o}{A}$), the P-C($\underline{sp}^3$) separation of 1.830(9) $\overset{o}{A}$ and

the C($\underline{sp}^2$)-C($\underline{sp}^2$) distances (mean values 1.375(7) and 1.375(9) $\overset{o}{A}$)

are similar to the corresponding values found in monotertiary

phosphine derivatives of platinum(II).[49] In addition, the Pt-P-C and

C-P-C angles display the expected deviations[48] from the ideal
tetrahedral value; respective ranges are 107.8(2) to 116.7(2)$^{\circ}$ and
105.4(3) to 107.0(3)$^{\circ}$.   Moreover, the endocyclic phenyl angles at
the _ipso_-carbon atoms [120.1(6) and 118.8(7)$^{\circ}$] are normal.[54]

In contrast, the P-CF$_3$ bond lengths in the trifluoromethylphosphine
ligand are longer than expected: the individual lengths are equal
and their mean value of 1.877(7) Å differs from the corresponding
P-C(phenyl) value by _ca._ 0.07 Å which is 0.04 Å longer than would be
predicted from the covalent radii[59] of _sp_^{3} and _sp_^{2} hybridised
carbon atoms (0.77 and 0.74 Å respectively).   Angular distortions
in the same sense as those found in the PPh$_2$ fragment are evident.
However, the C-P-C angles, which range from 99.7(4) to 104.4(4)$^{\circ}$,
are decidedly smaller; in particular, the CF$_3$-P-CF$_3$ angle is 7.3(5)$^{\circ}$
smaller than the corresponding C(Ph)-P-C(Ph) angle.

The respective ranges of Pt-P-C angles overlap but, on the whole,
the angles at the P(CF$_3$)$_2$ group (range 112.1(2) - 119.5(3)$^{\circ}$) are
slightly larger.   The bonding differences of the phosphine ligands are
discussed, in some detail, below.

The C-F bond lengths are in excellent agreement (χ^2 = 0.6 on 5
degrees of freedom); their mean value of 1.301(5) Å is somewhat
shorter than that obtained[50] from a number of fluoroparaffins
(1.333(5) Å), and the values in cyclic polyfluorophosphines of general
formula [P(CF$_3$)$_2$]$_n$ (mean 1.34 Å),[50] but it is in agreement with the
corresponding mean separation of 1.30(1) Å in the analogous complex
cis-[PtCl$_2$(F$_3$CSCHMeCH$_2$SCF$_3$)]:[72] this contraction can best be
attributed to the effects of the high thermal vibration of the

fluorine atoms. The P-C-F and F-C-F angles are nearly regular

with mean values of 110.9(9) and $107.6(6)^{\circ}$, respectively.

The P-C(methylene) bond lengths [1.846(7) and 1.830(9) Å] are

normal.[49] Moreover, the C(3)-C(4) separation of 1.519(10) Å is

similar to the accepted value[50] of 1.54 Å for a $C(\underline{sp}^3)-C(\underline{sp}^3)$ bond

length, and the $P-CH_2-CH_2$ interbond angles [110.1(5) and $108.7(6)^{\circ}$]

are close to $109^{\circ}28'$.

Metal-Ligand Bonding and <u>trans</u>-Influence   -   The most noteworthy

feature of the molecular structure is the extremely short $Pt-P(CF_3)_2$

bond [2.168(2) Å]. Prior to this work, the shortest Pt-P(phosphine)

distance observed in 56 monomeric platinum(II) phosphine complexes

for which structural data are available was that of 2.215(4) Å in the

$[PtCl_3(PEt_3)]^-$ anion.[64] Furthermore, the Pt-Cl(<u>trans</u> to P(2))

distance, 2.315(2) Å, indicates that the <u>trans</u>-influence of the $P(CF_3)_2$

group is substantially less than that of a trialkyl- or triarylphosphine,

being comparable with that of isocyanide or chloride:[3] the Pt-Cl(<u>trans</u> to C)

distance[47] in <u>cis</u>-$[PtCl_2(CNEt)(PEt_2Ph)]$ is 2.314(10) Å and the mean

length of the Pt-Cl(<u>trans</u> to Cl) bonds in five platinum (II) complexes

is 2.303(5) Å.[3] In contrast, the $Pt-PPh_2$ and Pt-Cl(<u>trans</u> to PPh_2)

distances [2.244(2) and 2.371(2) Å, respectively] are normal, being

equal within experimental error to the corresponding distances in five

other complexes of the type <u>cis</u>-$[PtCl_2L(PR_3)]$ where R is alkyl or

aryl, and L is carbenoid, isocyanide or phosphine (Table 2.7 and refs.

therein). The highly significant difference of 0.076(3) Å ($\Delta/\sigma = 25$) in the

Pt-P distances in the title complex must be predominantly of electronic origin

since the substituents on the atoms P(1) and P(2) appear to have similar steric

bulk but markedly different electron-withdrawing ability. Thus, the minimum cone angles of the phosphines are 120° (trifluoromethyl) and 125° (phenylphosphine), and the corresponding values of Tolman's $\sum \chi_i$ parameter are 41.0 and 10.4 cm^{-1}, respectively.[46]

The striking difference in the Pt-P bond lengths is paralleled by that in the $^1J(Pt-P)$ coupling constants: $^1J(Pt-PPh_2)$ = 3120 and $^1J(Pt-P(CF_3)_2)$ = 4013 Hz - a difference of ca. 900 Hz. However, in the complex cis-$[PtCl_2\{Ph_2PCH_2CH_2P(C_6F_5)_2\}]$ the coupling constants $^1J(Pt-PPh_2)$ [3445 Hz] and $^1J(Pt-P(C_6F_5)_2)$ [3845 Hz] differ by only ca. 400 Hz.[69] Thus, the coupling constant increases in the order $PPh_2 < P(C_6F_5)_2 < P(CF_3)_2$. It seems reasonable to relate this trend to increasing electron-withdrawing ability of the phosphine substituents. Thus, Tolman has assigned electron-withdrawing parameters (χ_i) 4.3, 11.2 and 19.6 cm^{-1} to the Ph^-, $C_6F_5^-$ and CF_3^- substituents, respectively; of the 47 substituents examined, trifluoromethyl was found to be the most electronegative.[46]

Bent considered bond lengths and angles in relation to hybridisation in PX_3, X_3PO and X_3PS derivatives.[73] His rules predict that the phosphorus atom with the more electronegative substituents will have the greater s-character/. Applied to the title complex, they lead to
in the lone pair orbital
a shorter Pt-P bond for the trifluoromethyl-substituted phosphine and a higher $^1J(Pt-P)$ coupling constant. In addition, the C-P-C angles should be smaller and the P-C bonds longer than the corresponding values of the phenyl-substituted phosphine (allowance, of course, being made for the difference in covalent radii of sp^3 and sp^2 hybridised carbon atoms). Although the structural parameters and coupling constants are in agreement with these predictions, there

are a number of objections to this interpretation. It implies that the less basic phosphorus atom forms a shorter and presumably stronger Pt-P bond. Moreover, it requires that the Pt-P bond lengths and the phosphine trans-influence be extremely sensitive to small variations in the hybridisation of the phosphorus atoms: an analogy can be drawn with the relative trans-influence of carbon-donor ligands where sp^3, sp^2 and sp hybridised carbon atoms have similar trans-influence on Pt-Cl bonds.[3] The extremely short Pt-P$(CF_3)_2$ bond can best be attributed to substantial backdonation from the platinum ion engendered by the electron-withdrawal of the trifluoromethyl groups. On this basis, the high $^1J(Pt-P(CF_3)_2)$ coupling constant arises from synergic enhancement of the Pt-P σ-bonding. Furthermore, the small trans-influence of the P$(CF_3)_2$ group is expected by analogy with carbon-donor ligand systems (Sec. 2.3.3) where it has been shown that there is a marked decrease in trans-influence if π-backdonation is significant.[3]

In conclusion, there are no significant differences between comparable bond lengths and angles in the present complex and its palladium analogue [66] with the exception of the M-P$(CF_3)_2$ bond length which is 0.025(4) Å shorter in the platinum complex.

TABLE 2.9

(a)   Fractional atomic co-ordinates $(\times 10^4)$ and vibrational parameters

for <u>cis</u>-$[PtCl_2\{Ph_2PCH_2CH_2P(CF_3)_2\}]$

Atom	x	y	z	$U\times 10^3 \text{Å}^2$
Pt	3539.7(2)	2003.9(1)	2342.9(1)	*
P(1)	2481(1)	2687(1)	1016(1)	*
P(2)	5464(2)	2618(1)	2234(1)	*
Cl(1)	1391(2)	1399(1)	2342(1)	*
Cl(2)	4669(2)	1232(1)	3719(1)	*
F(11)	7938(6)	2181(5)	2046(6)	*
F(12)	7658(7)	1579(6)	3202(5)	*
F(13)	6599(7)	987(5)	1970(6)	*
F(21)	7414(7)	3976(5)	2901(6)	*
F(22)	6624(9)	3331(5)	3861(4)	*
F(23)	5418(7)	4326(4)	2938(5)	*
C(1)	7020(10)	1805(7)	2379(7)	78(2)
C(2)	6312(10)	3613(7)	3039(7)	77(2)
C(3)	5210(8)	3160(5)	1144(5)	60(2)
C(4)	3725(7)	3557(5)	789(5)	49(1)
C(11)	902(6)	3390(4)	906(4)	39(1)
C(12)	1022(7)	4280(5)	1318(5)	53(2)
C(13)	-190(8)	4811(6)	1255(5)	63(2)
C(14)	-1469(8)	4453(5)	782(5)	63(2)
C(15)	-1596(8)	3582(6)	364(6)	66(2)
C(16)	-406(7)	3030(5)	431(5)	56(2)
C(21)	2040(6)	1800(4)	130(4)	44(1)
C(22)	1628(8)	2114(5)	-738(6)	66(2)
C(23)	1206(9)	1432(6)	-1431(6)	72(2)
C(24)	1225(10)	473(7)	-1251(6)	78(2)
C(25)	1589(10)	157(7)	-402(7)	88(3)

TABLE 2.9 (Cont'd)

Atom	x	y	z	$U \times 10^3 \mathring{A}^2$
C(26)	2033(9)	819(6)	297(6)	73(2)

* These atoms were assigned anisotropic temperature factors of the form $\exp\left[-2\pi^2 \sum\limits_{ij} U_{ij} a_i^* a_j^* h_i h_j\right]$. The final values of the U_{ij} parameters $(\times 10^3)$ are:

Atom	U_{11}	U_{22}	U_{33}	U_{12}	U_{13}	U_{23}
Pt	38.5(1)	33.8(1)	33.4(1)	-0.1(1)	12.4(1)	1.5(1)
P(1)	38.5(7)	33.0(6)	34.8(8)	0.7(5)	12.5(6)	1.2(6)
P(2)	37.5(8)	43.9(8)	56.9(11)	0.1(6)	13.0(7)	6.6(8)
Cl(1)	53.0(9)	63.0(10)	59.7(10)	-13.2(7)	25.0(8)	6.3(8)
Cl(2)	66.7(10)	76.0(12)	41.6(9)	5.0(9)	9.9(8)	16.9(8)
F(11)	65(3)	148(6)	213(8)	36(3)	85(4)	83(5)
F(12)	101(4)	165(6)	136(6)	73(4)	34(4)	72(5)
F(13)	105(5)	106(5)	236(9)	31(4)	73(6)	-33(6)
F(21)	108(5)	130(5)	194(8)	-79(4)	30(5)	-24(5)
F(22)	192(7)	93(4)	81(4)	-41(4)	-23(5)	-13(4)
F(23)	137(5)	66(3)	148(6)	4(3)	10(5)	-39(4)

TABLE 2.9 (Cont'd)

(b) Calculated fractional co-ordinates ($\times 10^3$) and assumed isotropic temperature factors for hydrogen atoms; each hydrogen atom is numbered according to the carbon atom to which it is attached.

Atom	x	y	z	$U \times 10^3 \text{Å}^2$
H(3a)	591	370	118	70
H(3b)	535	265	72	70
H(4a)	345	368	13	59
H(4b)	367	420	109	59
H(12)	197	456	168	63
H(13)	-12	547	154	73
H(14)	-235	483	77	75
H(15)	-255	335	0	76
H(16)	-50	238	11	66
H(22)	166	284	-87	75
H(23)	83	165	-208	83
H(24)	97	-3	-176	84
H(25)	161	-57	-26	97
H(26)	229	57	93	81

TABLE 2.10

Selected interatomic distances ($\overset{o}{A}$) and angles (^{o}) in

$\underline{cis}\text{-}[PtCl_2\{Ph_2PCH_2CH_2P(CF_3)_2\}]$
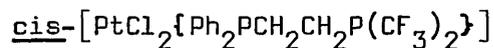
(a) Bond lengths

Pt-P(1)	2.244(2)	C(2)-F(21)	1.296(12)
Pt-P(2)	2.168(2)	C(2)-F(22)	1.304(12)
Pt-Cl(1)	2.315(2)	C(2)-F(23)	1.302(11)
Pt-Cl(2)	2.371(2)	Mean	1.301(5)
P(1)-C(11)	1.817(6)	C(11)-C(12)	1.371(9)
P(1)-C(21)	1.806(6)	C(12)-C(13)	1.396(10)
Mean	1.812(6)	C(13)-C(14)	1.358(11)
P(2)-C(1)	1.874(10)	C(14)-C(15)	1.352(11)
P(2)-C(2)	1.878(10)	C(15)-C(16)	1.391(10)
Mean	1.876(7)	C(16)-C(11)	1.382(9)
		Mean	1.375(7)
P(1)-C(4)	1.846(7)	C(21)-C(22)	1.379(11)
P(2)-C(3)	1.830(8)	C(22)-C(23)	1.404(12)
C(3)-C(4)	1.519(10)	C(23)-C(24)	1.343(13)
		C(24)-C(25)	1.354(14)
C(1)-F(11)	1.309(12)	C(25)-C(26)	1.394(13)
C(1)-F(12)	1.299(13)	C(26)-C(21)	1.370(10)
C(1)-F(13)	1.297(12)	Mean	1.375(9)

TABLE 2.10 (Cont'd)

(b) Interbond angles

Cl(1)-Pt-Cl(2)	90.7(1)	P(1)-C(4)-C(3)	110.1(5)
Cl(1)-Pt-P(1)	89.2(1)	P(2)-C(3)-C(4)	108.7(5)
P(2)-Pt-Cl(2)	94.1(1)		
P(2)-Pt-P(1)	86.0(1)	P(2)-C(1)-F(11)	112.7(7)
P(1)-Pt-Cl(2)	178.0(1)	P(2)-C(1)-F(12)	112.9(7)
P(2)-Pt-Cl(1)	175.2(1)	P(2)-C(1)-F(13)	109.0(7)
		P(2)-C(2)-F(21)	112.9(7)
Pt-P(1)-C(11)	116.6(2)	P(2)-C(2)-F(22)	112.4(7)
Pt-P(1)-C(21)	112.3(2)	P(2)-C(2)-F(23)	108.3(7)
Mean	115(2)	Mean	110.9(9)
Pt-P(1)-C(4)	107.8(2)		
		F(11)-C(1)-F(12)	108.5(8)
Pt-P(2)-C(1)	119.5(3)	F(11)-C(1)-F(13)	107.2(9)
Pt-P(2)-C(2)	116.7(3)	F(12)-C(1)-F(13)	106.1(9)
Mean	118.1(14)	F(21)-C(2)-F(22)	109.9(9)
Pt-P(2)-C(3)	112.1(3)	F(21)-C(2)-F(23)	106.6(8)
		F(22)-C(2)-F(23)	106.3(9)
C(11)-P(1)-C(4)	105.4(3)	Mean	107.6(6)
C(21)-P(1)-C(4)	107.1(3)		
Mean	106.2(8)		
C(11)-P(1)-C(21)	107.0(3)	C(11)-C(12)-C(13)	119.2(6)
		C(12)-C(13)-C(14)	120.2(7)
		C(13)-C(14)-C(15)	121.0(7)
C(1)-P(2)-C(3)	102.4(4)	C(14)-C(15)-C(16)	119.9(7)
C(2)-P(2)-C(3)	104.4(4)	C(15)-C(16)-C(11)	119.6(6)
Mean	103.4(10)	C(16)-C(11)-C(12)	120.1(6)
C(1)-P(2)-C(2)	99.6(4)	Mean	119.9(3)
		C(21)-C(22)-C(23)	120.0(6)
P(1)-C(11)-C(12)	119.0(5)	C(22)-C(23)-C(24)	120.2(8)

TABLE 2.10 (Cont'd)

P(1)-C(11)-C(16)	120.9(5)	C(23)-C(24)-C(25)	120.4(9)
P(1)-C(21)-C(22)	119.6(5)	C(24)-C(25)-C(26)	120.4(9)
P(1)-C(21)-C(26)	121.5(5)	C(25)-C(26)-C(21)	120.2(8)
Mean	119.9(6)	C(26)-C(21)-C(22)	118.8(6)
		Mean	119.9(3)

TABLE 2.10 (Cont'd)

(c) Torsion angles

Pt-P(1)-C(4)-C(3)   36.4(5)   Pt-P(2)-C(3)-C(4)   31.4(6)

P(1)-Pt-P(2)-C(3)   -7.4(3)   P(2)-Pt-P(1)-C(4)   -13.5(3)

P(2)-C(3)-C(4)-P(1) -42.0(6)

TABLE 2.10(Cont'd)

(d) Intramolecular non-bonded distances within the limits of the

contact radii (Å): $C(\underline{sp}^2)$ 1.85, $C(\underline{sp}^3)$ 2.0, Cl 1.8, F 1.35, P 1.9.

$$CF_3 \cdots CF_3$$

C(1)···F(21)	3.08	C(3)···F(11)	2.98
C(1)···F(22)	3.27	C(3)···F(21)	3.17
C(2)···F(11)	3.27	C(3)···F(23)	3.22
C(2)···F(12)	3.07		

$$C \cdots Cl$$

C(11)···Cl(1)	3.49	C(1)···Cl(2)	3.74
C(26)···Cl(1)	3.61		

$$C \cdots C$$

C(2)···C(4)	3.70	C(11)···C(22)	3.42
C(3)···C(21)	3.60	C(16)···C(21)	3.14
C(4)···C(12)	3.25	C(16)···C(22)	3.42
C(4)···C(22)	3.31		

TABLE 2.10 (Cont'd)

(e) Intermolecular non-bonded contacts within the limits of the van der Waals radii:

$Cl(1)\cdots C(13^{I})$*	3.59	$Cl(2)\cdots C(4^{II})$	3.72
$Cl(1)\cdots C(22^{II})$	3.62	$C(3)\cdots C(15^{III})$	3.84
$Cl(1)\cdots C(23^{II})$	3.59	$C(12)\cdots C(23^{II})$	3.66

* The Roman numeral superscripts refer to the following co-ordinate transformations:

I $-x$, $-1/2 + y$, $1/2 - z$ III $1 + x$, y, z

II x, $1/2 - y$, $1/2 + z$

TABLE 2.11

Least-squares planes of cis-[PtCl$_2$(Ph$_2$PCH$_2$CH$_2$P(CF$_3$)$_2$)]

Plane 1: Pt, P(1), P(2), Cl(1), Cl(2)

$$-0.314X +0.827Y +0.467Z -3.158 = 0$$

[Pt 0.019, P(1) -0.022, P(2) 0.012, Cl(1) 0.011, Cl(2) -0.020,

C(3) -0.237, C(4) 0.374]

Plane 2: C(11) - (16)

$$-0.349X -0.450Y +0.822Z +1.119 = 0$$

[P(1)0.034, C(11) 0.000, C(12) -0.006, C(13) 0.004, C(14) 0.003,

C(15) -0.009, C(16) 0.008]

Plane 3: C(21) - (26)

$$-0.997X +0.073Y -0.001Z + 1.800 = 0$$

[P(1)0.094, C(21) -0.002, C(22) 0.003, C(23) 0.007, C(24) -0.017,

C(25) 0.017, C(26) -0.008]

Angle (^{o}) between planes: (2) - (3)   71.7

Figure 2.4: A view of the cis-[PtCl$_2${Ph$_2$PCH$_2$CH$_2$P(CF$_3$)$_2$}]

molecule; thermal vibration ellipsoids

enclose 50% of probability. Hydrogen atoms

are not shown.
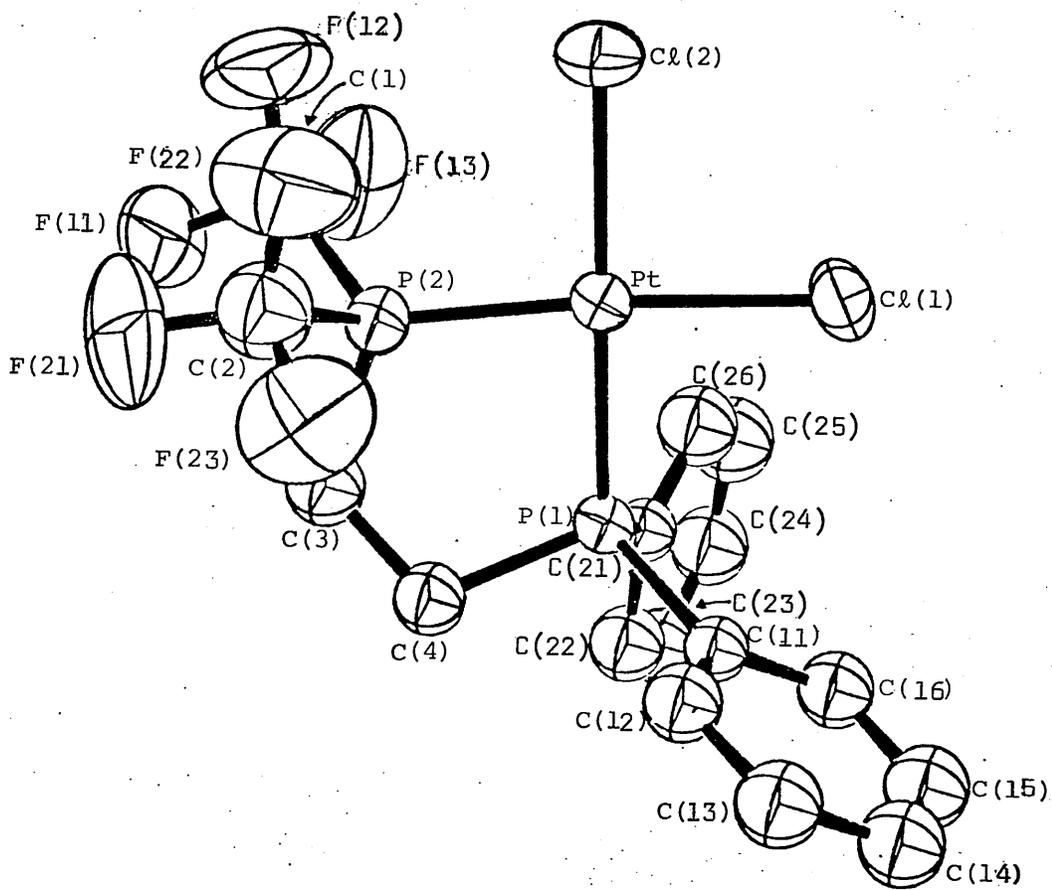
2.5. THE CRYSTAL AND MOLECULAR STRUCTURE OF THE PLATINUM(IV)

CARBENOID $[PtCl_2\{C(Cl.C_6H_3NH)(NHMe)\}(PEt_3)_2]ClO_4$

2.5.1. INTRODUCTION

Recently Chatt, Richards, and Royston showed that the platinum(II)

carbenoid complexes cis-$[PtCl_2\{C(NHR)(NHR')\}PEt_3]$ and trans-

$[PtCl\{C(NHR)(NHR')\}(PEt_3)_2]ClO_4$, where R = R' = Me, undergo oxidative

addition with dichlorine to give analogous platinum (IV) carbenoid

compounds. However, when R = Me or Et and R' = Ph a novel reaction

occurs, apparently involving 2-metallation and 4-chlorination of the

phenyl ring.[74]   Thus, the product from trans-$[PtCl\{C(NHMe)(NHPh)\}$-

$(PEt_3)_2]ClO_4$ was formulated as (I):
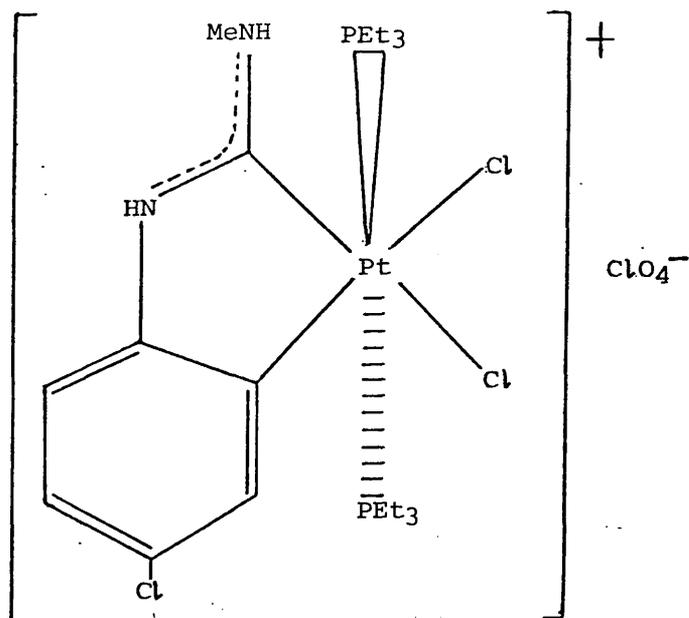
(I)

An X-ray structural analysis of this product was undertaken for the

following reasons.

(i)   Verification of this structural assignment seemed desirable

since reactions of co-ordinated carbenoid ligands are relatively

unusual.[75]

(ii) A metallation induced by oxidation rather than reduction is unusual.[76]

(iii)   The platinum-chlorine bond lengths would enable the relative

trans-influence of σ-phenyl and carbenoid ligands in platinum(IV)

complexes to be compared.   Thus, this work forms part of the

structural investigation of the trans-influence and bonding of

carbon-donor ligands in platinum complexes.[77]

Prior to this study, structural data were available only for carbenoid

complexes of metals in oxidation states 0 to II.[75]   However, the

analysis of a rhodium(III) carbenoid has been reported recently.[78]

A full account of the structure analysis of the title complex is

available.[79]   Accordingly, a brief description only is presented

here.

The observed and final calculated structure amplitudes are listed in

the Appendix [pp. 78 to 114].

2.5.2. RESULTS AND DISCUSSION

The crystals contain $[PtCl_2\{C(Cl.C_6H_3NH)(NHMe)\}(PEt_3)_2]^+$ complex

cations and perchlorate anions which are well separated. A perspec-

tive view of the cation is shown in Figure 2.5.

The structure of the complex cation agrees with that predicted by

Chatt et al.[74]   Mutually-cis phenyl and carbenoid carbon atoms,

trans phosphorus atoms, and cis chlorine atoms define a slightly

distorted octahedron about the platinum atom. The constraint imposed

by the chelate ring leads to a C(13)-Pt-C(19) angle of $80.3(4)^o$,

and also to a slight opening of the C(13)-Pt-Cl(2) and C(19)-Pt-Cl(3)

angles to 95.8(3) and $92.8(3)^o$, respectively. Other angles

subtended at the platinum atom by mutually-cis ligand donor atoms

are close to 90°.

The carbenoid carbon atom, C(19), is coplanar with the atoms N(1),

N(2) and Pt, to which it is directly bonded. The methyl carbon

atom, C(20), attached to N(1), also lies in this plane. The N-C

(carbenoid) bond lengths (1.327(13) and 1.347(17) $\overset{o}{A}$) are in agreement

and their mean value of 1.337(10) $\overset{o}{A}$ is much shorter than the other

N-C bonds in the cation [N-C(Ph) 1.394(13) $\overset{o}{A}$; N-C(Me) 1.496(18) $\overset{o}{A}$].

They are consistent with a bond order of approximately 1.7.[75]

The Pt-C(carbenoid) bond length of 1.973(11) $\overset{o}{A}$ is 0.061(16) $\overset{o}{A}$

shorter than the Pt-C(phenyl) bond length of 2.034(11) $\cdot\overset{o}{A}$. The latter

value is in turn 0.02 $\overset{o}{A}$ shorter than the mean Pt(IV)-C(methyl)

distance of 2.054 $\overset{o}{A}$ in several trimethylplatinum(IV) complexes,[80] and

this difference can be almost entirely accounted for by the difference

in covalent radii of sp^2 and sp^3 hybridised carbon atoms. The Pt-C(Ph)

bond thus appears to be single in character. It has been suggested that the order of a metal-carbon bond which is 0.1 Å shorter than the corresponding single bond will be approximately 1.2.[80] On this basis, it may be argued that the shortening of the Pt-C(carbenoid) bond is consistent with a bond order of about 1.1; such multiple character could arise from a small amount of Pt→C(carbenoid) backdonation.

From the lengths and coplanarity of the bonds involving the carbenoid carbon atom it may be concluded that the platinum-carbenoid bonding is predominantly that indicated by the canonical structure(I) (vide supra), in which the main interaction of the vacant p orbital of the sp^2 hybridised carbenoid carbon atom is with the filled p orbitals of the adjacent nitrogen atoms, which are also sp^2 hybridised. The C-N-C angles at the atoms N(1) and N(2), respectively 125.5(11) and 116.8(9)^{o}, are consistent with this view. Furthermore, there is also apparently a minor contribution from a second canonical structure, in which metal d electrons are donated to the vacant p orbital of the carbenoid carbon atom. This platinum(IV)-carbenoid bonding is strikingly similar to that observed in the platinum(II) complexes cis- and trans-[PtCl$_2${C(PhNCH$_2$)$_2$} PEt$_3$].[63]

The Pt-Cl (trans to carbenoid) bond length of 2.372(3) Å is 0.043(5) Å shorter than the Pt-Cl(trans to phenyl) distance of 2.415(4) Å but 0.040(6) Å longer than the mean Pt-Cl bond length of 2.332(5) Å in trans-[PtCl$_4$(PEt$_3$)$_2$].[81] These differences imply that in platinum(IV) complexes the trans-influence of the carbenoid ligand is less than that of σ-phenyl but greater than that of chloride. An identical trans-influence series pertains in complexes of platinum(II). Thus,

Pt(II)-Cl(<u>trans</u> to Cl) distances are normally close to 2.31 $\overset{o}{A}$, and a bond length of 2.362(3) $\overset{o}{A}$ has been reported for Pt(II)-Cl (<u>trans</u> to C(PhNCH$_2$)$_2$).[63] The length of a Pt(II)-Cl bond <u>trans</u> to σ-phenyl has apparently not been reported, but a value of 2.398(4) $\overset{o}{A}$ <u>trans</u> to σ-alkenyl has been observed.[82]

The mean Pt-P bond length of 2.388(4) $\overset{o}{A}$ is in good agreement with the corresponding value of 2.393(5) $\overset{o}{A}$ in <u>trans</u>-[PtCl$_4$(PEt$_3$)$_2$].[81] In square-planar complexes of platinum(II), however, mutually-<u>trans</u> Pt-P bond lengths lie in the range 2.27 - 2.32 $\overset{o}{A}$.[78] The greater length of Pt-P bonds in octahedral platinum(IV) complexes may be related to the presence of six, rather than eight, <u>d</u> electrons at the metal atom. In octahedral <u>trans</u>-[M^{IV}Cl$_4$(PR$_3$)$_2$] complexes, where M is a third row transition metal, addition of one <u>d</u> electron to M leads to a contraction of 0.05 $\overset{o}{A}$ in the M-P bond length.[81] It is, however, remarkable that the lengths of the Pt-C and Pt-Cl bonds in the [PtCl$_2${C(Cl.C$_6$H$_3$NH)(NHMe)}(PEt$_3$)$_2$]$^+$ cation are nearly the same as those of comparable bonds in square-planar platinum(II) complexes.

Figure 2.5: A view of the $[PtCl_2\{C(Cl.C_6H_3NH)(NHMe)\}(PEt_3)_2]^+$

cation. Hydrogen atoms are omitted for clarity.
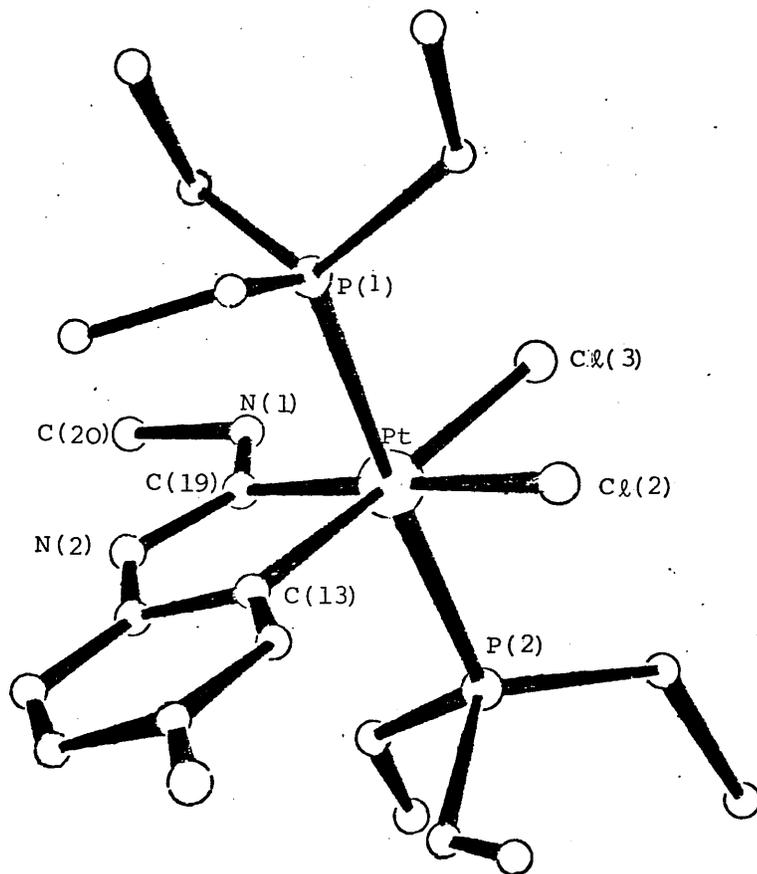
2.6. THE CRYSTAL AND MOLECULAR STRUCTURE OF THE

PLATINUM CYCLOOCTYNE $[Pt(C_8H_{12})(PPh_3)_2] \cdot 0.5C_6H_6$

2.6.1. INTRODUCTION

Cyclohexyne and cycloheptyne are too reactive to be isolated but form stable complexes with platinum (O).[83] The X-ray analyses of the complexes $[PtL(PPh_3)_2]$, L = cyclohexyne or cycloheptyne, have been reported.[84,85] In contrast, cyclooctyne is stable; an electron diffraction study of this molecule has been reported.[86] The present author undertook an X-ray analysis of the cyclooctyne complex $[Pt(C_8H_{12})(PPh_3)_2]$ for the following reasons.

(i) to obtain accurate molecular dimensions for comparison with those of the above cycloalkyne derivatives and with acyclic alkyne complexes;

(ii) to determine the mode of bonding of cyclooctyne to platinum (O); and

(iii) to compare the conformations of the free and complexed cyclooctyne molecules.

2.6.2. EXPERIMENTAL

Crystal Data. - $C_{47}H_{45}P_2Pt$, M = 866.9. Triclinic, a = 11.334(5), b = 15.931(6), c = 12.021(6) Å, α = 97.77(5), β = 113.66(4), γ = 90.79(3)°, T = 20°C, U = 1964.3 Å³, D_c = 1.466 gm cm^{-3}, Z = 2, F(000) = 870. Cu-K_α radiation, λ = 1.5418 Å, μ(Cu-K_α) = 78.2 cm^{-1}. Space group P$\bar{1}$.

The crystals are white, air-stable plates. The specimen used in the analysis displayed all members of the {100}, {010}, {110}, {1$\bar{1}$0}, and {011} forms, and also the (0$\bar{1}$1) face. It had dimensions of ca. 0.2 × 0.1 × 0.2 mm.

The crystal system and the dimensions of a Delaunay unit-cell were obtained from Weissenberg and precession photographs. Unit-cell dimensions were later adjusted by a least-squares treatment of the setting angles of 12 reflexions centred on a Hilger and Watts' Y290 diffractometer controlled by a PDP8 computer.[34a] The space group P$\bar{1}$ led to a satisfactory structural model.

Intensity Measurements. - The intensities of all independent reflexions with θ(Cu-K_α) $\leq$ 57° were measured on the Y290 instrument with the use of nickel-filtered copper radiation and a pulse-height analyser. A symmetrical θ - 2θ scan was employed, with a scan step in θ of 0.01° and a counting time per step of 1s. Each reflexion was scanned through a 2θ range of 1.4° and the local background was counted for 10s at each end of the scan range. To check crystal and electronic stability, the intensities of two strong low-angle reflexions were remeasured periodically throughout the experiment: they indicated total crystal decomposition of ca. 37% during the

course of the intensity measurements.

The integrated intensities, I, and their standard deviations, $\sigma(I)$, were derived in the usual manner (q 0.05).[35] They were corrected for Lorentz, polarisation and absorption effects. The transmission factors on $|F_o|$, calculated by Gaussian integration over a grid of 10 x 8 x 14 points, ranged from 0.61 to 0.75.[37]

Of 5200 reflexions measured, only 2579 for which $I \geqslant 3\sigma(I)$ were used in the subsequent calculations.

Structure Analysis. - The positions of the platinum and phosphorus atoms were derived from a Patterson synthesis, and the remaining non-hydrogen atoms were located in subsequent difference syntheses. The structural model was refined by least-squares minimisation of the function $\sum w \Delta^2$, where w is a weight and $\Delta = |F_o| - |F_c|$. Initially, the weights were taken as $1/\sigma^2(F_o)$, but this proved unsatisfactory and in the final stages of refinement another function was employed:
w = X.Y where X = 1 for $\sin\theta > 0.55$, else X = $(\sin\theta)/0.55$, and Y = 1 for $|F_o| > 50$, else Y = $50/|F_o|$. Atomic scattering factors were taken from ref.38a, except those for platinum[39] and hydrogen.[40] Allowance was made for the anomalous scattering of the platinum and phosphorus atoms using Cromer's values of $\Delta f'$ and $\Delta f''$.[41]

The refinement of a scale factor and of positional and isotropic thermal parameters of the platinum and phosphorus atoms led to R 0.29. When the remaining non-hydrogen atoms were included in the refinement and anisotropic temperature factors were assigned to the platinum and phosphorus atoms R fell to 0.16. Eight individual scale factors were included to account for the crystal decomposition,thus reducing

R to 0.11. The intensities were corrected for absorption. In addition, the hydrogen atom positions were inferred and the scattering of these atoms was included in subsequent structure factor calculations but their positional parameters were not varied. The refinement converged at R 0.093 and R' 0.122. In the final cycle of refinement all parameters shifted by less than 0.5σ . The mean values of $w\Delta^2$ showed no systematic trend when analysed as a function of $|F_o|$ or sin θ. The extreme function values in the final difference synthesis (2.1 and -3.0 e $\mathring{A}^{-3}$) were associated with the position of the platinum atom.

The observed structure amplitudes and calculated structure factors are listed in the Appendix (pp.115 to 131). Final atomic parameters and a selection of derived functions are presented in Tables 2.12 - 2.14. A view of the molecular structure is shown in Figure 2.6.

The computer programs used were those described in Sec. 2.3.2.

2.6.3. RESULTS AND DISCUSSION

The crystals are composed of discrete $[(C_8H_{12})Pt(PPh_3)_2]$ and benzene

(solvate) molecules in a 2:1 ratio. The distances between atoms in

neighbouring molecules are typical of van der Waals contacts (Table

2.13(e)).[44]

As a result of the rather severe crystal decomposition, the structural

parameters are ill-determined. The C-C bond distances of the

phenyl rings, for example, range from 1.22(7) to 1.50(5) $\overset{o}{A}$.

However, $\chi^2 = 43$ for 36 such distances and so it appears that the

standard deviations from the least-squares refinement are realistic

estimates of the true experimental errors.[87] Accordingly, the struc-

tural parameters are of sufficient accuracy for a discussion of the

salient features of the molecular structure.

The Metal Co-ordination. - As expected, the molecules of $[(C_8H_{12})Pt-$

$(PPh_3)_2]$ have a trigonal-planar co-ordination at the platinum atom

with one site occupied by a more or less symmetrically co-ordinated

multiple bond.[88] The metal co-ordination geometry is very similar to

that found in the analogous cyclohexyne and cycloheptyne complexes

and to that in the acyclic-alkyne complex $[(PhC{\equiv}CPh)Pt(PPh_3)_2]$.[89]

Selected bond lengths and interbond angles in the title complex, in

related complexes, and in cyclooctyne are presented in Table 2.15.

It can be seen that the corresponding Pt-P and Pt-C distances

and the C-Pt-C interbond angles are comparable in all the complexes.

The P-Pt-P angles vary from 102 to 111°. They fall into two

distinct groups: the values in the cyclooctyne and cyclohexyne

complexes are similar, as are those in the cycloheptyne and diphenyl-

acetylene derivatives. In addition, the dihedral angle of 1° between

the $[Pt, P(1), P(2)]$ and $[Pt, C(1), C(2)]$ planes in the title complex is in the range expected.[88]

The Cyclooctyne Ring. - It is a general feature of alkene or alkyne molecules co-ordinated to a transition metal that the C-C multiple bond is longer than that found in the free ligand.[88] On this basis, and by comparison with the dimensions of the acetylenic bonds in related complexes (Table 2.15), the co-ordinated alkyne linkage is a little short: bond distances in the free and bound cyclooctyne are 1.232(6) and 1.20(5) $\overset{o}{A}$, respectively, and the corresponding values in the related cycloalkyne complexes are equal at 1.29(2) $\overset{o}{A}$. However, the bond separations involving the acetylenic and adjacent carbon atoms [mean 1.52(4) $\overset{o}{A}$] and the remaining C-C bond lengths [mean $C(\underline{sp}^3)-C(\underline{sp}^3)$ distance = 1.51(5) $\overset{o}{A}$] are normal, being similar to the values observed in the related cyclic derivatives and in cyclooctyne itself.

The most generally applicable theory of the bonding of unsaturated hydrocarbons to transition metals appears to be the Dewar-Chatt model.[90] On this basis, the angular distortions at the acetylenic atoms indicate that the relative importance of C → M σ- and M → C π-interactions is similar in the three cycloalkyne complexes. Thus, the C-C≡C fragment bends by comparable amounts $[12 - 16^o]$ upon complexation as judged from the angles found in these three complexes, in free cyclooctyne, and predicted [83] for free cyclohexyne and cycloheptyne.

The interbond angles in the title complex involving $\underline{sp}^3$ hybridised carbon atoms [mean $120(3)^o$] are considerably greater than the ideal tetrahedral value $[109^o28']$ and comparable with those in the cyclo-heptyne complex [mean $120(1)^o$]; the corresponding angles in the cyclohexyne complex are somewhat smaller [mean 114°]. However, in free

cyclooctyne the $C(sp^3)-C(sp^3)-C(sp^3)$ angles are more nearly regular [mean 109.9(6)°]. These distortions may be attributed to ring strain engendered by the angular deformations at the acetylenic atoms upon complexation.

The conformations of the free and bound cyclooctyne molecules are different. In the gas phase the ring adopts a half-chair conformation with the atoms C(1)-(4) and C(7)-(8) coplanar, and C(5) and C(6) symmetrically displaced on opposite sides of the plane by 0.57 Å. In the title complex the ring displays a half-boat conformation with the same six atoms coplanar within experimental error and atoms C(5) and C(6) displaced on the same side of the plane by 0.87 and 1.14 Å, respectively. This conformation change presumably originates from non-bonded interactions arising from the deformations at the acetylenic atoms upon ligation rather than from crystal-packing forces. However, it is not possible to make a definite assertion since a molecular mechanics calculation [91] is not feasible at present due to lack of the necessary force-field parameters.

The Phosphine Ligand. - The geometry of the phosphine ligands is normal.[48] Thus, the Pt-P-C and C-P-C angles display the expected deviations from regular tetrahedral geometry. The mean P-C and C-C distances are 1.83(1) and 1.42(2) Å, respectively, and the phenyl rings are planar to within ± 0.04 Å.

The Benzene Solvate. - The C-C bond lengths [mean 1.34(4) Å] and internal interbond angles [mean 119(3)°] are close to the corresponding values for benzene.[50] The ring is planar to within ± 0.02 Å.

TABLE 2.12

Fractional co-ordinates $(\times 10^3)$ and vibrational parameters

for $\left[\text{Pt}(C_8H_{12})(\text{PPh}_3)_2\right] \cdot 0.5C_6H_6$

Atom	x	y	z	$U \times 10^3 \text{ Å}^2$
Pt	141.7(1)	279.6(1)	364.8(1)	*
P(1)	222.5(7)	247.4(4)	225.0(8)	*
P(2)	-71.6(7)	298.1(4)	273.6(8)	*
C(1)	206(3)	296(2)	550(3)	60(7)
C(2)	298(3)	278(2)	528(3)	76(8)
C(3)	443(4)	267(2)	568(4)	104(12)
C(4)	501(5)	278(3)	720(5)	130(15)
C(5)	470(5)	232(3)	789(5)	127(15)
C(6)	343(5)	228(3)	788(5)	137(16)
C(7)	271(4)	308(3)	778(4)	119(13)
C(8)	160(3)	305(2)	651(4)	85(10)
C(11)	325(3)	158(2)	262(3)	65(7)
C(12)	455(3)	165(2)	290(4)	96(11)
C(13)	528(4)	94(3)	334(4)	108(12)
C(14)	466(4)	23(3)	349(5)	122(14)
C(15)	341(3)	13(2)	321(4)	90(10)
C(16)	266(4)	84(2)	277(4)	101(11)
C(21)	337(2)	328(2)	223(3)	56(7)
C(22)	382(3)	327(2)	134(3)	65(7)
C(23)	472(3)	388(2)	137(4)	93(10)
C(24)	514(3)	456(2)	236(4)	82(9)
C(25)	470(4)	463(2)	319(4)	95(11)
C(26)	377(3)	399(2)	321(3)	78(9)
C(31)	128(3)	217(2)	58(3)	64(7)
C(32)	32(3)	267(2)	2(3)	80(9)
C(33)	-43(4)	247(2)	-135(4)	100(11)

<u>TABLE 2.12 (Cont'd)</u>

Atom	x	y	z	$U \times 10^3 \text{Å}^2$
C(34)	-15(4)	176(2)	-199(4)	103(12)
C(35)	76(5)	124(3)	-144(5)	134(16)
C(36)	150(3)	143(2)	-8(4)	87(10)
C(41)	-114(3)	380(2)	176(3)	67(8)
C(42)	-27(3)	450(2)	202(3)	78(9)
C(43)	-53(4)	514(2)	129(4)	100(11)
C(44)	-168(4)	510(2)	26(4)	100(11)
C(45)	-253(4)	441(3)	1(4)	107(12)
C(46)	-230(3)	376(2)	71(3)	84(9)
C(51)	-143(3)	333(2)	384(3)	64(7)
C(52)	-175(3)	280(2)	438(4)	92(10)
C(53)	-221(3)	301(2)	537(4)	95(11)
C(54)	-234(4)	391(2)	553(4)	99(11)
C(55)	-204(4)	446(3)	504(4)	108(12)
C(56)	-158(3)	421(2)	414(3)	71(8)
C(61)	-183(3)	209(2)	173(3)	62(7)
C(62)	-134(3)	151(2)	112(3)	73(8)
C(63)	-223(4)	82(2)	21(4)	99(11)
C(64)	-344(4)	75(2)	10(4)	101(11)
C(65)	-396(3)	130(2)	74(4)	93(10)
C(66)	-312(3)	201(2)	159(3)	71(8)
C(100)	101(4)	-28(3)	597(5)	122(14)
C(101)	119(5)	32(3)	538(5)	136(16)
C(102)	22(5)	61(3)	440(5)	139(17)

* These atoms were assigned anisotropic temperature factors of the form $\exp\left[-2\pi^2 \sum_{ij} U_{ij} a_i^* a_j^* h_i h_j\right]$. The final values of the U_{ij} parameters ($\times 10^3$) are:

TABLE 2.12 (Cont'd)

Atom	U_{11}	U_{22}	U_{33}	U_{12}	U_{13}	U_{23}
Pt	60(3)	56(2)	62(2)	-3(1)	-3(1)	-5(1)
P(1)	65(5)	50(4)	93(6)	-2(3)	-13(5)	-6(4)
P(2)	68(5)	59(4)	58(6)	-14(3)	12(4)	-5(3)

TABLE 2.13

Selected interatomic distances ($\overset{o}{A}$) and angles (^{o}) in

$$[\text{Pt}(C_8H_{12})(\text{PPh}_3)_2] \cdot 0.5C_6H_6$$
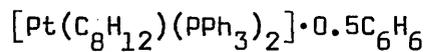
(a) **Bond lengths**

(i) $\text{PtP}_2(C_8H_{12})$

Pt-P(1)	2.22(1)	C(3)-C(4)	1.65(7)
Pt-P(2)	2.26(1)	C(4)-C(5)	1.32(9)
Mean	2.24(2)	C(5)-C(6)	1.44(8)
Pt-C(1)	2.02(3)	C(6)-C(7)	1.52(7)
Pt-C(2)	2.05(3)	C(7)-C(8)	1.53(5)
Mean	2.04(2)	Mean	1.51(5)
C(1)-C(2)	1.20(5)	P(1)-C(11)	1.84(3)
		P(1)-C(21)	1.83(3)
C(1)-C(8)	1.49(6)	P(1)-C(31)	1.85(3)
C(2)-C(3)	1.54(5)	P(2)-C(41)	1.81(3)
Mean	1.52(4)	P(2)-C(51)	1.84(4)
		P(2)-C(61)	1.82(2)
		Mean	1.83(1)

(ii) Phenyl and solvent

Ring atoms	Range	Mean
C(11)-(16)	1.32(6)-1.45(5)	1.41(2)
C(21)-(26)	1.28(7)-1.46(4)	1.40(2)
C(31)-(36)	1.35(6)-1.50(5)	1.42(2)
C(41)-(46)	1.37(5)-1.40(4)	1.39(2)
C(51)-(56)	1.22(7)-1.48(7)	1.40(4)
C(61)-(66)	1.33(6)-1.48(4)	1.42(2)
C(100)-(102)*	1.33(8)-1.38(7)	1.36(4)

* Benzene solvate

TABLE 2.13 (Cont'd)

(b) Interbond angles

(i) $PtP_2(C_8H_{12})$

P(1)-Pt-C(2)	103(1)	C(11)-P(1)-C(21)	101(1)
P(2)-Pt-C(1)	112(1)	C(11)-P(1)-C(31)	102(1)
Mean	108(5)	C(21)-P(1)-C(31)	99(1)
P(1)-Pt-P(2)	110.8(3)	C(41)-P(2)-C(51)	102(1)
C(1)-Pt-C(2)	34(1)	C(41)-P(2)-C(61)	101(1)
		C(51)-P(2)-C(61)	103(1)
P(1)-Pt-C(1)	138(1)	Mean	101.3(6)
P(2)-Pt-C(2)	146(1)		
Mean	142(4)	C(1)-C(2)-C(3)	152(3)
		C(2)-C(1)-C(8)	142(3)
Pt-C(1)-C(2)	74(2)	Mean	147(5)
Pt-C(2)-C(1)	71(2)		
Mean	73(2)	C(2)-C(3)-C(4)	104(4)
		C(1)-C(8)-C(7)	113(3)
Pt-P(1)-C(11)	110(1)	Mean	109(5)
Pt-P(1)-C(21)	115(1)		
Pt-P(1)-C(31)	126(1)	C(3)-C(4)-C(5)	128(4)
Pt-P(2)-C(41)	115(1)	C(4)-C(5)-C(6)	122(4)
Pt-P(2)-C(51)	113(1)	C(5)-C(6)-C(7)	119(4)
Pt-P(2)-C(61)	119(1)	C(6)-C(7)-C(8)	112(3)
Mean	116(2)	Mean	120(3)

(ii) Phenyl and solvent

Ring atoms	Range	Mean
C(11)-(16)	116(3)-124(4)	120(1)
C(21)-(26)	116(4)-123(3)	120(1)
C(31)-(36)	118(3)-123(4)	120(1)
C(41)-(46)	116(3)-124(3)	120(1)
C(51)-(56)	108(4)-129(5)	120(3)

TABLE 2.13 (Cont'd)

Ring atoms	Range	Mean
C(61)-(66)	117(3)-125(3)	121(2)
C(100)-(102)	116(4)-125(5)	119(3)

(c) Torsion angles

C(1)-C(2)-C(3)-C(4)	10(8)	C(5)-C(6)-C(7)-C(8)	106(5)
C(2)-C(3)-C(4)-C(5)	62(6)	C(6)-C(7)-C(8)-C(1)	-59(5)
C(3)-C(4)-C(5)-C(6)	-67(8)	C(7)-C(8)-C(1)-C(2)	-14(7)
C(4)-C(5)-C(6)-C(7)	-37(7)	C(8)-C(1)-C(2)-C(3)	-20(11)

TABLE 2.13 (Cont'd)

(d) Intramolecular non-bonded distances

C_8H_{12} Ring

C(1)···C(4)	3.19	C(3)···C(6)	3.39
C(1)···C(5)	3.50	C(3)···C(7)	3.76
C(1)···C(6)	3.02	C(3)···C(8)	3.75
C(2)···C(5)	3.15	C(4)···C(7)	2.99
C(2)···C(6)	3.17	C(4)···C(8)	3.66
C(2)···C(7)	3.11	C(5)···C(8)	3.53

C_8H_{12}···PPh_3

C(3)···P(1)	3.84	C(3)···C(26)	3.71
C(3)···C(11)	3.55	C(8)···C(51)	3.72
C(3)···C(12)	3.57	C(8)···C(52)	3.61

Ph···Ph

C(11)···C(36)	3.03	C(46)···C(61)	3.04
C(12)···C(21)	2.99	C(51)···C(66)	3.10
C(22)···C(31)	3.08	C(52)···C(61)	3.20
C(41)···C(56)	3.08	C(52)···C(66)	3.14

TABLE 2.13 (Cont'd)

(e) Intermolecular non-bonded distances

$C(5)\cdots C(65^{I})$	3.75	$C(24)\cdots C(55^{III})$	3.54
$C(6)\cdots C(35^{II})$	3.84	$C(24)\cdots C(56^{III})$	3.57
$C(12)\cdots C(65^{III})$	3.61	$C(25)\cdots C(55^{III})$	3.50
$C(12)\cdots C(66^{III})$	3.65	$C(36)\cdots C(63^{V})$	3.68
$C(13)\cdots C(65^{III})$	3.67	$C(42)\cdots C(55^{VI})$	3.60
$C(14)\cdots C(14^{IV})$	3.57	$C(43)\cdots C(44^{VII})$	3.67

The Roman numeral superscripts refer to the equivalent positions

relative to the reference molecule at x, y, z:

I	$1 + x,\quad y,\ 1 + z$	V	$- x,\quad -y,\quad - z$
II	$x,\quad y,\ 1 + z$	VI	$- x,\ 1 - y,\ 1 - z$
III	$1 + x,\quad y,\quad z$	VII	$- x,\ 1 - y,\quad - z$
IV	$1 - x,\ - y,\ 1 - z$		

TABLE 2.14

Least-squares planes of $[Pt(C_8H_{12})(PPh_3)_2] \cdot 0.5C_6H_6$

Plane 1: Pt, P(1), P(2)

$$-0.204X - 0.978Y - 0.036Z + 3.853 = 0$$

Plane 2: Pt, C(1), C(2)

$$0.220X + 0.975Y + 0.044Z - 3.865 = 0$$

Plane 3: Pt, P(1), P(2), C(1), C(2)

$$0.206X + 0.978Y + 0.043Z - 3.869 = 0$$

[Pt 0.007, P(1) 0.001, P(2) -0.005, C(1) 0.007, C(2) -0.010,

C(3) 0.071, C(8) -0.181]

Plane 4: C(1), C(2), C(3), C(4), C(7), C(8)

$$-0.151X - 0.986Y - 0.076Z + 4.063 = 0$$

[Pt 0.014, C(1) -0.062, C(2) 0.029, C(3) 0.016, C(4) -0.016,

C(5) 0.866, C(6) 1.144, C(7) -0.002, C(8) 0.035]

Angle between planes: (1) - (2) 1°

TABLE 2.15

Selected bond distances ($\overset{o}{A}$) and angles (^{o}) in the title complex

and related molecules

(a) Distances	(I)*	(II)	(III)	(IV)	(V)
Pt-P	2.24(2)$^{+}$	2.271(2)$^{+}$	2.268(4)$^{+}$	2.28(1)$^{++}$	-
Pt-C	2.04(2)$^{+}$	2.04(2)$^{+}$	2.05(2)$^{+}$	2.04(3)$^{++}$	-
C(sp)-C(sp)	1.20(5)	1.29(2)	1.29(2)	1.32(9)	1.232(6)
C(sp)-C(sp^3)	1.52(4)$^{+}$	1.50(1)$^{+}$	1.49(1)$^{+}$	-	1.459(12)
C(sp^3)-C(sp^3)	1.51(5)$^{+}$	1.54(1)$^{+}$	1.52(2)$^{+}$	-	1.55(3)$^{+}$

(b) Angles					
P-Pt-P	110.8(3)	109.3	102.5	102	-
C-Pt-C	34(1)	36.8	36.7	39	-
C(sp)-C(sp)-C(sp^3)	147(5)$^{+}$	127.5(5)$^{++}$	139(2)$^{++}$	139.5(5)$^{++}$	158.5(9)
C(sp^3)-C(sp^3)-C(sp^3)	120(3)$^{+}$	114^{+*}	120(1)$^{++}$	--	109.9(6)$^{+}$

* (I) is the title complex; (II) and (III) are, respectively, the analogous cyclohexyne[84] and cycloheptyne[85] derivatives; (IV) is $[(PhC{\equiv}CPh)Pt(PPh_3)_2]$;[89] and (V) is the cyclooctyne molecule.[86]

$^{+}$ Mean values

$^{++}$ The e.s.d. of the mean value was calculated from the range.

$^{+*}$ No estimate of error can be obtained from the available data.

Figure 2.6: A view of the $[Pt(C_8H_{12})(PPh_3)_2]$

molecule; thermal vibration ellipsoids

enclose 50% of probability. Hydrogen

atoms (and the benzene solvate) have

been omitted for clarity.
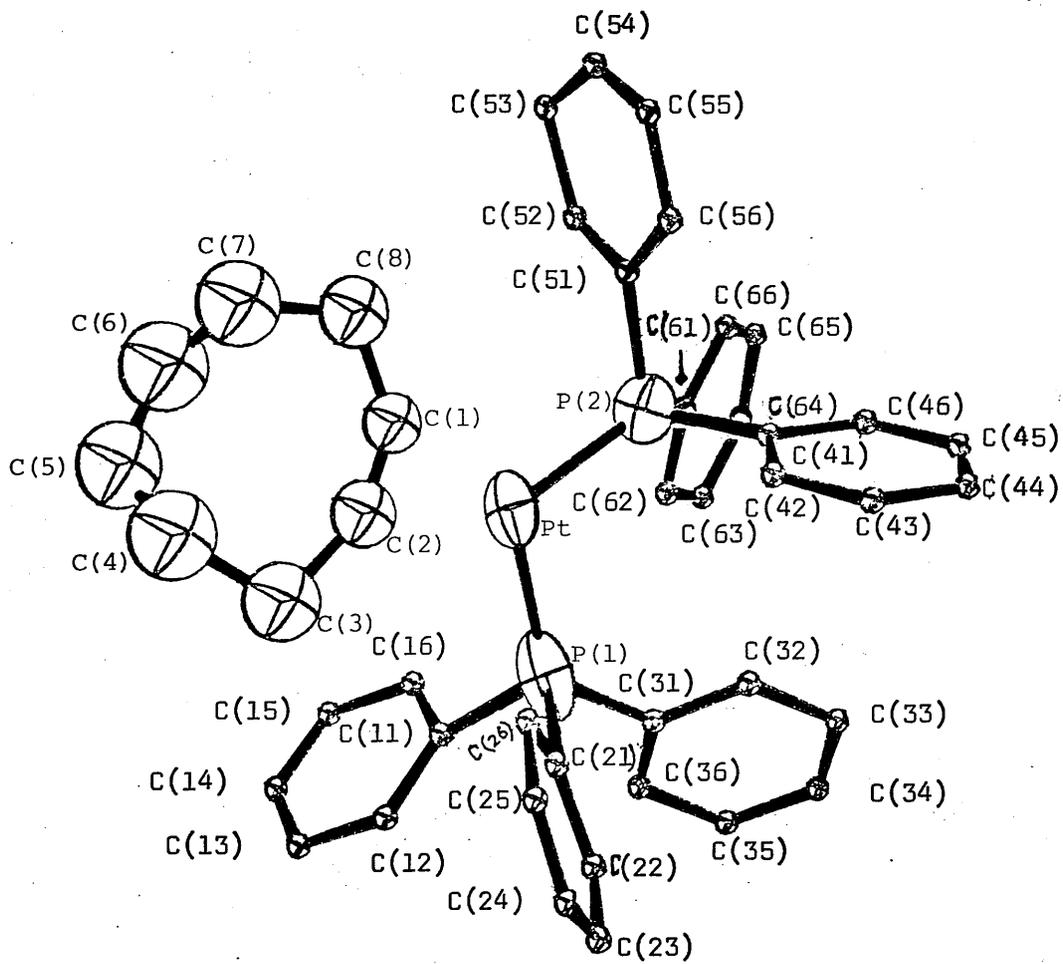
2.7. REFERENCES

1. F. Basolo and R. G. Pearson, Progr. Inorg. Chem., 1962, 4, 381.

2. A. Pidcock, R. E. Richards, and L. M. Venanzi, J. Chem. Soc. (A), 1966, 1707.

3. Lj. Manojlović-Muir and K. W. Muir, Inorg. Chim. Acta, 1974, 10, 47 and refs. therein.

4. T. G. Appleton, H. C. Clark, and L. E. Manzer, Co-ordination Chem. Rev., 1973, 10, 335.

5. A. A. Grinberg, Acta Physicochim. U.R.S.S., 1935, 3, 573; See also I.I. Chernyaev, Izv. Inst. Izuch. Platiny Drugikh Blagorod. Metal., Akad. Nauk.S.S.S.R., 1927, 5,109.

6. See, e.g., L. D. Pettit, Quart. Rev., The Chemical Society, London, 1971, 25, 1.

7. Y. K. Syrkin, Izv. Akad. Nauk.S.S.S.R., Otd. Khim. Nauk, 1948, 69.

8. M. Randić, J. Chem. Phys., 1962, 36, 3278.

9. (a) R. Mason, R. McWeeny, and A. D. C. Towl, Discuss. Faraday Soc., 1969, 47, 20; (b) R. Mason and A. D. C. Towl, J. Chem. Soc. (A) 1970, 1601.

10. S. S. Zumdahl and R. S. Drago, J. Amer. Chem. Soc., 1968, 90, 6669.

11. Derived from Table 3 in ref. 4.

12. J. A. Pople, Mol. Phys., 1958, 1, 216.

13. F. H. Allen and A. Pidcock, J. Chem. Soc. (A), 1968, 2700.

14. F. H. Allen, A. Pidcock, and C. R. Waterhouse, J. Chem. Soc. (A), 1970, 2087.

15. B. T. Heaton and A. Pidcock, J. Organometallic Chem., 1968, 14, 235; G. Socrates, J. Inorg. Nucl. Chem., 1969, 31, 1667.

16. F. H. Allen and S. N. Sze, J. Chem. Soc. (A), 1971, 2054.

17. M. J. Church and M. J. Mays, ibid., 1968, 3074.

18. Reference 4, p.381, and refs. therein.

19. G. G. Mather, A. Pidcock, and G. J. N. Rapsey, J. C. S. Dalton, 1973, 2095.

20. Sec.2.4.1 and ref. therein; A. N. Caldwell, Lj. Manojlović-Muir,

and K. W. Muir, J. C. S. Dalton, 1977, 2265.

21. Ref. 4, pp. 361, 379, 381 and 401, and refs. therein.

22. Lj. Manojlović-Muir, K. W. Muir, and T. Solomun, J. Organometallic

Chem., 1977, 142, 265.

23. F. R. Hartley, 'The Chemistry of Platinum and Palladium,'

Applied Science, London, 1973.

24. H. C. Clark, P. W. R. Corfield, K. R. Dixon, and J. A. Ibers,

J. Amer. Chem. Soc., 1967, 89, 3360.

25. M. Orchin and P. J. Schmidt, Co-ordination Chem. Rev., 1968, 3, 345.

26. E. M. Badley, J. Chatt, R. L. Richards, and G. A. Sim, Chem. Comm.,

1969, 1322.

27. J. S. Field and P. J. Wheatley, J. C. S. Dalton, 1974, 702.

28. K. W. Muir, in 'Molecular Structure by Diffraction Methods,' eds.

G. A. Sim and L. E. Sutton, The Chemical Society, London, 1973,

Vol. 1.

29. E. M. Badley, D. Phil. Thesis, University of Sussex, 1969.

30. S. O. Grim, R. L. Keiter, and W. McFarlane, Inorg. Chem., 1967, 6, 1133.

31. E. M. Badley, J. Chatt, and R. L. Richards, J. Chem. Soc. (A), 1971, 21;

ref. 4 and ref. therein.

32. Lj. Manojlović-Muir, K. W. Muir, and R. Walker, J. C. S. Dalton,

1976, 1279; ibid., J. Organometallic Chem., 1974, 66, C21.

33. W. H. Zacharaisen, Acta Cryst., 1965, 18, 705.

34. (a) W. R. Busing and H. A. Levy, Acta Cryst., 1967, 22, 457;

(b) The algorithm [related to that of ref. 34(a)] of the Hilger

'and Watts' software package for the Y290 diffractometer with D.E.C.

disc storage; this method produces no standard deviations of cell

parameters.

35. See Sec. 1.3.

36. See Sec. 1.4.

37. W. R. Busing and H. A. Levy, _Acta Cryst._, 1957, 10, 180.

38. (a) 'International Tables for X-Ray Crystallography,' Vol. III,
    Kynoch Press, Birmingham, 1962; (b) _ibid._, Vol. IV, 1974.

39. D. T. Cromer and J. T. Waber, _Acta Cryst._, 1965, 18, 104.

40. R. F. Stewart, E. R. Davidson, and W. T. Simpson, _J. Chem. Phys._,
    1965, 42, 3175.

41. D. T. Cromer, _Acta Cryst._, 1965, 18, 17.

42. W. C. Hamilton, 'Statistics in Physical Science,' Ronald Press,
    New York, 1964; _Acta Cryst._, 1965, 18, 502.

43. See Sec. 1.5, and ref. 14 therein.

44. L. Pauling, 'The Nature of the Chemical Bond,' Cornell University
    Press, Ithaca, New York, 1960.

45. W. C. Hamilton and J. A. Ibers, 'Hydrogen Bonding in Solids,'
    Benjamin, New York, 1968.

46. (a) C. A. Tolman, _J. Amer. Chem. Soc._, 1970, 92, 2956;
    (b) _Chem. Rev._, 1977, 77, 313; (c) ref. 46(a), p.2953.

47. B. Jovanović and Lj. Manojlović-Muir, _J. Chem. Soc. Dalton_, 1972, 1176.

48. M. A. Bush, A. D. U. Hardy, Lj. Manojlović-Muir, and G.A. Sim,
    J. Chem. Soc. (A) 1971, 1003.

49. B. Jovanović, Lj. Manojlović-Muir, and K. W. Muir, _J. C. S. Dalton_,
    1974, 195.

50. L. E. Sutton, 'Tables of Interatomic Distances,' _Chem. Soc._
    Special Publ., No.18, 1965.

51. M. R. Churchill, K. L. Kalra, and M. V. Veidis, _Inorg. Chem._,
    1973, 12, 1656.

52. J. J. Daly, _J. Chem. Soc._, 1964, 3799.

53. The prefix _ipso_ indicates the position bearing the substituent, as
    proposed by C. L. Perrin and G. A. Skinner, _J. Amer. Chem. Soc._,
    1971, 93, 3389.

54. A. Domenicano, A. Vaciago, and C. A. Coulson, Acta Cryst.,

1975, B31, 1630.

55. S. F. A. Kettle, Inorg. Chem., 1965, 4, 1661.

56. C. J. Cardin, D. J. Cardin, M. F. Lappert, and K. W. Muir,

J. Organometallic Chem., 1973, 60, C70.

57. P. S. Braterman, R. J. Cross, Lj. Manojlović-Muir, K. W. Muir,

and G. B. Young, J. Organometallic Chem., 1975, 84, C40.

58. R. J. D. Gee and H. M. Powell, J. Chem. Soc. (A), 1971, 1956.

59. M. J. S. Dewar and H. N. Schmeising, Tetrahedron, 1959, 5, 166.

60. B. Jovanović, Lj. Manojlović-Muir, and K. W. Muir, J. C. S. Dalton,

1972, 1178.

61. F. A. Cotton and G. Wilkinson, 'Advanced Inorganic Chemistry,'

3rd edn., Interscience, New York, 1972, p.685.

62. G. G. Messmer, E. L. Amma, and J. A. Ibers, Inorg. Chem.,

1967, 6, 725.

63. D. J. Cardin, B. Çetinkaya, E. Çetinkaya, M. F. Lappert,

Lj. Manojlović-Muir, and K. W. Muir, J. Organometallic Chem.,

1972, 44, C59; Lj. Manojlović-Muir and K. W. Muir, J. C. S. Dalton,

1974, 2427.

64. G. W. Bushnell, A. Pidcock, and M. A. R. Smith, J. C. S. Dalton,

1975, 572.

65. Average of following: 2.234(3) Å in cis-[PtCl$_2${C(NPhCH$_2$)$_2$}(PEt$_3$)],

ref. 63; 2.240(8) Å in cis-[PtCl$_2${C(OEt)NHPh}(PEt$_3$)], ref. 26;

2.238(8) Å in cis-[PtCl$_2$(CNPh)(PEt$_3$)], refs. 26 and 29;

2.244(8) Å in cis-[PtCl$_2$(CNEt)(PEt$_2$Ph)], ref. 47; 2.244(2) Å in

cis-[PtCl$_2${(CF$_3$)$_2$PCH$_2$CH$_2$PPh$_2$}] (ligating phosphorus atom is

underlined), Sec. 2.4.3, this thesis; 2.248(9) Å (mean) in

cis-[PtCl$_2$(PMe$_3$)$_2$], ref. 62; 2.255(5) Å (mean) in

cis-$[PtCl_2(PMe_2Ph)_2]HgCl_2$, R. W. Baker, M. J. Braithwaite,

and R. S. Nyholm, J. C. S. Dalton, 1972, 1924.

66. Lj. Manojlović-Muir, D. Millington, K. W. Muir, D. W. A. Sharp,

W. E. Hill, J. V. Quagliano, and L. M. Vallarino, Chem. Comm.,

1974, 999.

67. See, e.g., ref. 28; ibid., vols. II - IV, 1974, 1975, 1976.

68. J. A. McGinnety, N. C. Payne, and J. A. Ibers, J. Amer. Chem. Soc.,

1969, 91, 6301.

69. I. D. McLeod, Lj. Manojlović-Muir, D. Millington, K. W. Muir,

D. W. A. Sharp, and R. Walker, J. Organometallic Chem., 1975, 97, C7.

70. J. R. Gollogly and C. J. Hawkins, Inorg. Chem., 1969, 8, 1168.

71. M. C. Hall, B. T. Kilbourn, and K. A. Taylor, J. Chem. Soc. (A),

1970, 2539.

72. R. J. Cross, Lj. Manojlović-Muir, K. W. Muir, D. S. Rycroft,

D. W. A. Sharp, T. Solomun, and H. T. Miguel, J. C. S. Chem. Comm.,

1976, 291.

73. H. A. Bent, Chem. Rev., 1961, 61, 275.

74. J. Chatt, R. L. Richards, and G. H. D. Royston, J. C. S. Dalton,

1976, 599.

75. F. A. Cotton and C. M. Lukehart, Progress in Inorg. Chem.,

1973, 16, 487; D. J. Cardin, B. Çetinkaya, M. J. Doyle, and

M. F. Lappert, Chem. Soc. Rev., 1973, 2, 99.

76. A. J. Cheney, W. S. McDonald, K. O'Flynn, B. L. Shaw, and

B. L. Turtle, J. C. S. Chem. Comm., 1973, 128, and refs. therein.

77. See Secs. 2.1.3(c), 2.3, 2.4 and refs. therein.

78. P. B. Hitchcock, M. F. Lappert, G. M. McLaughlin and A. J. Oliver,

J. C. S. Dalton, 1974, 68.

79. R. Walker and K. W. Muir, J. C. S. Dalton, 1975, 272; K. W. Muir,

R. Walker, J. Chatt, R. L. Richards, and G. H. D. Royston,

J. Organometallic Chem., 1973, 56, C30.

80. M. R. Churchill, Perspectives in Structural Chem., 1970, 3, 91.

81. L. Aslanov, R. Mason, A. G. Wheeler, and P. O. Whimp, Chem. Comm.,
    1970, 30.

82. C. J. Cardin and K. W. Muir, J. C. S. Dalton, 1977, 1593.

83. A. Krebs, in 'Chemistry of Acetylenes,' ed. H. G. Viehe, Marcel
    Dekker, New York, 1969, Ch.15

84. G. B. Robertson and P. O. Whimp, J. Organometallic Chem., 1971, 32, C69.

85. M. A. Bennett, G. B. Robertson, P. O. Whimp, and T. Yoshida,
    J. Amer. Chem. Soc., 1971, 93, 3797.

86. J. Haase and A. Krebs, Z. Naturforsch, 1971, 26 A, 1190.

87. R. A. Fisher and F. Yates, 'Statistical Tables,' Oliver and Boyd,
    Edinburgh, 1953.

88. Ref. 28, p.622.

89. J. O. Glanville, J. M. Stewart, and S. O. Grim, J. Organometallic
    Chem., 1967, 7, P9.

90. Ref. 9(a); M. J. S. Dewar, Bull. Soc. chim. Fr., 1951, 18, C71;
    J. Chatt and L. A. Duncanson, J. Chem. Soc., 1953, 2939.

91. M. Hanack, 'Conformation Theory,' Academic Press, New York, 1965.

CHAPTER   THREE

The Crystal and Molecular Structures of

1,1-Dimethyl-2,5-Diphenyl-1-Silacyclo-

pentadiene and its Tricarbonylruthenium

complex

3.1   INTRODUCTION

Silacyclopentadiene (silole) metal complexes are of recent discovery and current interest.[1-3] Direct high-yield syntheses are available and complexes of chromium, iron, cobalt, molybdenum, ruthenium and rhodium have been prepared.[4]

The crystal and molecular structures[4] of 1,1-dimethyl-2,5-diphenyl-1-silacyclopentadiene (I) and its tricarbonylruthenium complex (II) have been determined. This work establishes the nature of the bonding

```
        H            H                    H   Ru(CO)3   H
         \          /                      \     |    /
          C ====== C                        C ===|== C
         /          \                      /     |    \
   Ph ---C          C--- Ph          Ph---C      |    C---Ph
          \        /                       \          /
           Si                               Si
          /  \                             /  \
        Me    Me                         Me    Me

         (I)                                 (II)
```

in an uncomplexed silole ring. Moreover, it permits an assessment of the changes in structure and bonding which occur when the silole is bonded to a transition metal. This is the first case in which the structures have been determined of the uncomplexed and complexed forms of the same cyclopentadiene heterocycle, where the hetero-atom belongs to the second short period. The results are, thus, relevant to those on the related phosphorus and sulphur heterocyclic complexes $[(C_5H_5)Co\{C(CF_3)_4C_4PO.OH\}]$ and $[\{(CF_3)_4C_4S(C_6F_5)\}Mn(CO)_3]$.[5]

Brief details are available of the structure of the silole (I) co-

crystallised with diphenylacetylene.[6] In the same paper, reference

was made to a structure analysis of (I) but, as yet, no publication

of this work has appeared. In addition, the dimensions of 1,2,5-

triphenylphosphacyclopentadiene (a phosphole) have been reported.[7]

3.2. EXPERIMENTAL

<u>Crystal Data</u> - <u>Structure (I)</u>. $C_{18}H_{18}Si$, $M = 262.4$. Orthorhombic, $a \doteqdot 15.669$, $b = 7.500$, $c = 6.548$ Å, $T = 23°C$, $U = 769.5$ Å^3, $D_c = 1.133$ gm cm^{-3}, $Z = 2$, $F(000) = 280$. Mo-K$_\alpha$ radiation, $\lambda = 0.71069$ Å, μ(Mo-K$_\alpha$) = 1.39 cm^{-1}. Space group Pmn2$_1$.

<u>Structure (II)</u>. $C_{21}H_{18}O_3RuSi$, $M = 447.5$. Monoclinic, $a = 18.112$, $b = 8.013$, $c = 27.455$ Å, $\beta = 97.22°$, $T = 20°C$, $U = 3952.7$ Å^3, $D_c = 1.504$ gm cm^{-3}, $Z = 8$, $F(000) = 1808$. Mo-K$_\alpha$ radiation, μ (Mo-K$_\alpha$) = 8.5 cm^{-1}. Space group I2/c(C_{2h}^6, No.15). Equivalent positions: $\pm$ (x,y,z), $\pm$ ($\bar{x}$,y, 1/2-z), $\pm$ (1/2 + x, 1/2 + y, 1/2 + z), $\pm$ (1/2 - x, 1/2 + y, $\bar{z}$).

<u>Crystallographic Measurements</u>. - Crystals of (I) are fluorescent-yellow air-stable polyhedra. The specimen used in the analysis had dimensions of <u>ca</u>. 0.6 x 0.4 x 0.4 mm. Crystals of (II) are fluorescent-orange air-stable needles. The specimen chosen displayed all faces of the {100} and {001} forms, and also the (01$\bar{1}$) and (0$\bar{1}\bar{1}$) faces, and its dimensions were 0.13 x 0.17 x 0.61 mm.

In each analysis the Laue group, the space group extinctions and unit-cell dimensions were derived by X-ray photography. For crystals of (II) a non-standard body-centred monoclinic cell was chosen in order that β would be close to 90°. The unit-cell parameters were then adjusted by a least-squares treatment of the setting angles of 12 reflexions centred on a Hilger and Watts' Y290 diffractometer controlled by a PDP8 computer.[8]

<u>Intensity Measurements</u>. - The intensities of all independent reflexions for which θ(Mo-K$_\alpha$) $\leq$ 30° (I) or 27° (II) were measured on the Y290 instrument with the use of graphite-monochromated molybdenum radiation

and a pulse-height analyser. A symmetrical $\theta - 2\theta$ scan was employed, with a scan step in θ of 0.02° and a counting time per step of 3 s (I) or 2.5 s (II). Each reflexion was scanned through a 2θ range of 0.96° (I) or 1.4° (II) and the local background was counted for 15 s (I) or 10 s (II) at each end of the scan range. The intensities of three strong reflexions, remeasured periodically throughout each experiment, displayed random fluctuations no greater than $\pm$ 3% (I) or $\pm$ 5% (II) of their mean values.

The integrated intensities, I, and their standard deviations, $\sigma(I)$, were derived in the usual way (q 0.04).[9] They were corrected for Lorentz, polarisation and counting-loss effects. No absorption correction was applied; for (II) a test calculation with a Gaussian integration grid[10] of 14 x 14 x 14 points indicated that the transmission factors on $|F_o|$ were constant to within $\pm$ 1%.

Of the reflexions measured [892,(I) ; 3498,(II)], only those for which $I \gtrsim 3\ \sigma(I)$ [828,(I); 3363,(II)] were used in the subsequent calculations.

Structure Analysis - In both analyses, the position of the heaviest atom was derived from a Patterson synthesis. The remaining atoms were located in subsequent difference syntheses, except that in the analysis of the ruthenium complex the positions of the hydrogen atoms were, in general, derived from those of the attached heavier atoms.

The structural parameters were refined by the method of full-matrix least-squares. The function minimised was $\Sigma w \Delta^2$, where $w = 1/\sigma^2(F_o)$ and $\Delta = |F_o| - |F_c|$. Atomic scattering factors were taken from ref.11, except those of hydrogen.[12] Allowance was made for the

anomalous scattering of the silicon and ruthenium atoms using values
of $\Delta f'$ and $\Delta f''$ from ref. 13.

(i) <u>Silole</u> - The systematic absences h0l when h + l = 2n + 1
are consistent with the space groups Pmnm and Pmn2$_1$. The former
centrosymmetric space group has eight general positions per unit-cell
whereas the latter non-centrosymmetric space group has four general
positions. With two silole molecules per unit-cell, the centrosym-
metric space group imposes mm symmetry on the molecules and the
silicon atom must be located at the special position (0, y, 0).
However, in the non-centrosymmetric space group only m symmetry is
required of the molecules, with the silicon atom situated at the
special position (0, y, z).

Initially, a solution was sought in the centrosymmetric space group.
Refinement of a scale factor and the isotropic thermal parameter of
the silicon atom led to R 0.39. A difference synthesis revealed
pseudo-symmetric sets of atomic peaks and indicated that the silole
molecules possess only one mirror plane. Accordingly, all subsequent
calculations were performed with the polar non-centrosymmetric space
group. The origin of this space group was defined by holding z(Si)
fixed at 1/4. Refinement of a scale factor, the positional para-
meters of all non-hydrogen atoms, and isotropic thermal parameters
led to R 0.089. Several cycles of Fourier synthesis and least-squares
were necessary for the location of all the hydrogen atoms; peak
heights of these atoms ranged from 0.22 to 0.44 e$\AA^{-3}$. The hydrogen
atom parameters were held invariant until the shifts in the carbon
parameters were insignificant and thereafter were refined. Anisotropic
temperature factors were assigned to the silicon and carbon atoms. The
refinement converged at R 0.034 and R' 0.040. The enantiomeric model
gave identical R-ratios and was not considered further. In the final cycle

of least-squares calculations all parameters shifted by less than

$0.10\,\sigma$. The standard deviation of an observation of unit weight,

S.D.,was 1.5 suggesting that the accuracy of the observed structure

amplitudes has been slightly overestimated. However, the absence of

significant trends in the mean values of $w\Delta^2$, when analysed as a

function of $|F_0|$ or $\sin\theta$, suggests that the relative weights are

satisfactory. In the final difference synthesis the extreme

function values were 0.2 and $-0.2\ e\mathring{A}^{-3}$; the positive peak was

situated between the Si and C(1) atoms and the negative one was

close to the silicon atom. The minimum peak height for a carbon

atom in the final electron-density synthesis was $5.7\ e\mathring{A}^{-3}$. Corrections

for secondary extinction effects did not appear to be necessary.

(ii) (silole)tricarbonylruthenium. - The systematic absences hkl

when $h + k + l = 2n + 1$ and h0l when $l = 2n + 1$ are consistent with

the space groups $I2/c$ (centrosymmetric) and Ic (non-centrosymmetric).

With eight formula units per unit-cell the centrosymmetric space

group leads to one (silole)tricarbonylruthenium molecule per

asymmetric unit with the atoms located in general positions. However,

the non-centrosymmetric space group has only four general positions

per cell and, hence, the asymmetric unit would need to possess two

formula units. A solution was attempted in the centrosymmetric space

group and this led to a satisfactory analysis.

Refinement of a scale factor and of the positional and isotropic

thermal parameter of the ruthenium atom led to R 0.34. After the

remaining non-hydrogen atoms were included with isotropic thermal

parameters R and R' were 0.060 and 0.082, respectively. Anisotropic

temperature factors were then assigned to the ruthenium and silicon

atoms. In addition, the positions of the phenyl hydrogen atoms were
inferred and the scattering of these atoms was included in subsequent
structure factor calculations but no hydrogen parameter was varied.
This led to R 0.055 and R' 0.079. The hydrogen atoms bonded to the
methyl carbon atom C(2) were located in a difference synthesis; the
positions of the hydrogen atoms of the butadiene unit were inferred.
Furthermore, anisotropic temperature factors were assigned to the
butadiene atoms C(3) - (6). R and R' decreased to 0.049 and 0.066,
respectively. Anisotropic thermal parameters were then assigned to
the carbon and oxygen atoms of the carbonyl groups and to four of
the phenyl carbon atoms - regions of electron density in a difference
synthesis had indicated that the thermal vibrations of these carbon
atoms were significantly anisotropic.[14] The refinement converged
at R 0.038 and R' 0.049. In the final cycle of least-squares refine-
ment all parameters shifted by less than 0.2σ. The value of S.D.
was 1.9. However, the relative correctness of the weights employed
was indicated by the absence of obvious trends when the data were
analysed as a function of $|F_0|$ or $\sin\theta$. In the final difference
synthesis there were no significant features: the function values
ranged from 0.7 to -0.5 $e\overset{\circ}{A}^{-3}$ with the extreme values associated with
the positions of the C(1) and C(15) atoms, respectively. The minimum
peak height for a carbon atom in the final electron density synthesis
was 4.5 $e\overset{\circ}{A}^{-3}$.

Observed and calculated structure amplitudes are listed in the Appendix
(pp. 132 to 140,(I), and 141 to 165, (II)). Atomic parameters are given in
Tables 3.1 and 3.2, and a selection of derived functions - interatomic
distances and angles, and mean planes - are presented in Tables 3.3
to 3.6. The atomic numbering schemes are indicated and views of the

molecular structures are shown in Figures 3.3 to 3.5.

The computer programs employed have been described previously.[15]

3.3. RESULTS AND DISCUSSION

The crystals of (I) and (II) are composed, respectively, of discrete

monomeric silole and (silole)tricarbonylruthenium molecules. The

separations between atoms in neighbouring molecules are in the range

of normal van der Waals contacts (Tables 3.3(d) and 3.4(d)).[16]

(i) <u>Structure (I)</u>. - The molecules of (I) display exact C_s

symmetry, with the silicon and methyl carbon atoms lying on the

mirror plane at x = 0 to which the butadiene unit is perpendicular.

The butadiene fragment of the silole ring is exactly planar, with the

silicon atom displaced from it by 0.08 Å, leading to a dihedral angle

of 3.7° between the butadiene and SiC(3)C(3') planes. The phenyl

ring is approximately coplanar with the butadiene unit with a dihedral

angle between these planes of 13.7°. This small rotation about the

C(butadiene)-C(phenyl) bond appears to result from intramolecular

steric effects. Thus, there are a number of short intramolecular

contacts between phenyl ortho-carbon and -hydrogen atoms and buta-

diene carbon and hydrogen atoms (Table 3.3(c)). The most noteworthy

of these separations are H(5)···H(10) 2.26Å and C(4)···C(10) 3.00Å.

The bond lengths within the silole ring are consistent with complete

localisation of the double bonds: the C(3)-C(4) and C(4)-C(4')

distances of 1.345(4) and 1.466(6) respectively, are typical of

values found in <u>cis</u>-1,3-butadienes.[17] The Si-C(3) bond length is

that of a Si-C(sp^2) single bond (<u>vide infra</u>). In addition, the

butadiene-phenyl bond C(3)-C(5) has a length, 1.478(4)Å, which is

that of a C(sp^2)-C(sp^2) single bond.[17]

The interbond angles of the heterocyclic ring are qualitatively as

expected. Thus, the C(3)-C(4)-C(4') angle at the central carbon

atom C(4), 117.6(2)$^{\mathrm{o}}$, is close to 120$^{\mathrm{o}}$ as expected for sp^2 hybridisation of the carbon atoms. However, the Si-C(ring)-C(ring) and C(ring)-Si-C(ring) angles are reduced [from the normal values of 120$^{\mathrm{o}}$ and 109$^{\mathrm{o}}$58'] to 106.0(2) and 92.5(2)$^{\mathrm{o}}$, respectively, and this may be attributed to constraints imposed by the formation of the five-membered ring. They result in an opening of the exocyclic Si-C(ring)-C(Ph) and C(ring)-C(ring)-C(Ph) angles to 128.9(2) and 125.0(2)$^{\mathrm{o}}$, respectively; the latter angle may also arise, to some extent, from the intramolecular steric effects dis-cussed above.

The silicon atom has a distorted tetrahedral configuration. Con-comitant with the reduction of the C(3)-Si-C(3') angle there is an opening of the C(Me)-Si-C(Me) and C(Me)-Si-C(ring) angles to 112.5(3) and 112.6(3)$^{\mathrm{o}}$ (mean), respectively. The Si-C(Me) bond lengths are equal: their mean distance, 1.867(6) Å, agrees well with the standard value [1.870(5) Å].[17] The Si-C(sp^2) bonded distance, 1.878(3) Å, appears long by comparison with the Si-C(sp^3) distances in the same molecule. However, it is in the range expected. Thus, in 10 silicon derivatives the Si-C(Ph) bond lengths vary from 1.855(6) to 1.894(5) Å;[18] the Si-C bond distances in PhSiH$_3$ and [(C$_5$H$_5$)$_2$ZrCl(SiPh$_3$)] are 1.843(5) and 1.913(4) Å, respectively.[17, 19] In several cyclosiloxanes the Si-C(Me) and Si-C(Ph) distances display the same trend as in (I): this has been attributed to an effect of the relatively high thermal motion of the methyl carbon atoms.[20]

The phenyl geometry is normal.[21] Thus, the ring [atoms C(5) - (10)] is accurately planar, the root mean-square deviation from planarity of the carbon atoms being 0.003 Å. The mean C-C distance, 1.384(7) Å,

is slightly shorter than the spectroscopic value [1.397(1) Å] for

benzene.[17] The mean internal interbond angle is 119.9(1)°.

The C-H bond lengths range from 0.83(5) to 1.05(3) Å; mean distances

are 0.95(4)Å (Me) and 0.95(2)Å (Ph). These distances are, as

expected, slightly shorter than the values [ca. 1.08 Å] obtained by

neutron diffraction or spectroscopic methods.[22] Such contractions

have been attributed to the displacement of the electron density of

the hydrogen atom from its nuclear position when it bonds to a

heavier atom such as carbon.[23]

In addition, the Si-C-H and H-C(Me)-H angles range, respectively,

from 102(3) to 122(5)°, and 92(3) to 115(4)°, but the corresponding

mean values, 110(3) and 107(6)°, are close to the ideal tetrahedral

angle [109°28']. The C(Ph)-C(Ph)-H angles vary from 115(2) to 124(2)°

and their mean value is 120(1)°.

(ii) **Structure II.** - Approximate C_s symmetry is retained in the

molecules of (II) (Fig.3.5.). The metal co-ordination can be

described, in terms of canonical form (A), as a distorted square

(A)   (B)

Fig. 3.1. Metal-Butadiene bonding: valence bond model.

pyramid with the metal atom displaced by 1.85 Å from the plane of

the butadiene carbon atoms or, in terms of form (B), as a distorted

octahedron with three _facial_ sites occupied by carbonyl ligands and

a further three by diene atoms C(3) and C(6) and the midpoint of

the diene C(4)-C(5) bond. The disposition of the carbonyl ligands

and the   M-C(butadiene) bonded distances are in accord with

features[24] observed in many (diene)M(CO)$_3$ structures. Thus, when

the molecule is viewed in a direction normal to the butadiene plane

the carbonyl groups C(100)-O(1) and C(101)-O(2) project across

the formally double bonds C(3)-C(4) and C(5)-C(6) of the diene

(Fig. 3.5). Moreover, the ruthenium atom is slightly closer to the

central carbon atoms of the diene than it is to the terminal atoms:

equivalent metal-carbon separations are equal and mean values are

Ru-C(central) 2.189(3) Å and   Ru-C(terminal) 2.293(4) Å . These

values agree well with the corresponding distances of 2.182(6) and

2.265(6) Å in (C$_8$H$_8$)Ru(CO)$_3$.[25]

The butadiene unit remains accurately planar. However, the presence

of the ruthenium atom results in substantial changes in the bonding

of the silole ring. Thus, the formally double bonds C(3)-C(4) and

C(5)-C(6) are lengthened by 0.103(5) Å (21σ) to a mean distance

of 1.448(3) Å, a value close to that expected for a C(sp^2)-C(sp^2)

single bond.[17] There is also a highly significant reduction of

0.059(8) Å (7σ) in the length of the central C(4)-C(5) bond of

the butadiene to 1.407(5) Å. However, the Si-C(ring), Si-Me and

C(Ph)-C(ring) distances remain unchanged. The changes in the

bonding within, and the conformation (vide infra) of the silole ring

are reflected in minor (but statistically significant) variations

of the valency angles of this ring by up to 5°. Thus, the C(terminal)-

C(central)-C(central) angles, C(3)-C(4)-C(5) and C(4)-C(5)-C(6)

are reduced by 3.2(5)^o to 114.4^o (mean). However, the Si-C(ring)-

C(ring) angles, mean 105.7(4)^o, show little change. The

C(ring)-Si-C(ring) angle is only 87.7(1)^o [cf. 92.5(2)^o in

(I)]. There is an opening of the C(Me)-Si-C(ring) angles to

114.9(11)^O (mean). However, the C(Me)-Si-C(Me) angle becomes

more nearly regular (108.4(2)^O).

There are a number of short intramolecular contacts (Table 3.4(c)).
The most noteworthy are C(4)···C(16) 3.04 $\overset{O}{A}$ and C(5)···C(22)

2.99 $\overset{O}{A}$ which involve ortho-carbon atoms of the phenyl groups and

central carbon atoms of the butadiene. Similar interactions are

observed in the molecules of (I). However, in the complex, these

repulsive forces are apparently relieved by the greater rotations

about the C(Ph)-C(ring) bonds leading to phenyl/butadiene dihedral

angles of 24.5 and 18.4^O[cf. 13.7^O in (I)]; the C(ring)-C(ring)-C(Ph)

angles, mean 121.7(6)^O, are close to 120° [cf. 125.0(2)^O in (I)].

A rationalisation of the metal-diene bonding[26] can be given in terms

of a valence bond treatment, where the bonding is considered to be

a hybrid of π and σ- canonical forms (Fig. 3.1) or in terms of a

molecular orbital approach such as that of Hückel (Fig. 3.2).
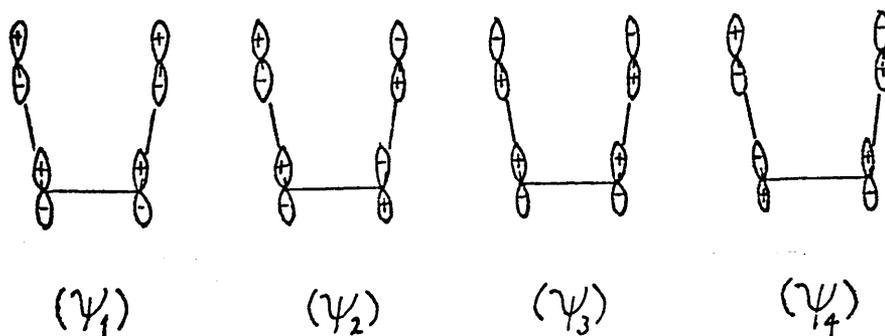
Fig. 3.2. Metal-butadiene bonding: Hückel
molecular orbitals.

In this treatment the orbitals ψ_1, ψ_2, ψ_3 and ψ_4 are obtained for

the description of the butadiene bonding. The ψ_1- and ψ_2- orbitals

are filled and are of appropriate symmetry for σ-donation to a

metal, whereas the vacant ψ_3- and ψ_4- orbitals are capable of

bonding to filled metal d_π orbitals. Two interactions are expected: donation of electron density from the highest filled orbital (ψ_2) of the butadiene to the metal and donation of metal d_π electrons to the butadiene ψ_3-orbital. These processes lead to a weakening of the terminal double bonds and a strengthening of the central C-C bond, which corresponds to an increased contribution from canonical form (B). From the changes in the butadiene bond lengths upon ligation, it is concluded that there is significant backdonation from the metal atom to the butadiene unit. In valence bond terms a significant contribution from canonical form (B) must be present. However, as is often found, there is little evidence of any partial $\underline{sp}^3$ hybridisation at the terminal carbon atoms C(3) and C(6).[26] The valence bond description of butadiene metal systems is of limited usefulness.

There is one further major difference in geometry of the free and complexed silole rings. The butadiene $\diagup$ SiC$_2$(ring) dihedral angle opens up considerably to 32.2$^\mathrm{o}$ in (II) [$\underline{cf}$. 3.7$^\mathrm{o}$ in (I)], so that the silicon atom is situated 0.72 $\overset{\mathrm{o}}{\mathrm{A}}$ from the butadiene plane on the side opposite to that of the metal atom. This envelope conformation is typical of the ligands in such cyclic butadiene systems: it has been attributed to an inward twisting of the $\underline{p}$ orbitals of the terminal carbon atoms of the diene in order to maximise their overlap with the metal orbitals.[27] The folding about the C(3)-C(6) vector results in a Ru$\cdots$Si separation of 2.992(2) $\overset{\mathrm{o}}{\mathrm{A}}$: any possibility of normal bonding between these atoms is excluded since the lengths of the Ru-Si single bonds in six complexes[28] for which structural data are available are in the range 2.39 - 2.51 $\overset{\mathrm{o}}{\mathrm{A}}$ (mean 2.45 $\overset{\mathrm{o}}{\mathrm{A}}$) and the sum of the covalent radii of ruthenium (1.30 $\overset{\mathrm{o}}{\mathrm{A}}$) and silicon (1.10 $\overset{\mathrm{o}}{\mathrm{A}}$) is 2.40 $\overset{\mathrm{o}}{\mathrm{A}}$;[29] Pauling's empirical relationship between the lengths of single and

fractional bonds suggests a Ru-Si bond order of about 0.12.[16]

In the related P- and S-heterocyclic complexes $[(C_5H_5)Co\{C(CF_3)_4-C_4PO.OH\}]$ and $[\{(CF_3)_4C_4S(C_6F_5)\}Mn(Co)_3]$, where again there is no direct bond between the metal and the ring hetero-atoms, the tetrahapto rings are also folded about the line through the terminal carbon atoms of the butadiene.[5] The resulting dihedral angles, respectively 32 and 31°, agree well with the corresponding angle in (II). In all three molecules the non-bonded separations between the metal atom and the hetero-atom appear surprisingly small, since subtraction of the van der Waals radius of the hetero-atom suggests that the contact radii of the metal atoms are in the range 0.8 - 1.0 Å.

The environments of the carbonyl groups C(100)-O(1) and C(101)-O(2) are similar and they are markedly different from that of the C(102)-O(3) group (Fig. 3.5.). The ruthenium-carbonyl Ru-C distances range from 1.906(4) to 1.941(4) Å [mean 1.923(10) Å], the largest value being associated with the C(102) atom of the unique carbonyl group. They are similar to those observed in $[(C_8H_8)Ru(CO)_3]$ (mean 1.916(7) Å) and in $[(C_8H_8)Ru_2(CO)_6]$ (mean 1.89(2) Å). This is to be expected since in all three complexes the ratios of olefin-ligand atoms to ruthenium atoms to carbonyl groups are similar.[25] The non-equivalence of the carbonyl groups of (II) is reflected in the CO-Ru-CO angles which are 90.0, 94.7 and 96.9°: the last two values, which involve the unique carbonyl, are the largest of the set, as has been noted in other systems.[24]

The C-O bond lengths are in agreement and their mean distance, 1.133(3) Å, is near to the spectroscopic value [1.128 Å] for carbon monoxide.[17] The Ru-C-O angles deviate from 180° by up to 5°.

Distortions of such an amount are common in metal carbonyls. In the case of $M(CO)_3$ fragments symmetry considerations indicate that the π^* electron density of each CO group has twofold rotational symmetry rather than full cylindrical symmetry.[30] The resulting angular distortion is a function of the difference in population of the π^* orbitals. Since in (II) the ligand trans to the CO groups does not present a cylindrically-symmetric bonding electron distribution to the metal atom, bending at carbonyl is expected. The Ru-C(100)-O(1) and Ru-C(101)-O(2) angles are equal at 178.7(4)$^\circ$, whereas the Ru-C(102)-O(3) angle is only 175.2(4)$^\circ$.

The phenyl geometries are normal, with root-mean square deviations from planarity of the carbon atoms of $\leq$ 0.006 Å.[21] The mean C-C lengths are 1.387(8) Å [C(11) - (16)] and 1.390(5) Å [C(21) - (26)]. The internal interbond angles are close to 120°.

3.4. REFERENCES

1. J.C. Brunet, B. Resibois, and J. Betrand, *Bull. Soc. chim. France*, 1969, 3424.

2. W. Fink, *Helv. Chim. Acta*, 1974, 57, 167.

3. H. Sakurai and J. Hayashi, *J. Organometal. Chem.*, 1973, 63, C.10.

4. K.W. Muir, R. Walker, E.W. Abel, T. Blackmore, and R.J. Whitley, *J.C.S. Chem. Comm.*, 1975, 698; E.W. Abel, T. Blackmore, and R.J. Whitley, *J.C.S. Dalton*, 1976, 2484.

5. M.J. Barrow, J.L. Davidson, W. Harrison, D.W.A. Sharp, G.A. Sim, and F.B. Wilson, *J.C.S. Chem. Comm.*, 1973, 583; M.J. Barrow, A.A. Freer, W. Harrison, G.A. Sim, D.W. Taylor, and F.B. Wilson, *J.C.S. Dalton*, 1975, 197.

6. J. Clardy and T.J. Barton, *J.C.S. Chem. Comm.*, 1972, 690.

7. W.P. Ozbirn, R.A. Jacobson, and J.C. Clardy, *ibid.*, 1971, 1062.

8. W.R. Busing and H.A. Levy, *Acta Cryst.*, 1967, 22, 457.

9. See Sec. 1.3.

10. W.R. Busing and H.A. Levy, *Acta Cryst.*, 1957, 10, 180.

11. 'International Tables for X-Ray Crystallography,' Vol. IV, Kynoch Press, Birmingham, 1974.

12. R.F. Stewart, E.R. Davidson, and W.T. Simpson, *J. Chem. Phys.*, 1965, 42, 3175.

13. D.T. Cromer, *Acta Cryst.*, 1965, 18, 17.

14. See, for example, G.H. Stout and L.H. Jensen, 'X-Ray Structure Determination,' Collier-Macmillan, London, 1968, p.380.

15. See Sec. 2.3.2.

16. L. Pauling, 'The Nature of the Chemical Bond,' Cornell University Press, Ithaca, New York, 1960.

17. L.E. Sutton, _Chem. Soc. Spec. Publ._, Supplement No.18, 1965.

18. A Domenicano, A. Vaciago, and C.A. Coulson, _Acta. Cryst._,
    1975, _B 31_, 221.

19. K.W. Muir, _J.C.S.(A).,_ 1971, 2663.

20. M. Söderholm, _Acta Chem. Scand._, 1978, _B 32_, 171.

21. A. Domenicano, A. Vaciago, and C.A. Coulson, _Acta Cryst._,
    1975, _B 31_, 1630; see also ref. 18.

22. M.R. Churchill, _Inorg. Chem._, 1973, _12_, 1213.

23. J. Tomiie, _J. Phys. Soc. Japan_, 1958, _13_, 1030; W.C. Hamilton
    and J.A. Ibers, 'Hydrogen Bonding in Solids,' Benjamin,
    New York, 1968.

24. M.G. Waite and G.A. Sim, _J. Chem. Soc.(A)_ , 1971, 1009.

25. F.A. Cotton and R. Eiss, _J. Amer. Chem. Soc._, 1969, _91_, 6593.

26. M.R. Churchill and R. Mason, _Advan. Organometal. Chem._ 1967,
    _5_, 93.

27. M.R. Churchill, _J. Organometal. Chem._, 1965, _4_, 258.

28. M.M. Crozat and S.F. Watkins, _J.C.S. Dalton_, 1972, 2512;
    J.A.K. Howard, S.A.R. Knox, V. Riera, B.A. Sosinsky, F.G.A.
    Stone, and P. Woodward, _J.C.S. Chem. Comm._, 1974, 673;
    J. Howard and P. Woodward, _J.C.S. Dalton_, 1975, 59;
    J.D. Edwards, R. Goddard, S.A.R. Knox, R.J. McKinney,
    F.G.A. Stone and P. Woodward, _J. Chem. Soc._, _Chem. Commun._,
    1975, 828; P.J. Harris, J.A.K. Howard, S.A.R. Knox, R.J.
    McKinney, R.P. Phillips, F.G.A. Stone, and P. Woodward,
    J.C.S. Dalton, 1978, 403.

29. J.C. Slater, _J. Chem. Phys._, 1964, _41_, 3199.

30. S.F.A. Kettle, _Inorg. Chem._, 1965, _4_, 1661.

TABLE 3.1

Fractional co-ordinates (x10^3) and vibrational parameters for (I)

Atom	x	y	z	B Å^2
Si	0	172.3(1)	1/4	*
C(1)	0	-66.9(6)	174.5(9)	*
C(2)	0	202.9(8)	533.8(8)	*
C(3)	-86.6(2)	305.4(3)	123.3(5)	*
C(4)	-46.8(2)	433.9(4)	16.3(5)	*
C(5)	-180.0(2)	279.8(3)	132.6(5)	*
C(6)	-215.7(2)	163.7(4)	272.0(8)	*
C(7)	-304.0(2)	136.2(4)	281.2(7)	*
C(8)	-356.8(2)	224.5(4)	149.1(7)	*
C(9)	-322.8(2)	338.5(5)	11.2(7)	*
C(10)	-235.2(2)	366.9(4)	-0.5(6)	*
H(1)	0	-60(7)	34(10)	6(1)
H(2)	49(2)	-122(4)	233(7)	6(1)
H(3)	0	310(8)	592(12)	8(2)
H(4)	53(3)	168(5)	604(9)	9(1)
H(5)	-74(2)	515(4)	-62(5)	5(1)
H(6)	-185(2)	104(4)	367(6)	5(1)
H(7)	-324(2)	65(4)	391(7)	6(1)
H(8)	-422(2)	192(4)	155(5)	6(1)
H(9)	-352(2)	392(5)	-75(8)	7(1)
H(10)	-212(2)	433(4)	-99(6)	6(1)

TABLE 3.1 (cont'd)

* These atoms were assigned anisotropic temperature factors of the form exp $\left[-\sum_i\sum_j B_{ij}h_ih_j\right]$. The final values of the B_{ij} parameters $(\times 10^4)$ are:

Atom	B_{11}	B_{22}	B_{33}	B_{12}	B_{13}	B_{23}
Si	36.6(4)	160.1(15)	228.2(23)	0**	0**	15.7(25)
C(1)	43(2)	196(8)	368(18)	0**	0**	-2(8)
C(2)	70(3)	286(12)	228(11)	0**	0**	-4(10)
C(3)	39(1)	173(4)	235(6)	8(2)	0(2)	2(5)
C(4)	45(1)	202(5)	319(9)	11(2)	-6(3)	63(6)
C(5)	38(1)	158(4)	265(7)	8(2)	7(3)	-13(5)
C(6)	43(1)	235(5)	344(10)	14(2)	13(3)	68(8)
C(7)	46(1)	254(6)	388(14)	-6(2)	19(4)	59(9)
C(8)	41(1)	223(5)	422(10)	-4(2)	6(3)	-30(7)
C(9)	45(1)	251(7)	395(11)	5(3)	-29(3)	25(8)
C(10)	48(1)	236(6)	308(9)	-5(2)	-14(3)	50(7)

** $B_{12}=B_{13}=0$ by symmetry

TABLE 3.2

(a) Fractional co-ordinates ($\times 10^4$) and vibrational parameters for (II)

Atom	x	y	z	$U \times 10^3$ Å^2
Ru	2382.7(1)	1942.3(3)	1523.3(1)	*
Si	2848.0(5)	-849.8(12)	905.8(3)	*
C(1)	3438(3)	-2750(6)	834(2)	64(1)
C(2)	2290(2)	-395(5)	301(1)	58(1)
C(3)	3410(2)	919(4)	1214(1)	*
C(4)	3430(2)	619(4)	1735(1)	*
C(5)	2841(2)	-362(4)	1866(1)	*
C(6)	2322(2)	-908(4)	1452(1)	*
C(11)	3973(2)	1951(5)	1011(1)	51(1)
C(12)	4122(2)	1714(5)	534(2)	63(1)
C(13)	4656(3)	2690(8)	343(2)	*
C(14)	5048(2)	3876(7)	634(2)	*
C(15)	4923(3)	4116(6)	1106(2)	76(1)
C(16)	4397(2)	3169(5)	1296(2)	64(1)
C(21)	1660(2)	-1910(4)	1524(1)	47(1)
C(22)	1395(2)	-2014(5)	1978(2)	62(1)
C(23)	779(3)	-3015(7)	2041(2)	81(1)
C(24)	416(3)	-3879(6)	1649(2)	*
C(25)	663(2)	-3780(6)	1200(2)	*
C(26)	1283(2)	-2819(5)	1137(2)	61(1)
C(100)	2761(2)	4057(5)	1753(1)	*
C(101)	1576(2)	2168(5)	1911(1)	*
C(102)	1860(2)	2810(5)	916(1)	*
O(1)	3000(2)	5305(4)	1892(1)	*
O(2)	1107(2)	2275(5)	2143(1)	*
O(3)	1577(2)	3420(4)	569(1)	*

TABLE 3.2 (Cont'd)

* These atoms were assigned anisotropic temperature factors of the form exp $[-2\pi^2 \Sigma\Sigma_{ij} U_{ij} a_i^* a_j^* h_i h_j]$. The final values of the U_{ij} parameters ($\times 10^3$) are:

Atom	U_{11}	U_{22}	U_{33}	U_{12}	U_{13}	U_{23}
Ru	43.9(2)	39.7(2)	42.5(2)	1.9(1)	5.2(1)	-2.9(1)
Si	43.5(5)	41.8(5)	43.1(4)	1.3(4)	6.7(4)	-3.0(4)
C(3)	41(2)	42(2)	51(2)	4(1)	5(1)	0(1)
C(4)	45(2)	44(2)	50(2)	1(1)	-2(1)	-3(1)
C(5)	49(2)	45(2)	42(2)	7(1)	3(1)	3(1)
C(6)	45(2)	40(2)	44(2)	2(1)	7(1)	1(1)
C(13)	66(3)	111(4)	82(3)	4(3)	24(2)	41(3)
C(14)	46(2)	80(3)	143(5)	-8(2)	4(3)	43(3)
C(24)	58(2)	70(3)	127(4)	-11(2)	27(3)	14(3)
C(25)	55(2)	68(3)	106(4)	-12(2)	5(2)	-14(3)
C(100)	64(2)	47(2)	58(2)	5(2)	4(2)	-4(2)
C(101)	60(2)	57(2)	54(2)	5(2)	10(2)	-5(2)
C(102)	52(2)	51(2)	56(2)	2(2)	10(2)	-3(2)
O(1)	105(3)	49(2)	81(2)	-7(2)	1(2)	-13(1)
O(2)	73(2)	100(3)	73(2)	12(2)	30(2)	-8(2)
O(3)	81(2)	79(2)	58(2)	16(2)	4(1)	14(1)

TABLE 3.2 (Cont'd)

(b)   Calculated fractional co-ordinates $(\times 10^3)$ and assumed isotropic vibrational parameters for hydrogen atoms; each hydrogen atom is numbered according to the carbon atom to which it is attached.

Atom	x	y	z	$U \times 10^3$ $\mathring{A}^2$
H(2a)	182	0	33	69
H(2b)	204	-155	18	69
H(2c)	250	0	0	69
H(4)	383	108	199	58
H(5)	279	-67	222	54
H(12)	382	83	32	72
H(13)	479	251	-1	95
H(14)	544	460	49	91
H(15)	523	500	131	88
H(16)	430	335	166	74
H(22)	166	-139	227	73
H(23)	59	-313	237	89
H(24)	-4	-459	168	91
H(25)	39	-442	91	84
H(26)	147	-277	80	69

TABLE 3.3

Selected interatomic distances (Å) and angles ($^\circ$) in (I)

(a) **Bond lengths**

Si-C(1)	1.861(5)	H(1)-C(1)	0.92(6)
Si-C(2)	1.872(5)	H(2)-C(1)	0.95(3)
Mean	1.867(6)	H(3)-C(2)	0.89(7)
Si-C(3)	1.878(3)	H(4)-C(2)	0.99(5)
		Mean	0.95(2)
C(3)-C(4)	1.345(4)		
C(3)-C(5)	1.478(4)	H(5)-C(4)	0.90(3)
C(4)-C(4')*	1.466(6)		
		H(6)-C(6)	0.90(4)
C(5)-C(6)	1.380(5)	H(7)-C(7)	0.95(4)
C(6)-C(7)	1.400(4)	H(8)-C(8)	1.05(3)
C(7)-C(8)	1.367(5)	H(9)-C(9)	0.83(5)
C(8)-C(9)	1.353(6)	H(10)-C(10)	0.90(4)
C(9)-C(10)	1.391(5)	Mean	0.95(4)
C(10)-C(5)	1.391(4)		
Mean	1.384(7)		

* Co-ordinates of primed atoms are derived from those of the corresponding atoms in Table 3.1 by the transformation ($\bar{x}$, y, z).

TABLE 3.3 (Cont'd)

(b) Interbond angles

C(1)-Si-C(2)	112.5(3)	C(3)-C(5)-C(6)	120.7(3)
C(3)-Si-C(3')	92.5(2)	C(3)-C(5)-C(10)	121.9(3)
		Mean	121.3(6)
C(1)-Si-C(3)	113.3(1)		
C(2)-Si-C(3)	111.9(1)	C(5)-C(6)-C(7)	121.4(4)
Mean	112.6(7)	C(6)-C(7)-C(8)	119.9(4)
		C(7)-C(8)-C(9)	119.3(3)
Si-C(1)-H(1)	102(3)	C(8)-C(9)-C(10)	121.5(3)
Si-C(1)-H(2)	108(2)	C(9)-C(10)-C(5)	120.5(3)
Si-C(2)-H(3)	122(5)	C(10)-C(5)-C(6)	117.3(3)
Si-C(2)-H(4)	116(3)	Mean	119.9(1)
Mean	110(3)		
		H(6)-C(6)-C(5)	124(2)
Si-C(3)-C(4)	106.0(2)	H(6)-C(6)-C(7)	115(2)
Si-C(3)-C(5)	128.9(2)	H(7)-C(7)-C(6)	116(2)
		H(7)-C(7)-C(8)	124(2)
H(1)-C(1)-H(2)	115(3)	H(8)-C(8)-C(7)	117(2)
H(2)-C(1)-H(2')	108(3)	H(8)-C(8)-C(9)	124(2)
H(3)-C(2)-H(4)	92(3)	H(9)-C(9)-C(8)	123(3)
H(4)-C(2)-H(4')	115(4)	H(9)-C(9)-C(10)	116(3)
Mean	107(6)	H(10)-C(10)-C(5)	117(2)
		H(10)-C(10)-C(9)	122(2)
C(4)-C(3)-C(5)	125.0(2)	Mean	120(1)
C(3)-C(4)-C(4')	117.6(2)		
C(3)-C(4)-H(5)	124(2)		
C(4')-C(4)-H(5)	118(2)		

TABLE 3.3 (Cont'd)

(c) Intramolecular non-bonded distances within the limits of the van der Waals radii ($\overset{o}{A}$): C($\underline{sp}$), 1.7; C($\underline{sp}^2$), 1.85; C($\underline{sp}^3$), 2.0; H, 1.2; O, 1.4; Si, 1.95.

(i) Phenyl⋯Butadiene

H(6)⋯C(3)	2.69	C(5)⋯H(5)	2.74
H(10)⋯C(3)	2.62	C(10)⋯H(5)	2.80
H(10)⋯C(4)	2.69	C(10)⋯C(4)	3.00
H(10)⋯H(5)	2.26		

(ii) Phenyl⋯Methyl

H(6)⋯C(2)	3.19	C(6)⋯C(2)	3.80

(iii) Phenyl⋯Silicon

H(6)⋯Si	3.05	C(6)⋯Si	3.38

TABLE 3.3 (Cont'd)

(d) Intermolecular non-bonded distances within the limits of the contact radii:

$C(2)\cdots C(4^{I})^{*}$	3.68	$C(5)\cdots H(7^{III})$	3.03
$C(4)\cdots H(3^{II})$	3.02	$C(8)\cdots H(5^{IV})$	2.93

* The Roman numeral superscripts refer to the following co-ordinate transformations:

I	x, y, 1 + z	III	-1/2 -x, -y, -1/2 + z
II	x, y, -1 + z	IV	-1/2 -x, 1 -y, 1/2 + z

TABLE 3.4

Selected interatomic distances ($\overset{o}{A}$) and angles (^{o}) in (II)

(a) Bond lengths

Ru-C(3)	2.293(3)	C(3)-C(4)	1.447(5)
Ru-C(6)	2.294(3)	C(5)-C(6)	1.448(4)
Mean	2.294(2)	Mean	1.448(3)
Ru-C(4)	2.187(3)		
Ru-C(5)	2.187(3)	C(4)-C(5)	1.407(5)
Mean	2.187(2)		
		C(3)-C(11)	1.475(5)
Ru-C(100)	1.906(4)	C(6)-C(21)	1.477(5)
Ru-C(101)	1.921(4)	Mean	1.476(4)
Ru-C(102)	1.941(4)		
Mean	1.923(10)	C(11)-C(12)	1.385(6)
		C(12)-C(13)	1.396(7)
C(100)-O(1)	1.136(5)	C(13)-C(14)	1.380(8)
C(101)-O(2)	1.128(6)	C(14)-C(15)	1.355(8)
C(102)-O(3)	1.134(5)	C(15)-C(16)	1.371(7)
Mean	1.133(3)	C(16)-C(11)	1.415(6)
		Mean	1.387(8)
Si-C(1)	1.885(5)	C(21)-C(22)	1.394(6)
Si-C(2)	1.868(4)	C(22)-C(23)	1.402(7)
Mean	1.875(8)	C(23)-C(24)	1.374(8)
		C(24)-C(25)	1.367(8)
Si-C(3)	1.883(3)	C(25)-C(26)	1.391(6)
Si-C(6)	1.876(3)	C(26)-C(21)	1.394(5)
Mean	1.880(4)	Mean	1.390(5)

TABLE 3.4 (Cont'd)

(b) Interbond angles

Ru-C(100)-O(1)	178.7(4)	C(3)-C(4)-C(5)	114.8(3)
Ru-C(101)-O(2)	178.7(4)	C(4)-C(5)-C(6)	114.0(3)
Ru-C(102)-O(3)	175.2(4)	Mean	114.4(4)
Mean	177.5(12)		
		C(4)-C(3)-C(11)	122.3(3)
C(100)-Ru-C(101)	90.0(2)	C(5)-C(6)-C(21)	121.1(3)
C(100)-Ru-C(102)	94.7(2)	Mean	121.7(6)
C(101)-Ru-C(102)	96.9(2)		
Mean	94(2)	C(3)-C(11)-C(12)	120.5(3)
		C(3)-C(11)-C(16)	122.1(3)
C(1)-Si-C(2)	108.4(2)	C(6)-C(21)-C(22)	122.0(3)
C(3)-Si-C(6)	87.7(1)	C(6)-C(21)-C(26)	120.7(3)
		Mean	121.3(4)
C(1)-Si-C(3)	111.9(2)		
C(1)-Si-C(6)	114.5(2)	C(11)-C(12)-C(13)	120.3(4)
C(2)-Si-C(3)	117.0(2)	C(12)-C(13)-C(14)	119.9(5)
C(2)-Si-C(6)	116.3(2)	C(13)-C(14)-C(15)	121.0(5)
Mean	114.9(11)	C(14)-C(15)-C(16)	119.5(4)
		C(15)-C(16)-C(11)	121.8(4)
Si-C(3)-C(4)	105.3(2)	C(16)-C(11)-C(12)	117.4(4)
Si-C(6)-C(5)	106.0(2)	Mean	119.9(6)
Mean	105.7(4)	C(21)-C(22)-C(23)	120.9(4)
		C(22)-C(23)-C(24)	120.2(5)
Si-C(3)-C(11)	127.8(2)	C(23)-C(24)-C(25)	119.9(5)
Si-C(6)-C(21)	128.5(2)	C(24)-C(25)-C(26)	120.3(4)
Mean	128.2(4)	C(25)-C(26)-C(21)	121.4(4)
		C(26)-C(21)-C(22)	117.4(3)
		Mean	119.7(7)

TABLE 3.4 (Cont'd)

(c) <u>Intramolecular non-bonded distances</u>

Ru···Si	2.992	C(2)···C(26)	3.66
Si···C(12)	3.34	C(2)···C(102)	3.22
Si···C(26)	3.37	C(4)···C(16)	3.04
Si···C(102)	3.44	C(5)···C(22)	2.99
C(1)···C(4)	3.66	C(16)···C(100)	3.43
C(1)···C(5)	3.69	C(21)···C(101)	3.44
C(2)···C(12)	3.71	C(22)···C(101)	3.37

<u>TABLE 3.4 (Cont'd)</u>

(d) Intermolecular non-bonded distances within the limits of the
van der Waals radii:

$C(1)\cdots C(2^{I})$*	3.86	$C(1)\cdots C(16^{II})$	3.84
$C(1)\cdots C(15^{II})$	3.69	$C(14)\cdots C(102^{III})$	3.54

* The Roman numeral superscripts refer to the following co-ordinate
transformations:

I $1/2 - x, - 1/2 + y, - z$ III $1/2 + x, 1/2 - y, z$

II $x, - 1 + y, z$

TABLE 3.5

Equations of least-squares planes of (I) in which X, Y, Z refer

to orthogonal co-ordinates in $\overset{o}{A}$. Deviations of selected atoms

from the plane are given in square brackets.

Plane 1: C(3), C(3'), C(4), C(4')

$$0.589Y + 0.809Z -2.001 = 0$$

[Si 0.083, C(3), C(3'), C(4), C(4') 0, C(5) -0.064, C(6) 0.162,

H(5) -0.055]

Plane 2: Si, C(1), C(2)

$$X = 0$$

Plane 3: Si, C(3), C(3')

$$0.639Y + 0.769Z -2.085 = 0$$

[C(3) 0.017, C(4) -0.192, C(5) -0.003, C(6) 0.003, C(7) 0.000

C(8) 0.000, C(9) -0.003, C(10) 0.005, H(6) -0.028, H(7) -0.097

H(8) 0.071, (9) 0.027, H(10) 0.089]

Angles (^{o}) between planes:

(1) - (2)	90*	(1) - (4)	13.7
(1) - (3)	3.7		

* By symmetry

TABLE 3.6

Least-squares-planes of (II)

Plane 1: C(3) - (6)

$$0.561X - 0.824Y - 0.080Z - 2.361 = 0$$

[Ru -1.848, Si 0.722, C(3) -0.001, C(4) 0.003, C(5) -0.003,

C(6) 0.001, C(11) -0.028, C(16) -0.518, C(21) -0.040, C(26) 0.337]

Plane 2: Si, C(1), C(2)

$$0.772X + 0.586Y - 0.246Z - 2.733 = 0$$

Plane 3: Si, C(3), C(6)

$$0.609X - 0.656Y + 0.446Z - 4.497 = 0$$

Plane 4: C(11) - (16)

$$0.661X - 0.684Y + 0.308Z - 4.313 = 0$$

[C(3) 0.009, C(4) 0.515, C(11) -0.008, C(12) 0.009, C(13) -0.003,

C(14) -0.006, C(15) 0.001, C(16) 0.007]

Plane 5: C(21) - (26)

$$0.574X - 0.784Y + 0.238Z - 3.610 = 0$$

[C(5) 0.410, C(6) 0.027, C(21) 0.000, C(22) -0.006, C(23) 0.010,

C(24) 0.000, C(25) -0.008, C(26) 0.006]

Angles (°) between planes:

(1) - (2)	91.7	(1) - (4)	24.5
(1) - (3)	32.2	(1) - (5)	18.4

Figure 3.3: A view of the silacyclopentadiene

molecule (I). Thermal ellipsoids

enclose 50% of probability.

Hydrogen atoms are shown with arbitrary

radii for clarity.
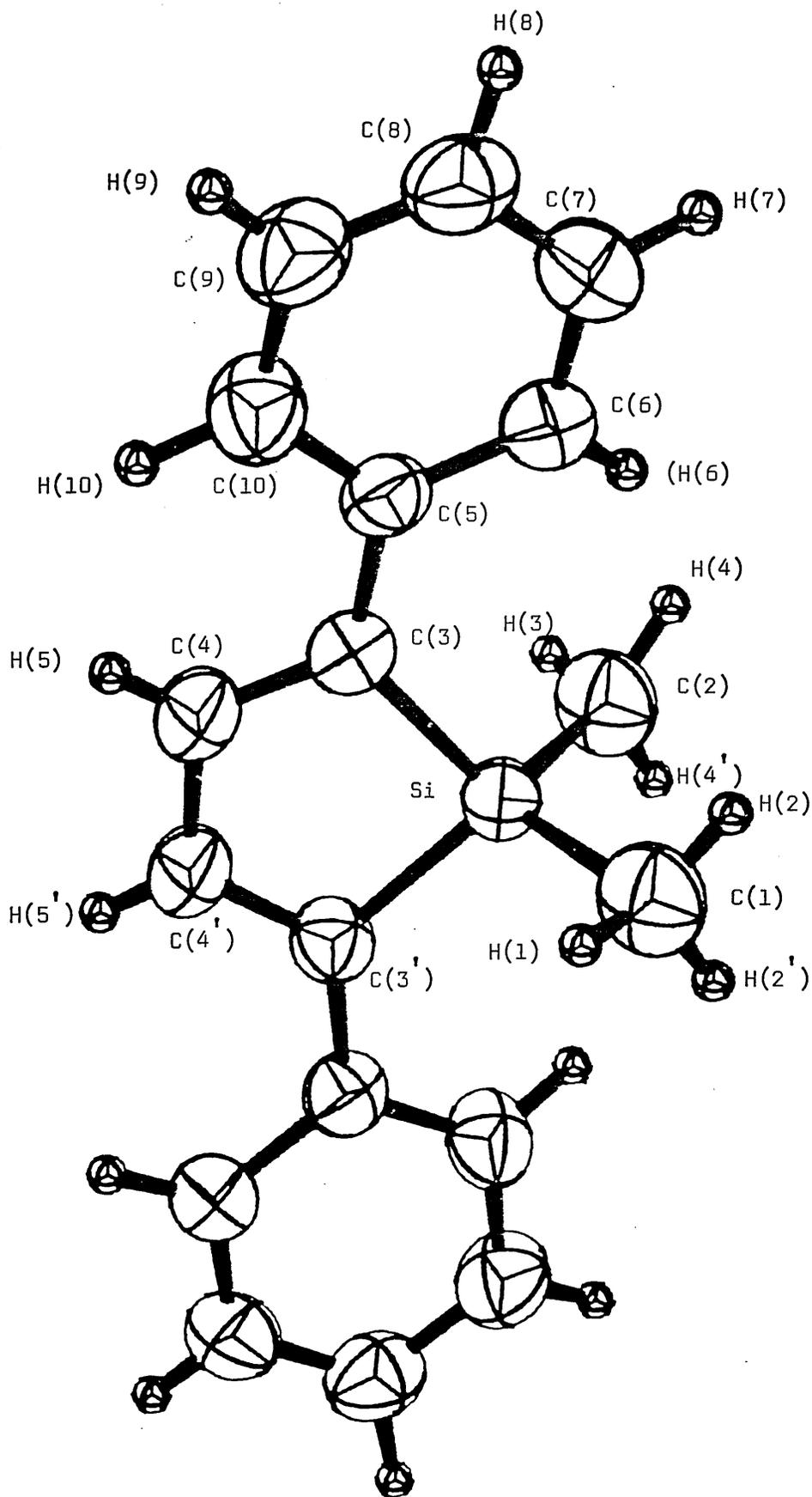
Figure 3.4: A view of the (silacyclopentadiene) -

tricarbonylruthenium molecule (II);

thermal ellipsoids enclose 50% of

probability. Hydrogen atoms are

not shown.
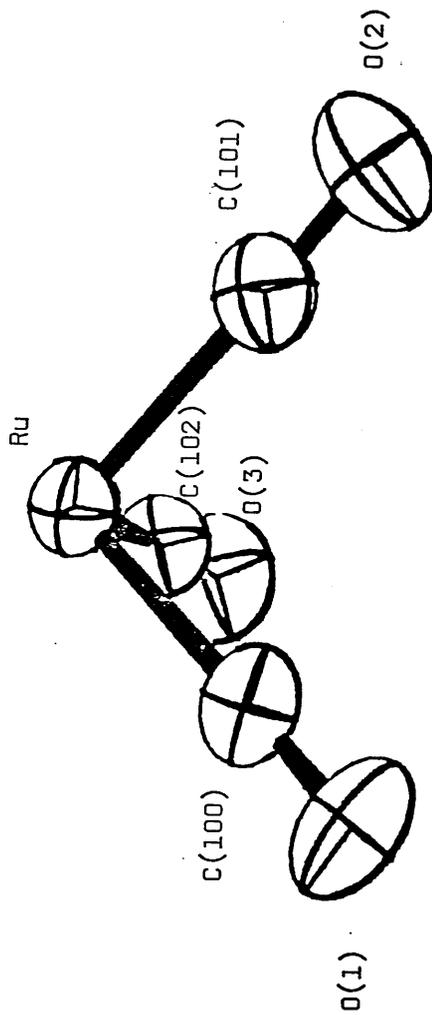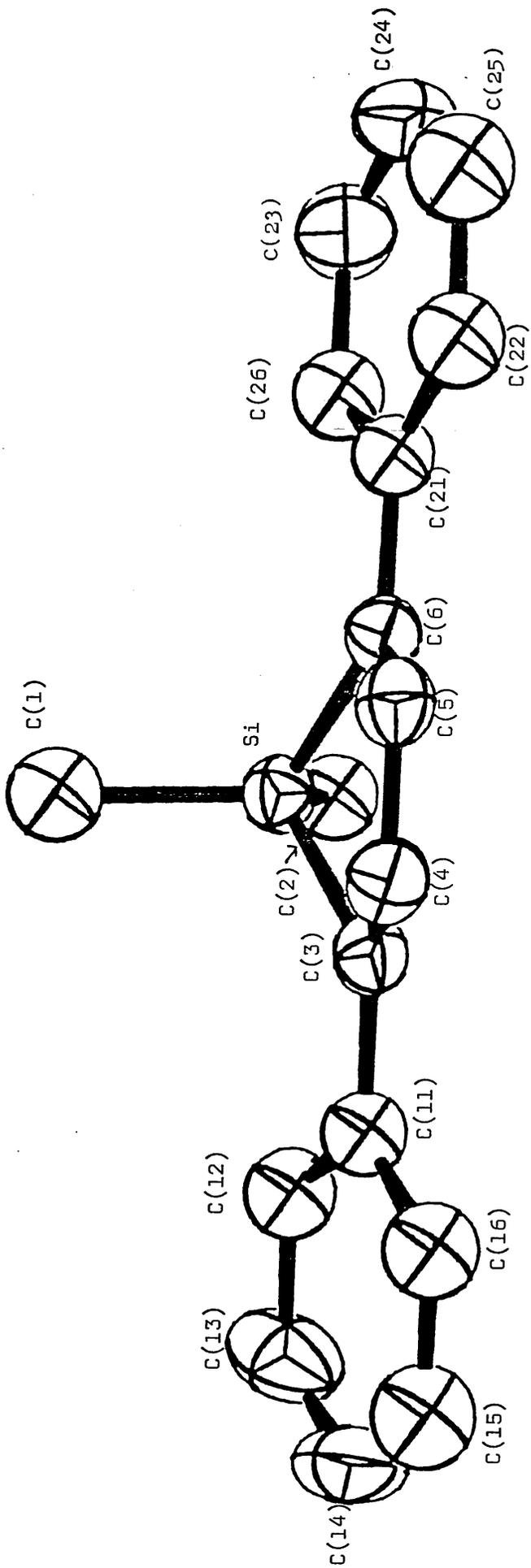
Figure 3.5: A view of the molecular structure

of (II) in projection onto the butadiene

plane.

C(11)

O(1)

C(100)

C(3)

C(4)

C(102)

O(3)

Ru

Si

C(5)

C(6)

C(101)

O(2)

C(21)
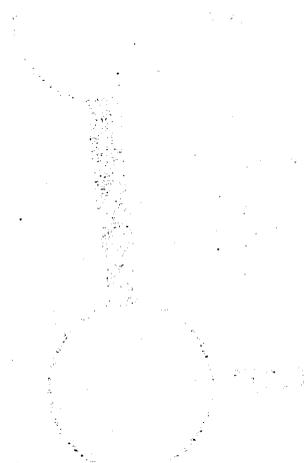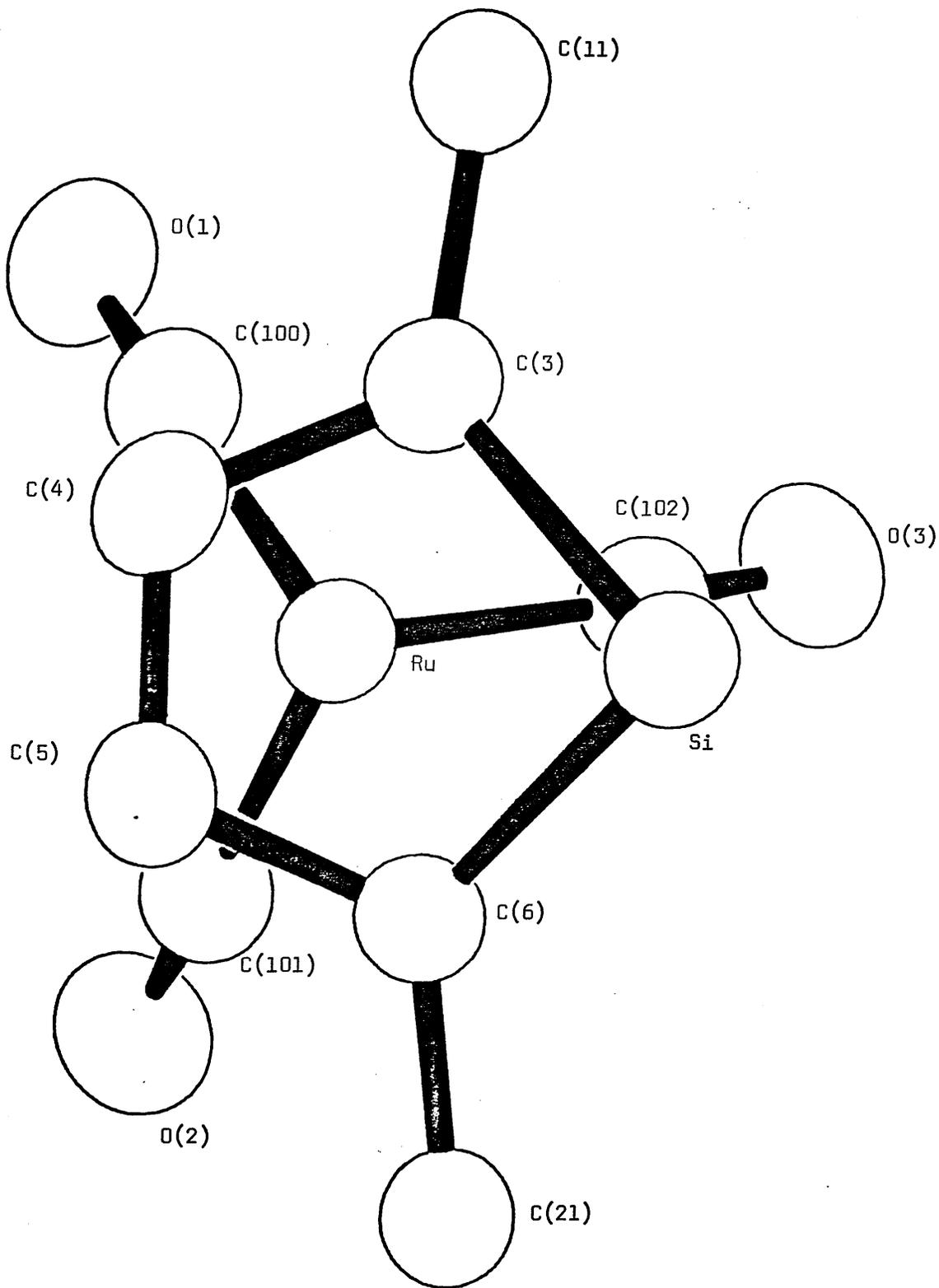
CHAPTER FOUR

The Crystal and Molecular Structures of

the Isocyanide Complexes

trans-$[M(CNMe)_2(Ph_2PCH_2CH_2PPh_2)_2]$(M=Mo and W)
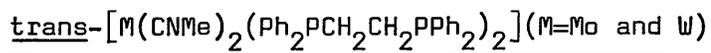
4.1. INTRODUCTION

It has been observed that the co-ordination of isocyanides to transition metals in their intermediate or higher oxidation states results in an increase of the $\nu(NC)$ stretching frequency relative to that of the free ligand.[1] This may be attributed to the use, in bonding to the metal, of the essentially lone pair orbital on the donor carbon atom, thereby enhancing the $C(\underline{sp})-N$ σ-bonding. In some cases nucleophilic attack at the donor atom is facilitated.[1] However, low-valent metals produce a decrease of $\nu(NC)$ relative to that of the free isocyanide. This arises from backdonation to the isocyanide π^* orbitals.[2] Interestingly, there is apparently no report of electrophilic attack at the ligating isocyanide in such cases, possibly because in the majority of systems studied to date the iso-cyanide competes with carbon monoxide or isocyanide co-ligands for metal d_π electrons.[3]

A series of complexes trans-$[M(CNR)_2(dppe)_2]$ (M = Mo or W; R = Me, Bu^t, Ph, C_6H_4Me-4, C_6H_4Cl-4, $C_6H_3Cl_2-2$, 6, or C_6H_4OMe-4; dppe = $Ph_2PCH_2CH_2PPh_2$) has been prepared by Chatt and co-workers.[4] These derivatives contain metal sites which are such powerful electron donors that they activate dinitrogen.[5] In these isocyanide complexes the build-up of charge on the carbon-donor ligand gives it some "carbene-like" character, engendering ready electrophilic attack at the nitrogen atom and producing the greatest observed decrease in $\nu(NC)$ for terminal isocyanide ligands in uncharged complexes.[4] Thus, for example, $\nu(NC)$ for the complex trans-$[Mo(CNMe)_2(dppe)_2]$ is 1886 cm^{-1} in tetrahydrofuran solution, which is 279 cm^{-1} smaller than the corresponding value for free methyl isocyanide. The corres-

ponding frequencies of the analogous tungsten derivative are 1850

and 315 cm^{-1}, respectively. The ν(NC) frequencies throughout the

series of bis-isocyanide complexes are very low relative to those

of the unbound isocyanides and close to the range (ca. 1750 - 1800

cm^{-1}) of bridging isocyanides which display[6] CNC interbond angles

of ca. 125°.

In order to obtain structural information on the metal-isocyanide

bonding in these systems accurate X-ray analyses of two representative

complexes trans-$[M(CNMe)_2(dppe)_2]$ (M = Mo and W) were undertaken.

A preliminary account of this work has been published.[4]

A full description of the analysis of the molybdenum derivative, (I),

is now given. For comparison, brief details of the tungsten analogue

(II) are also presented.

4.2. EXPERIMENTAL

Crystal Data - Complex (I). $C_{56}H_{54}N_2P_4Mo$, M = 974.9. Triclinic, a = 10.747, b = 10.555, c = 12.565 Å, α = 72.37, β = 87.78, γ = 61.80°, T = 20°C, U = 1187.9 Å^3, D_c = 1.363 gm cm^{-3}, Z = 1, F(000) = 506. Mo - K$_\alpha$ radiation, λ = 0.71069 Å, μ(Mo - K$_\alpha$) = 4.5 cm^{-1}. Space group P$\bar{1}$.

Complex (II). $C_{56}H_{54}N_2P_4W$, M = 1062.8. Triclinic, a = 10.731, b = 10.535, c = 12.552 Å, α = 72.38, β = 87.83, γ = 61.98°, T = 20°C, U = 1184.6 Å^3, D_c = 1.490 gm cm^{-3}, Z = 1, F(000) = 538. Mo - K$_\alpha$ radiation, μ (Mo - K$_\alpha$) = 16.7 cm^{-1}. Space group P$\bar{1}$.

Crystallographic Measurements - Complex (I). The crystals are red air-stable plates. The specimen used in the analysis displayed all members of the {100}, {001} and {221} forms, and the perpendicular distances between parallel faces were 0.16, 0.06 and 0.30 mm.

The crystal system and the dimensions of a reduced triclinic cell were obtained by X-ray photography. The unit-cell dimensions were later adjusted by a least-squares treatment of the setting angles of 11 reflexions measured on a Hilger and Watts' Y290 diffractometer controlled by a PDP8 computer.[7] The space group P$\bar{1}$ led to a satisfactory structural analysis which included the location of hydrogen atoms.

Complex(II). The crystals are deep-red air-stable plates. The specimen used in the structural measurements had dimensions ca. 0.21 x 0.30 x 0.45 mm.

The crystal system and unit-cell dimensions were derived by X-ray

photography. Final values of the cell dimensions were obtained by a least-squares method.[7] The crystals are nearly isomorphous with those of the molybdenum analogue.[4]

Intensity Measurements - Complex (I). The intensities of all independent reflexions for which $\theta(Mo - K_\alpha) \leq 28°$ were measured on the Y290 diffractometer with the use of graphite-monochromated molybdenum radiation and a pulse-height analyser. A symmetrical $\theta - 2\theta$ scan was employed, with a scan step in θ of $0.02°$ and a counting time per step of 2.5 s. Each reflexion was scanned through a 2θ range of $1.2°$ and the local background was counted for 15 s at each end of the scan range. The intensities of three strong reflexions, measured periodically throughout the experiment, showed only random fluctuations of up to $\pm$ 5% of their mean values.

The integrated intensities, I, and their standard deviations, $\sigma(I)$, were derived from standard relationships described earlier in the text (q 0.04).[8] They were corrected for Lorentz, polarisation and counting-loss effects. No correction for the effects of absorption was applied, since a test calculation with a Gaussian integration grid[9] of 14 x 14 x 14 points indicated that the transmission factors were in the narrow range 0.96 - 0.98.

Of 3816 reflexions measured only 3620 for which $I \geq 3\sigma(I)$ were used in subsequent calculations.

Complex (II). The intensities of all independent reflexions for which $\theta(Mo - K_\alpha) \leq 28°$ were measured on the Y290 diffractometer in a manner comparable to that adopted for complex (I).

The integrated intensities, I, and their standard deviations, $\sigma(I)$,

were derived using standard relationships (q 0.04).[8] They were

corrected for Lorentz and polarisation effects.

Of 5660 reflexions measured only 5657 for which $I \geq 3\sigma(I)$ were used

in subsequent calculations.

Structure Analysis - Complex (I). The position of the molybdenum

atom at the origin of the unit cell, and the co-ordinates of each

phosphorus atom were deduced from a Patterson synthesis. The remain-

ing non-hydrogen atoms were located in subsequent difference syntheses.

The structure was refined by the method of full-matrix least-squares.

The function minimised was $\sum w \Delta^2$, where $w = 1/\sigma^2(F_o)$ and $\Delta =$

$|F_o| - |F_c|$. Atomic scattering factors were taken from ref.10,

except those for hydrogen atoms.[11] Allowance was made for the

anomalous scattering of the molybdenum and phosphorus atoms using

values of $\Delta f'$ and $\Delta f''$ from ref.12.

A structure factor calculation based on the molybdenum and phosphorus

atoms with isotropic temperature factors gave R 0.30. When the

remaining non-hydrogen atoms were included R decreased to 0.092.

Anisotropic temperature factors were then assigned to the molybdenum

and phosphorus atoms, and to the carbon and nitrogen atoms of the

isocyanide ligand, giving rise to R 0.059 and R' 0.068. A difference

synthesis was then calculated using only the 1075 reflexions for which

$\sin\theta/\lambda \leq 0.40$. This indicated the position of every hydrogen atom

except that attached to the phenyl carbon atom C(16); the peak

heights of these atoms ranged from 0.60 to 0.94 $e\text{Å}^{-3}$. The methyl

geometry was rather ill-determined: ranges were l(C-H) 0.96 -

1.35Å, $\angle$N-C(Me)-H 94.8 - $112.3°$, and $\angle$H-C(Me)-H 101.7 - $121.6°$;

the value of 1.35 Å was associated with the rather diffuse

peak of the atom H(4a).   The phenyl and methylene geometries were

idealised and the scattering of all the hydrogen atoms was included

in the subsequent structure factor calculations but the positional

and assumed vibrational parameters of these atoms were not varied.

The refinement converged at R 0.048 and R' 0.058. In the final

cycle of least-squares all parameters shifted by $< 0.2 \, \sigma$.   In

addition, the standard deviation of an observation of unit weight

was 1.9, suggesting that the accuracy of the data was slightly over-

estimated.   However, the absence of significant trends when the mean

values of $w\Delta^2$ were analysed as a function of $|F_o|$ or $\sin\theta$ indicated

that the relative weights were satisfactory. In the final difference

synthesis the extreme function values were 0.8 and $-0.5 \, e\overset{\circ}{A}^{-3}$.   The

positive peak was situated between the atoms C(33) and C(34), and

the negative peak was close to the atom P(2). The minimum peak

height for a carbon atom in the final electron density synthesis was

$4.0 \, e\overset{\circ}{A}^{-3}$.

Observed and calculated structure amplitudes are listed in the Appendix

(pp. 166-189). Atomic parameters are given in Table 4.1 and a selection

of derived functions is presented in Tables 4.2 and 4.3. The atomic

numbering scheme is indicated and a view of the molecular structure

is shown in Figure 4.1.

The computer programs employed have been described previously.[13]

Complex (II).   The structural parameters[4] of the molybdenum analogue

(I) were used in a trial solution and this led to a satisfactory

analysis.

The model was refined by the least-squares method ($w = 1/\sigma^2(F_o)$).

Atomic scattering factors were taken from refs.10 and 11. Correction

for the anomalous scattering of the tungsten and phosphorus atoms was applied.[12]

Refinement of the scale factor and of the positional and isotropic thermal parameters of the non-hydrogen atoms led to R 0.085 and R' 0.094. When anisotropic temperature factors were assigned to the tungsten and phosphorus atoms R and R' decreased significantly to 0.045 and 0.061, respectively. In the final cycle of refinement the shifts in the parameters were close to 1σ except those of the tungsten thermal parameters $(1 - 5\sigma)$. The analysis was terminated at this stage.

A selection of bond lengths and interbond angles is presented in Table 4.4. The atomic labelling scheme is that of Fig. 4.1 (with molybdenum replaced by tungsten).

4.3. RESULTS AND DISCUSSION

(a) Complex (I)

The crystals are composed of discrete monomeric trans $-[Mo(CNMe)_2-$ $(dppe)_2]$ molecules. The intermolecular distances (Table 4.2(e)) are in the range expected for normal van der Waals contacts.[14]

The Metal Co-ordination - As expected, the molybdenum co-ordination is distorted octahedral. The isocyanide ligands occupy axial trans positions, and the phosphorus atoms and the molybdenum atom define an equatorial plane. Moreover, exact C_i crystallographic symmetry is imposed on each molecule as a space group requirement.

The Mo-C(donor) vector is not strictly normal to the equatorial plane but is inclined to it at an angle of 82.4^o. The metal co-ordination is, thus, strikingly similar to that observed in the analogous dinitrogen complex trans $-[Mo(N_2)_2(dppe)_2]$ (III).[15] The distortions of the P-Mo-CNMe angles appear to arise from steric effects. Thus, the intramolecular non-bonded contacts $[C(3)... C(16^*)$ 3.44, $C(3)... C(26)$ 3.32, $C(3)... C(36)$ 3.38, and $C(3)... C(41^*)$ 3.40 $\overset{o}{A}]$ (Table 4.2(d)) involving the carbon-donor and the phenyl carbon atoms suggest that the molecules of (I) are subject to some steric strain.

The Diphosphine Geometry - The molybdenum-phosphorus Mo-P(1) and Mo-P(2) bonded distances, respectively 2.442(1) and 2.457(2) $\overset{o}{A}$, are comparable to the values found in other arylphosphine or diphosphine complexes of molybdenum(0).[16] Moreover, they are in good agreement with the corresponding bond lengths [2.445(1) and 2.462(1) $\overset{o}{A}$] in the dinitrogen complex (III).[15] The highly significant difference of ca.

0.02 $\overset{o}{A}$ in the lengths of the cis-Mo-P bonds in each of these

complexes may be attributed to intramolecular steric overcrowding

(vide supra). These values are all significantly shorter than the

estimated Mo(0)-P single bond length of 2.71 $\overset{o}{A}$ derived from the

covalent radii of molybdenum[17] and phosphorus[14] atoms (1.61 and 1.10 $\overset{o}{A}$,

respectively). This contraction has been attributed either to

significant Mo-P d_π - d_π backbonding[16a] or to distortions from

exact d^2sp^3 hybridisation.[18]

Steric strain is also apparent in highly significant differences in

the lengths of equivalent P-C bonds in both (I) and (III). Thus, in

(I) the P-C(sp^3) distances differ by 0.026(8) $\overset{o}{A}$ (Δ/σ = 3.25).

Moreover, the P-C (sp^2) bond lengths range from 1.841(3) to

1.860(5) $\overset{o}{A}$. The same pattern of bond length variation is also seen

in (III), the individual distances being in excellent agreement with

those of (I). Despite these distortions the mean distances are

normal: those of (I) are P-C(sp^2) 1.847(4) $\overset{o}{A}$ and P-C(sp^3) 1.869(13) $\overset{o}{A}$.[19]

In addition, the CH_2-CH_2 bond length of 1.508(7) $\overset{o}{A}$ is close to the

accepted value of 1.54 $\overset{o}{A}$ for a C(sp^3)-C(sp^3) distance.[20]

The P(1)-Mo-P(2) interbond angle involving mutually-cis phosphorus

atoms is only 79.6(1)° [cf. 79.4(2)° in (III)] and this may be

attributed to a constraint of chelation. Other valency angles at the

phosphorus atoms also display significant distortions. Thus, the

Mo-P-C(Ph) interbond angles [range 117.0(2) - 124.7(2)°] are

considerably greater than the ideal tetrahedral value of 109°28'.

Furthermore, the C-P-C angles [range 96.7(2) - 103.0(2)°] are

much less than the latter value. This pattern of distortion is commonly

observed in transition metal complexes of arylphosphines.[16a] However,

the magnitude cf the effect in the title complex (I) is somewhat

greater than is typically observed, providing further evidence of

steric strain in the molecules of (I). In addition, the Mo-P-C(sp^3)

and P-C(sp^3)-C(sp^3) angles are regular, having mean values of 109(2)

and 110(1)^0, respectively; that there are no appreciable distortions

of these angles may be attributed to constraints imposed by ring

formation.

The five-membered chelate ring is puckered, as expected,[21] with the

methylene carbon atoms C(1) and C(2) displaced on the same side of

the equatorial plane by 0.84 and 0.21 Å, respectively. The ring

conformation is, thus, unsymmetrical: torsion angles about the Mo-P

bonds are P(1)-Mo-P(2)-C(2) -6.4(2)^0 and P(2)-Mo-P(1)-C(1) 28.6(2)^0,

and the P-CH$_2$-CH$_2$-P dihedral angle is -47.1(6)^0. These values are

normal, being in the range observed in a variety of metal-diphosphine

systems.[22]

The Molybdenum-Isocyanide Bonding - The molybdenum-carbon Mo-C(3)

bond length of 2.095(4) Å is appreciably shorter than the estimated

Mo-C(sp) single-bond length[23] [2.32 Å] indicating that there is

considerable Mo(4d)$\longrightarrow$(C≡N) π* backdonation. Indeed, it is only

slightly longer than the Mo-CO(trans to CO) bonds in [Mo(CO)$_6$]

(2.06 Å)[24] and [Mo(CO)$_4$(Ph$_2$PCH$_2$PPh$_2$)] (2.04 Å).[25] This trend is also

displayed in the complex [Mo(π-C$_5$H$_5$)I(CO)$_2$(CNPh)] where the

Mo-CO and Mo-CNR bond lengths differ by about 0.05 Å.[23] The

bond length data, therefore, imply that isocyanide is almost as good

a π-acceptor as carbon monoxide, as has been noted in other systems.[23]

The most interesting feature of the molecular structure is the geo-

metry of the isocyanide ligand. The Mo-C-N angle of 176.2(5)^0 is

close to 180^0, as expected. However, the C(sp)-N-C(sp^3) angle

is only $155.1(5)^O$, much smaller than the approximately 180° usually

found in terminal isocyanide derivatives.[3] Prior to the present

work,the only cases of considerable bending at the nitrogen atom were

those observed in the derivatives cis -$[Fe(CN)_2(CNMe)_4].4CHCl_3$

and cis -$[PtCl_2(CNPh)(PEt_3)]$. [26, 27] C-N-C angles of 156(7) and

$165.5(30)^O$, respectively, were noted in these complexes. However,

the crystal used in the X-ray analysis of the iron compound had a

large proportion of disordered chloroform solvate: the distortion of

the isocyanide group could result from crystal packing effects.

Moreover, the pronounced non-linearity observed in the above platinum

(II) - isocyanide complex does not appear to be a general feature of

such systems since it is not paralleled in the geometries of cis—

$[PtCl_2(CNEt)(PEt_2Ph)]$ and cis-$[PtCl_2(CNPh)_2]$.[28]   However, a very

pronounced bending has been reported recently for the derivative

$[Ru(CNBu^t)_4(PPh_3)]$:   the C-N-C angle of $130(2)^O$ is believed to be of

electronic rather than steric origin.[29]

Although relatively sophisticated molecular orbital treatments of

isocyanide systems[30] have been carried out, it is, perhaps, instruc-

tive to consider the valence bond formulation.[14] Thus, in valence

bond terms the electronic structure can be represented as an appro-

priately weighted combination of the forms (A) and (B), with

$$(A) \quad \overset{-}{M} - C \equiv \overset{+}{N}R \quad \longleftrightarrow \quad M = C = \overset{..}{N}_{\diagdown R} \quad (B)$$

a major contribution from structure (B) in cases of large bending at

the nitrogen atom. If form (B) is predominant in a particular

molecule, a short M-C bond and a long C-N bond would be expected.

A relatively short   Mo-C(donor) distance is, indeed, found in (I)

(as noted above). However, the C(sp)-N   distance of $1.094(7)$ Å

is similar to that in methyl isocyanide itself $[1.166 \text{ Å}]$.[31] Further-
more, the corresponding values in other complexes with terminal iso-
cyanide ligands are also close to those found in the free isocyanides.[3]
This is, perhaps, not surprising since in transition metal complexes
containing the isoelectronic carbonyl ligand the C-O bond lengths
are insensitive to bond order changes in the region 2 - 3.[32] In
addition, the N-C($\underline{sp}^3$) distance, 1.449(10) Å, is normal.[20]

Although a steric mechanism could produce an unusually large bending
at the isocyanide nitrogen atom, an electronic effect is strongly
indicated by the following observations:

(a) There are no exceptionally short intramolecular contacts involving
the methyl carbon atom either in its observed position or that calcu-
lated assuming linearity of the C($\underline{sp}$)-N-C($\underline{sp}^3$) fragment.

(b) Throughout the series of $\underline{bis}$-isocyanide complexes $\underline{trans}$ —
$[\text{M(CNR)}_2\text{(dppe)}_2]$ the lowering of the ν(NC) stretching frequency in
the spectra of the solids, relative to that found for the free
isocyanide, is very large [Mo, 303-221 cm^{-1}; W, 336-230 cm^{-1}] and
is not altered significantly when the solid is dissolved in tetra —
hydrofuran.[4]

(c) The isocyanide complexes protonate readily at their nitrogen atoms.[4]

The Phenyl Geometry - The phenyl rings display only expected features.[33]
Thus, they are planar within experimental error. Furthermore, the
C($\underline{sp}^2$)-C($\underline{sp}^2$) bond lengths range from 1.344(7) to 1.420(8) Å and have
a mean value of 1.387(3) Å which is only slightly shorter than the
spectroscopic value[20] [1.397(1) Å] for benzene. Moreover, the C-C-C
interbond angles are close to $120°$. The smallest values of this set
involve the $\underline{ipso}$-carbon atoms with a range of 117.4(3) to 118.9(4)°:

they are, thus, consistent with the P - C(Ph) distances and with the postulated Mo → P backdonation.[33]

(b) Complex (II)

The molecular structure is very similar to that of the analogous molybdenum complex (I).

Of particular interest is the metal-isocyanide geometry (Table 4.4). Thus, the M–C(donor) and C(sp)–N bond lengths, 2.065(5) and 1.12(1) Å respectively, are in good agreement with the corresponding distances of (I). The C(sp)–N–C(sp^3) angle again deviates significantly from 180° with a value of 151(1)$^\circ$ [cf. 155.1(5)$^\circ$ in (I)]. This observation strongly suggests that the pronounced non-linearity of the isocyanide ligand is a characteristic feature of the trans-[M(CNR)$_2$(dppe)$_2$] system rather than an artifact.

4.4. REFERENCES

1. J. Chatt, R.L. Richards, and G.H.D. Royston, J.C.S. Dalton, 1973, 1433, and refs. therein.

2. L. Malatesta and F. Bonati, 'Isocyanide Complexes of Metals,' Wiley, New York, 1969.

3. F. Bonati and G. Minghetti, Inorg. Chim. Acta., 1974, 9, 95, and refs. therein.

4. J. Chatt, A.J.L. Pombeiro, R.L. Richards, G.H.D. Royston, K.W. Muir, and R. Walker, J.C.S. Chem. Comm., 1975, 708; J. Chatt, C.M. Elson, A.J.L. Pombeiro, R.L. Richards, and G.H.D. Royston, J.C.S. Dalton, 1978, 165.

5. J. Chatt, G.A. Heath, and R.L. Richards, J.C.S. Dalton, 1974, 2074, and refs. therein.

6. F.A. Cotton and B.A. Frenz, Inorg. Chem., 1974, 13, 253, and refs. therein.

7. Ref. 34(b) of Sec. 2.7.

8. See Sec. 1.3.

9. W.R. Busing and H.A. Levy, Acta Cryst., 1957, 10, 180.

10. 'International Tables for X-Ray Crystallography,' Vol. IV, Kynoch Press, Birmingham, 1974.

11. R.F. Stewart, E.R. Davidson, and W.T. Simpson, J. Chem. Phys., 1965, 42, 3175.

12. D.T. Cromer and D. Liberman, J. Chem. Phys., 1970, 53, 1891.

13. See Sec. 2.3.2.

14. L. Pauling, 'The Nature of the Chemical Bond,' 3rd edition, Cornell University Press, Ithaca, New York, 1960.

15. T. Uchida, Y. Uchida, M. Hidai, and T. Kodama, Acta Cryst., 1975, B31, 1197.

16. (a)   M.A. Bush, A.D.U. Hardy, Lj. Manojlović-Muir, and

         G.A. Sim, J. Chem. Soc.(A), 1971, 1003;

    (b)   W.S. Sheldrick, Acta Cryst., 1975, B31, 1789;

    (c)   D.S. Payne, J.A.A. Mokuolu, and J.C. Speakman, Chem. Comm.,

         1965, 599.

17. M.J. Bennett and R. Mason, Proc.Chem.Soc., 1963, 273.

18. R. Mason and L. Randaccio, J.Chem.Soc.(A), 1971, 1150.

19. B. Jovanović, Lj. Manojlović-Muir, and K.W. Muir, J.C.S. Dalton,

     1974, 195.

20. L.E. Sutton, 'Tables of Interatomic Distances,' Chem. Soc.

     Special Publ., No.18, 1965.

21. J.R. Gollogly and C.J. Hawkins, Inorg. Chem., 1969, 8, 1168.

22. M.C. Hall, B.T. Kilbourn, and K.A. Taylor, J. Chem. Soc.(A),

     1970, 2539.

23. G.A. Sim, J.G. Sime, D.I. Woodhouse, and G.R. Knox, J. Organometallic

     Chem., 1974, 74, C7.

24. S.P. Arnesen and H.M. Seip, Acta Chem. Scand., 1966, 20, 2711.

25. K.K. Cheung, T.F. Lai, and K.S. Mok, J. Chem. Soc. (A), 1971,

     1644.

26. J.B. Wilford, N.O. Smith, and H.M. Powell, J. Chem. Soc.(A),

     1968, 1544.

27. E.M. Badley, D. Phil. Thesis, University of Sussex, 1969;

     cited in ref. 28.

28. B. Jovanović and Lj. Manojlović-Muir, J.C.S. Dalton, 1972,

     1176; B. Jovanović, Lj. Manojlović-Muir, and K.W. Muir,

     ibid., 1178.

29. G.K. Barker, A.M.R. Galas, M. Green, J.A.K. Howard, F.G.A. Stone,

     T.W. Turney, A.J. Welch, and P. Woodward, J.C.S. Chem. Comm.,

     1977, 256.

30. A.C. Sarapu and R.F. Fenske, _Inorg. Chem._, 1972, _11_, 3021;

    See also B.M. Gimarc, _J. Amer.Chem.Soc._, 1971, _93_, 815.

31. C.C. Costain, _J. Chem. Phys._, 1958, _29_, 864.

32. F.A. Cotton and R.M. Wing, _Inorg. Chem._, 1965, _4_ , 314.

33. A. Domenicano, A. Vaciago, and C.A. Coulson, _Acta Cryst._, 1975,

    _B31_, 221; _ibid._, 1630.

TABLE 4.1

Fractional co-ordinates ($\times 10^4$) and vibrational parameters of

<u>trans</u>-[Mo(CNMe)$_2$(Ph$_2$PCH$_2$CH$_2$PPh$_2$)$_2$]
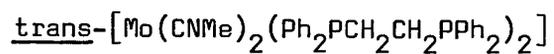
Atom	x	y	z	$U \times 10^3 \text{Å}^2$
Mo	0	0	0	*
P(1)	254(1)	1966(1)	-1469(1)	*
P(2)	678(1)	1138(1)	1154(1)	*
N	-3336(5)	1948(5)	40(4)	*
C(1)	1577(4)	2297(5)	-861(3)	40(1)
C(2)	1168(4)	2573(5)	242(4)	42(1)
C(3)	-2188(5)	1326(5)	12(3)	*
C(4)	-4629(8)	2326(12)	570(7)	*
C(11)	1036(4)	1729(5)	-2778(3)	38(1)
C(12)	1073(5)	2911(5)	-3626(4)	47(1)
C(13)	1775(5)	2649(6)	-4557(4)	55(1)
C(14)	2423(5)	1216(6)	-4655(4)	57(1)
C(15)	2381(5)	29(6)	-3823(4)	54(1)
C(16)	1700(5)	284(5)	-2889(4)	46(1)
C(21)	-1285(4)	3885(4)	-2015(3)	38(1)
C(22)	-1251(5)	5224(5)	-2115(4)	45(1)
C(23)	-2457(5)	6630(5)	-2546(4)	52(1)
C(24)	-3694(5)	6734(6)	-2917(4)	58(1)
C(25)	-3751(6)	5431(6)	-2836(5)	65(1)
C(26)	-2561(5)	4022(6)	-2367(4)	52(1)
C(31)	-560(4)	2369(5)	1935(4)	42(1)
C(32)	-237(5)	2233(5)	3044(4)	52(1)
C(33)	-1221(6)	3255(6)	3546(5)	66(1)
C(34)	-2488(6)	4359(7)	2965(5)	70(1)
C(35)	-2854(6)	4519(7)	1887(5)	72(2)

TABLE 4.1 (Cont'd)

Atom	x	y	z	$U \times 10^3 \text{Å}^2$
C(36)	-1872(6)	3507(6)	1354(4)	60(1)
C(41)	2263(4)	-149(5)	2212(3)	40(1)
C(42)	3604(5)	-315(6)	2004(4)	55(1)
C(43)	4783(6)	-1303(7)	2805(5)	69(1)
C(44)	4652(6)	-2180(6)	3825(5)	67(1)
C(45)	3355(6)	-2076(6)	4031(4)	59(1)
C(46)	2156(5)	-1072(5)	3234(4)	52(1)

* These atoms were assigned anisotropic temperature factors of the form

$$\exp\left[-2\pi^2 \sum_i \sum_j U_{ij} a_i^* a_j^* h_i h_j\right].$$ The final values of the U_{ij} parameters

$(\times 10^3)$ are:

Atom	U_{11}	U_{22}	U_{33}	U_{12}	U_{13}	U_{23}
Mo	43.7(3)	31.6(3)	28.7(3)	-24.8(2)	7.9(2)	-10.0(2)
P(1)	43.8(6)	35.5(6)	31.9(5)	-24.4(5)	6.4(5)	-9.9(4)
P(2)	47.0(6)	37.5(6)	32.8(5)	-25.5(5)	5.3(5)	-11.4(4)
N	66(3)	64(3)	59(3)	-29(3)	9(2)	-14(2)
C(3)	49(3)	38(2)	32(2)	-27(2)	9(2)	-11(2)
C(4)	69(5)	168(9)	104(6)	-17(5)	28(4)	1(6)

TABLE 4.1 (Cont'd)

(b) Fractional co-ordinates $(\times 10^3)$ and assumed isotropic vibrational parameters for hydrogen atoms; each hydrogen atom is numbered according to the carbon atom to which it is attached.

Atom	x	y	z	$U \times 10^3 \text{Å}^2$
H(1a)	256	138	-73	51
H(1b)	163	320	-140	51
H(2a)	198	253	66	52
H(2b)	33	363	9	52
H(4a)	-535	227	-25	134
H(4b)	-427	147	138	134
H(4c)	-515	338	50	134
H(12)	58	398	-357	57
H(13)	180	352	-516	65
H(14)	294	103	-534	66
H(15)	286	-103	-390	65
H(16)	169	-59	-228	56
H(22)	-33	518	-188	55
H(23)	-243	758	-258	62
H(24)	-456	778	-326	68
H(25)	-466	550	-311	75
H(26)	-263	307	-229	62
H(32)	72	139	348	62
H(33)	-100	316	435	75
H(34)	-320	509	334	79
H(35)	-382	535	146	83
H(36)	-213	362	55	69
H(42)	372	30	125	66
H(43)	575	-139	264	80

TABLE 4.1 (Cont'd)

Atom	x	y	z	$U \times 10^3 \, \text{Å}^2$
H(44)	551	-290	442	77
H(45)	325	-273	477	69
H(46)	119	-100	340	61

TABLE 4.2

Selected interatomic distances (Å) and angles (°) in

$$\underline{trans}\text{-}[Mo(CNMe)_2(Ph_2PCH_2CH_2PPh_2)_2]$$
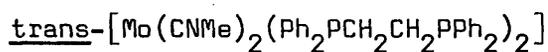
(a) Bond lengths

Mo-P(1)	2.442(1)	C(14)-C(15)	1.386(8)
Mo-P(2)	2.457(2)	C(15)-C(16)	1.387(7)
Mean	2.450(8)	C(16)-C(11)	1.395(7)
Mo-C(3)	2.095(4)	C(21)-C(22)	1.398(8)
		C(22)-C(23)	1.388(5)
C(3)-N	1.094(7)	C(23)-C(24)	1.371(9)
N-C(4)	1.449(10)	C(24)-C(25)	1.378(10)
		C(25)-C(26)	1.387(6)
P(1)-C(1)	1.856(6)	C(26)-C(21)	1.384(8)
P(2)-C(2)	1.882(5)	C(31)-C(32)	1.398(7)
Mean	1.869(13)	C(32)-C(33)	1.400(8)
C(1)-C(2)	1.508(7)	C(33)-C(34)	1.344(7)
		C(34)-C(35)	1.363(10)
P(1)-C(11)	1.849(4)	C(35)-C(36)	1.420(6)
P(1)-C(21)	1.841(3)	C(36)-C(31)	1.382(6)
P(2)-C(31)	1.860(5)	C(41)-C(42)	1.391(8)
P(2)-C(41)	1.847(4)	C(42)-C(43)	1.385(7)
Mean	1.847(4)	C(43)-C(44)	1.383(8)
		C(44)-C(45)	1.366(9)
C(11)-C(12)	1.390(6)	C(45)-C(46)	1.397(6)
C(12)-C(13)	1.394(7)	C(46)-C(41)	1.396(6)
C(13)-C(14)	1.378(8)	Mean	1.387(3)

TABLE 4.2 (Cont'd)

(b) Bond angles

P(1)-Mo-P(2)	79.6(1)	P(1)-C(11)-C(12)	122.7(4)
P(1)-Mo-C(3)	95.6(1)	P(1)-C(11)-C(16)	118.7(3)
P(2)-Mo-C(3)	94.2(2)	P(1)-C(21)-C(22)	124.4(4)
		P(1)-C(21)-C(26)	118.1(4)
Mo-C(3)-N	176.2(5)	P(2)-C(31)-C(32)	124.4(3)
C(3)-N-C(4)	155.1(5)	P(2)-C(31)-C(36)	116.7(4)
		P(2)-C(41)-C(42)	122.3(3)
Mo-P(1)-C(1)	107.1(1)	P(2)-C(41)-C(46)	119.8(4)
Mo-P(2)-C(2)	110.4(2)	Mean	121(1)
Mean	109(2)		
Mo-P(1)-C(11)	124.7(2)	C(11)-C(12)-C(13)	120.5(5)
Mo-P(1)-C(21)	119.4(2)	C(12)-C(13)-C(14)	120.3(5)
Mo-P(2)-C(31)	124.5(2)	C(13)-C(14)-C(15)	119.9(5)
Mo-P(2)-C(41)	117.0(2)	C(14)-C(15)-C(16)	119.9(5)
Mean	121(2)	C(15)-C(16)-C(11)	120.9(4)
		C(16)-C(11)-C(12)	118.5(4)
C(1)-P(1)-C(11)	98.0(2)	C(21)-C(22)-C(23)	120.9(5)
C(1)-P(1)-C(21)	103.0(2)	C(22)-C(23)-C(24)	120.4(6)
C(2)-P(2)-C(31)	96.7(2)	C(23)-C(24)-C(25)	119.8(4)
C(2)-P(2)-C(41)	102.8(2)	C(24)-C(25)-C(26)	119.9(6)
Mean	100(2)	C(25)-C(26)-C(21)	121.6(6)
C(11)-P(1)-C(21)	100.9(2)	C(26)-C(21)-C(22)	117.4(3)
C(31)-P(2)-C(41)	101.9(2)	C(31)-C(32)-C(33)	120.2(4)
Mean	101.4(5)	C(32)-C(33)-C(34)	120.0(6)
		C(33)-C(34)-C(35)	121.7(6)
P(1)-C(1)-C(2)	109.5(3)	C(34)-C(35)-C(36)	119.5(5)
P(2)-C(2)-C(1)	111.4(4)	C(35)-C(36)-C(31)	119.7(5)
Mean	110(1)	C(36)-C(31)-C(32)	118.9(4)

TABLE 4.2 (Cont'd)

Bond angles

C(41)-C(42)-C(43)	121.3(5)	C(44)-C(45)-C(46)	120,9(5)
C(42)-C(43)-C(44)	120.2(6)	C(45)-C(46)-C(41)	120.3(5)
C(43)-C(44)-C(45)	119.4(5)	C(46)-C(41)-C(42)	119.9(4)
Mean	119.7(3)		

TABLE 4.2 (Cont'd)

(c) Torsion angles

Mo-P(1)-C(1)-C(2)	-52.1(5)	Mo-P(2)-C(2)-C(1)	-22.6(5)
P(1)-Mo-P(2)-C(2)	-6.4(2)	P(2)-Mo-P(1)-C(1)	28.4(2)
P(2)-C(2)-C(1)-P(1)	-47.1(6)		

TABLE 4..2 (Cont'd)

(d) Intramolecular non-bonded contacts

Isocyanide···Phenyl

C(3)···C(16*)	3.44	C(3)···C(41*)	3.40
C(3)···C(21)	3.58	C(3)···C(42*)	3.65
C(3)···C(26)	3.32	C(4)···C(16*)	3.69
C(3)···C(36)	3.38		

Isocyanide···Methylene

C(3)···C(1*)   3.38

Phenyl···Phenyl

C(11)···C(22)	3.67	C(26)···C(45*)	3.70
C(11)···C(26)	3.58	C(26)···C(46*)	3.44
C(12)···C(21)	3.16	C(31)···C(46)	3.34
C(12)···C(22)	3.53	C(32)···C(41)	3.10
C(16)···C(31*)	3.45	C(32)···C(46)	3.15

Methylene···Phenyl

C(1)···C(12)	3.35	C(2)···C(21)	3.41
C(1)···C(16)	3.74	C(2)···C(22)	3.47
C(1)···C(22)	3.13	C(2)···C(32)	3.76
C(1)···C(41)	3.81	C(2)···C(36)	3.32
C(1)···C(42)	3.77	C(2)···C(42)	3.14

* Co-ordinates of the starred atoms are related to those of the corresponding unstarred ones by the transformation $(\bar{x}, \bar{y}, \bar{z})$.

TABLE 4.2 (Cont'd)

(e) Intermolecular non-bonded contacts

$C(2)\cdots C(22^{I})$	3.81	$C(14)\cdots C(23^{II})$	3.57
$C(2)\cdots C(23^{I})$	3.73	$C(22)\cdots C(32^{I})$	3.63
$C(13)\cdots C(23^{II})$	3.61	$C(23)\cdots C(32^{I})$	3.59

* The Roman numeral superscripts refer to the following co-ordinate transformations:

I -x, 1-y, -z   II -x, 1-y, -1-z

TABLE 4.3

Least-squares planes/line of <u>trans</u>-[Mo(CNMe)$_2$(Ph$_2$PCH$_2$CH$_2$PPh$_2$)$_2$]

Plane 1: Mo, P(1), P(2)

$$7.930X - 2.594Y - 2.101z = 0$$

[C(1) 0.836, C(2) 0.208]

Plane 2: C(11) - (16)

$$9.414X + 3.870Y + 5.904Z = 0.001$$

[P(1) 0.131, C(11) 0.002, C(12) -0.006, C(13) 0.004, C(14) 0.002,

C(15) -0.006, C(16) 0.004]

Plane 3: C(21) - (26)

$$-3.313X + 0.934Y + 11.781Z = -1.580$$

[P(1) -0.051, C(21) -0.006, C(22) -0.009, C(23) 0.014, C(24) -0.004,

C(25) -0.011, C(26) 0.016]

Plane 4: C(31) - (36)

$$8.347X + 8.829Y - 1.456Z = 1.337$$

[P(2) 0.065, C(31) 0.006, C(32) -0.006, C(33) 0.001, C(34) 0.004

C(35) -0.004, C(36) -0.001]

Plane 5: C(41) - (46)

$$2.229X + 9.355Y + 8.438Z = 2.214$$

[P(2) -0.025, C(41) 0.018, C(42) -0.014, C(43) 0.000, C(44) 0.011,

C(45) -0.007, C(46) -0.007]

Line 6: Mo, C(3), N

[Mo 0.011, C(3) 0.031, N 0.020]

$$X = -0.184 + 0.105t, \quad y = 0.109 - 0.061t, \quad z = 0.002 - 0.001t$$

TABLE 4.3 (Cont'd)

Angles (^{o}) between functions:

(1) - (6)	82.4	(4) - (5)	59.7
(2) - (3)	81.2		

TABLE 4.4

Selected interatomic distances ($\overset{o}{A}$) and angles (^{o}) in

$\underline{trans}$-$[W(CNMe)_2(Ph_2PCH_2CH_2PPh_2)_2]$
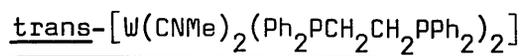
(a) Bond lengths

W-P(1)	2.429(2)	W-C(3)	2.065(5)
W-P(2)	2.442(4)	C(3)-N	1.12(1)
		N-C(4)	1.46(1)

(b) Bond angles

P(1)-W-P(2)	79.6(2)	W-C(3)-N	177.3(6)
P(1)-W-C(3)	95.7(2)	C(3)-N-C(4)	151(1)
P(2)-W-C(3)	94.3(3)		

Figure 4.1:   A view of the <u>trans</u>-$[Mo(CNMe)_2(Ph_2PCH_2CH_2PPh_2)_2]$

molecule; thermal ellipsoids enclose 50% of

probability.   Hydrogen atoms have been omitted

for clarity.
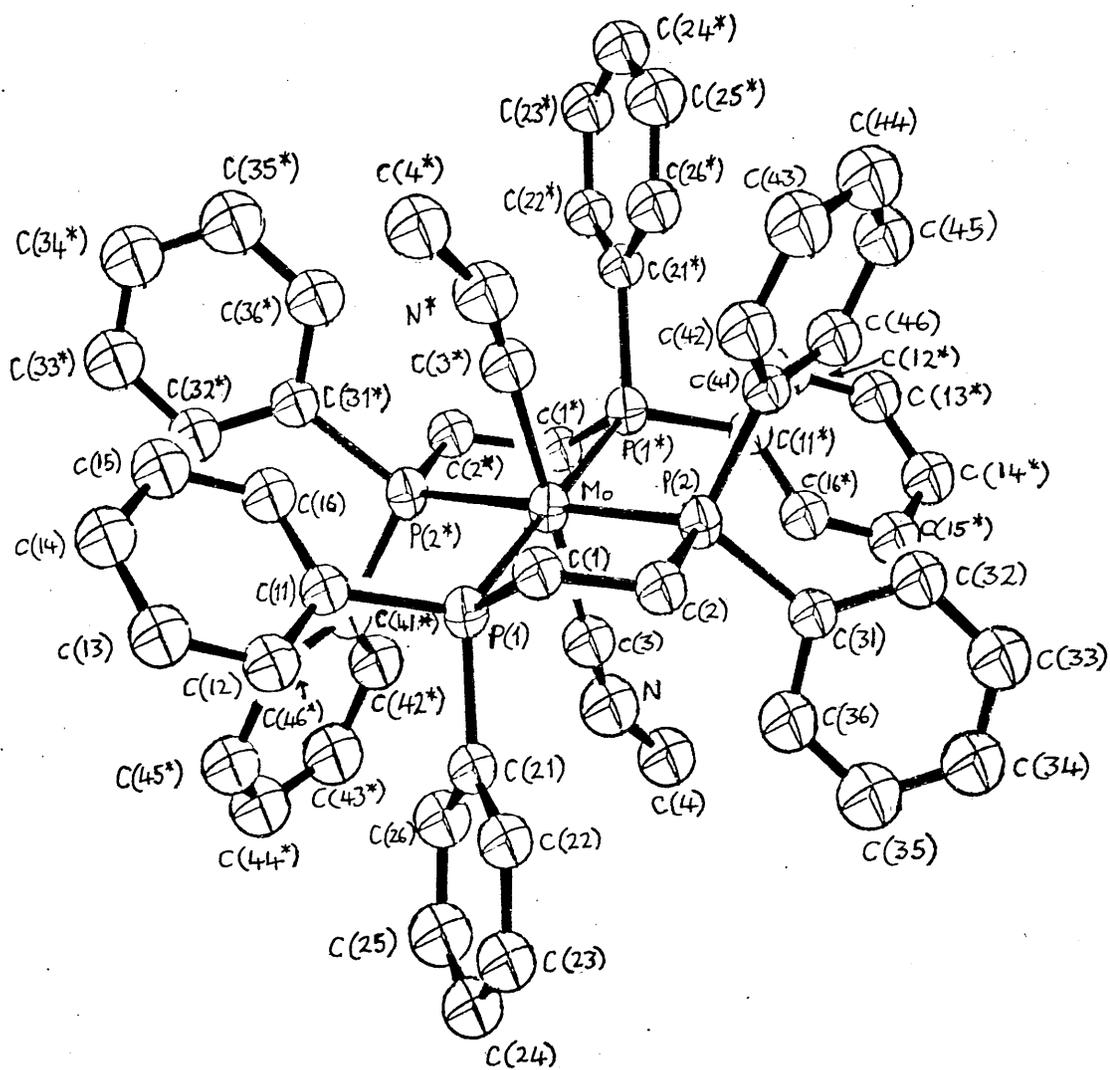
CHAPTER FIVE

The Crystal and Molecular Structures of

the Rhenium Nitrosyl Complexes

$\left[\text{ReCl}_2(\text{NO})(\text{PMePh}_2)_2\text{L}\right]$, (I) L = Cl,

and (II)   L = MeOH

5.1.   INTRODUCTION

Recently, Chatt and co-workers devised a synthetic route to novel

rhenium nitrosyl complexes (Fig. 5.1):
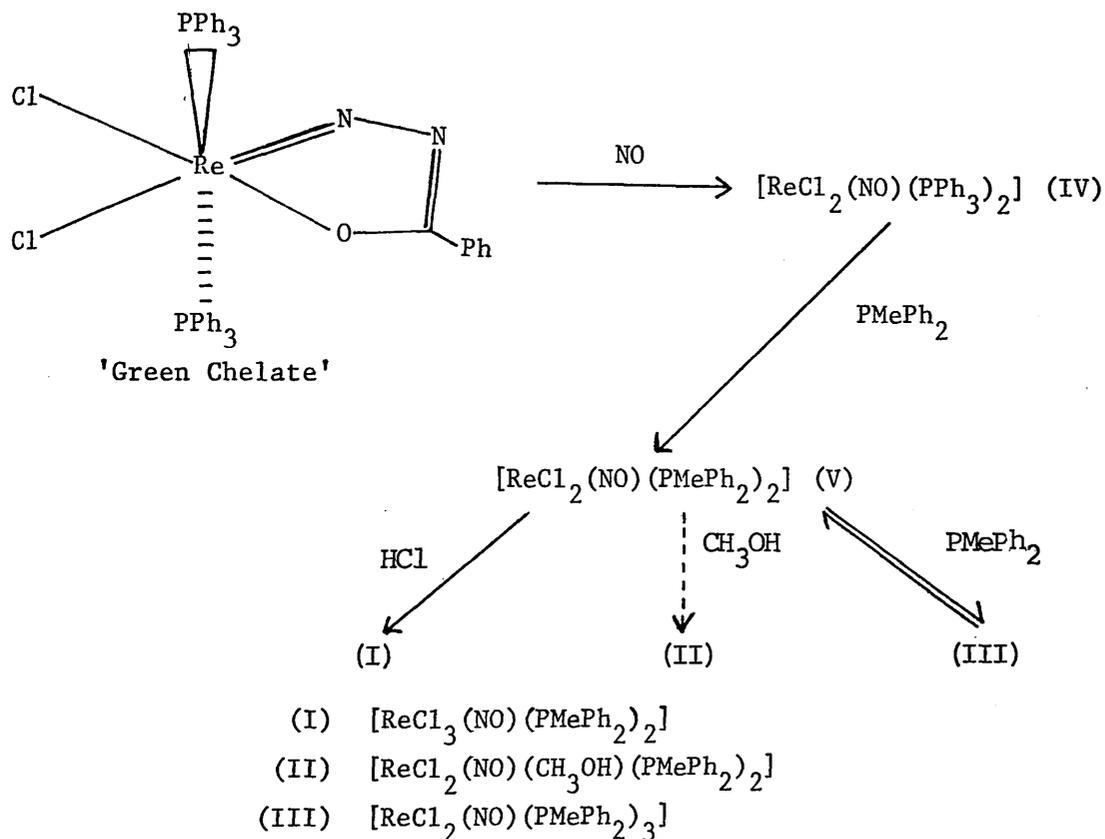
Figure 5.1:   Synthesis of Rhenium nitrosyls.

(I) $[ReCl_3(NO)(PMePh_2)_2]$

(II) $[ReCl_2(NO)(CH_3OH)(PMePh_2)_2]$

(III) $[ReCl_2(NO)(PMePh_2)_3]$

The "Green chelate" gives rise to $[ReCl_2(NO)(PPh_3)_2]$ (IV) which is

the parent compound of a variety of related five- and six-co-

ordinate rhenium nitrosyl derivatives.[1]

A preliminary account of the structure analysis of complex (III)

has been reported.[1] In that study it was observed that the molecules

had a linear Re-N-O arrangement, consistent with the formulation

of nitrosyl as the three-electron donor NO^+. From the similarity of

the ν(NO) stretching frequencies in (I), (III) and (V) [1740, 1690

and 1725 cm^{-1}, respectively, in chloroform solution],one can predict that the three complexes contain NO^+ ligands. However, the magnetic properties of (V) appear to be anomalous.[1] Thus, (V) has formally a Re(II) d^5 metal ion. However, the metal oxidation state is either Re(I) or Re(III), depending on whether the nitrosyl is co-ordinated as NO^+ or NO^-. A d^6 metal NO^+ complex should be diamagnetic, whereas a d^4 NO^- species could exhibit temperature-independent paramagnetism for octahedral co-ordination and can be either paramagnetic or diamagnetic when five-co-ordinate. It is observed that (V) displays paramagnetism which is _not_ temperature-independent.[1] Hence, it is difficult to assign a definite structure to (V) from magnetic and spectroscopic data.

The present author undertook the structure analysis of two represen-tative complexes $[ReCl_3(NO)(PMePh_2)_2]$ (I) and $[ReCl_2(NO)(PMePh_2)_2]$ (V) for the following reasons.

(i)   Unambiguous evidence of the structure of (V) was required in order to understand its anomalous magnetic behaviour.

(ii) Provision of additional structural information on rhenium nitrosyls should aid the assessment of the metal-nitrosyl bonding.

(iii) Interest also centred on the relative _trans_-influence of the nitrosyl ligand.

The results, unfortunately, have yielded no structural information on complex (V) because the crystal specimen used in the diffraction experiment was found to consist entirely of the octahedral complex $[ReCl_2(NO)(CH_3OH)(PMePh_2)_2]$ (II), which contains co-ordinated methanol originating from the recrystallisation solvent.

5.2. EXPERIMENTAL

Crystal Data.   Complex (I). $C_{26}H_{26}Cl_3NOP_2Re$, $M = 723.0$.
Triclinic, $a = 9.751$, $b = 9.627$, $c = 8.919$ Å, $\alpha = 116.69$,
$\beta = 88.24$, $\gamma = 113.50°$, $T = 20-28°C$, $U = 674.7$ Å^3,
$D_c = 1.780$ gm cm^{-3}, $Z = 1$, $F(000) = 353$.   Mo-K$_\alpha$ radiation,
$\mu(Mo-K_\alpha) = 52.0$ cm^{-1}.   Space group P$\bar{1}$.

Complex(II). $C_{27}H_{30}Cl_2NO_2P_2Re$, $M = 719.6$.   Monoclinic,
$a = 21.998(7)$, $b = 15.333(5)$, $c = 9.822(3)$ Å, $\beta = 115.26(2)°$,
$T = 20°C$, $U = 2996.1$ Å^3, $D_c = 1.595$ gm cm^{-3}, $Z = 4$,
$F(000) = 1416$.   Mo-K$_\alpha$ radiation, $\lambda = 0.71069$ Å, $\mu(Mo-K_\alpha) =$
46.0 cm^{-1};   Cu-K$_\alpha$ radiation, $\lambda = 1.5418$ Å, $\mu(Cu-K_\alpha) = 105.1$
cm^{-1}.   Space group P2$_1$/a.

Crystallographic Measurements.   The crystals of (I) are purple
air-stable polyhedra. The specimen used had dimensions ca.
0.67 x 0.18 x 0.10 mm. Crystals of (II) are brown air-stable
extremely thin needles. The specimen chosen for the analysis was
elongated along the c-axis and its dimensions were ca. 0.58 x
0.05 x 0.05 mm.

The crystal systems and unit-cell dimensions were determined by
X-ray photography. For (I), the space group P$\bar{1}$ led to a satis-
factory structural analysis which included the location of some of
the hydrogen atoms. For (II), the systematic absences 0k0 when
k = 2n + 1 and h0l when h = 2n + 1 uniquely determine the space
group as P2$_1$/a. The unit-cell dimensions were adjusted by a least-
squares treatment of the setting angles of a number [11,(I); 12(II)]

of reflexions centred on a Hilger and Watts' Y 290 diffractometer controlled by a PDP8 computer;[2] θ ranges of these reflexions were $12 \lesssim \theta \lesssim 17^{o}$ (I) and $8 \lesssim \theta \lesssim 12^{o}$ (II). For (II), reflexions with $\theta > 12^{o}$ and strong enough for setting purposes could not be found.

Complex (I). - The intensities of the unique reflexions for which $\theta(\text{Mo-}K_{\alpha}) \leq 30^{o}$ were measured on the Y 290 diffractometer with graphite-monochromated molybdenum radiation and a pulse-height analyser. A symmetrical $\theta - 2\theta$ scan was used, with a scan step in θ of 0.02^{o} and a counting time per step of 2.5 s. Each reflexion was scanned through a 2θ range of 1.52^{o}, and the local background was sampled for 15 s at each end of the scan. The intensities of three strong reflexions, measured periodically throughout the experiment, displayed systematic variations of up to +12 and -16% of their mean values because of changes in the ambient humidity and temperature attributed to malfunctioning of the laboratory air-conditioning system.

The integrated intensities, I, and their standard deviations, $\sigma(I)$, were derived in the usual manner (q 0.05).[3] They were scaled according to the variations of the intensities of the standard reflexions and corrected for Lorentz, polarisation and counting-loss effects.[3]

Of 3897 reflexions measured, 3869 for which $I \geq 3\sigma(I)$ were used in subsequent calculations.

Complex (II). - (a) Diffractometric Intensities

The intensities of all independent reflexions for which $\theta(\text{Mo-}K_{\alpha}) \leq 18^{o}$ were measured on the Y 290 instrument with the use of zirconium-filtered molybdenum radiation and a pulse-height analyser. A

symmetrical $\theta - 2\theta$ scan was used with a scan step of 0.02° in θ and a counting-time per step of 5s. Each reflexion was scanned through a 2θ range of 0.96° and the local background was counted for 20 s at each end of the scan range. The intensities of two strong low-angle reflexions measured periodically throughout the experiment showed only random fluctuations of up to $\pm$ 2% of their mean values.

The integrated intensities, I, and their standard deviations, $\sigma(I)$, were derived in the usual way (q 0.04).[3] They were corrected for Lorentz and polarisation effects;[3] correction for dead-time losses was considered unnecessary.

Of 2129 reflexions measured, only 1327 for which $I \geqslant 1.5\sigma(I)$ were used in the subsequent calculations.

(b) Photographic Intensities

In an attempt to include more high angle data, the intensities for (II) were re-collected by film methods. Multiple-film photographs of the hk0-8 levels were obtained by the equi-inclination Weissenberg technique, with the use of copper radiation.[4] The time of irradiation for a particular level was in the range 2-7 days.

The intensities were estimated visually with the aid of a calibrated strip and corrected for Lorentz and polarisation effects.[5] The hk8 layer intensities showed signs of significant crystal decomposition and were considered unworthy of measurement. 1272 unique intensities were estimated and used in subsequent calculations.

Structure Analysis. - In each analysis the position of the rhenium

atom was derived from a Patterson synthesis and the remaining non-hydrogen atoms were located in subsequent difference syntheses.

Each structural model was refined by the method of full-matrix least-squares, with minimisation of the function $\Sigma w \Delta^2$, where w is a suitable weight and $\Delta = |F_o| - |F_c|$. The weights were defined as $w = (A+B|F_o| + C |F_o|^2)^{-1}$ for (I) and $w = 1/\sigma^2(F_o)$ (diffractometric intensities) or $w = 1$(photographic intensities) for (II); the parameters A, B and C were adjusted during the refinement of (I) so that $\langle w \Delta^2 \rangle$ was approximately constant when analysed as a function of $|F_o|$ or $\sin \theta$. The final values employed for the parameters were A = 4.425, B = -0.421 and C = 0.012. Atomic scattering factors were taken from ref.6, except those for rhenium[7] and hydrogen.[8] Allowance was made for the anomalous scattering of the rhenium, chlorine and phosphorus atoms with Cromer's values of $\Delta f'$ and $\Delta f''$.[9]

<u>Complex (I)</u>. - With one molecule per unit cell there are alternative structural models: (a) the space group is P1 with one molecule per asymmetric unit; and (b) the space group is P$\bar{1}$ with the asymmetric unit consisting of half a molecule. The second alternative, which requires positional disorder, led to a successful solution.

A difference synthesis, based on phases calculated from the position of the rhenium atom, revealed the positions of most of the non-hydrogen atoms. In particular, it indicated a positional disorder of mutually-<u>trans</u> chloro and nitrosyl ligands.

Refinement of a scale factor and of the positional and isotropic thermal parameters of all non-hydrogen atoms led to R 0.067 and

R' 0.083. When anisotropic vibrational parameters were assigned
to the Re, P and Cl(2) atoms, R and R' decreased to 0.053 and 0.069,
respectively. A difference synthesis revealed the positions of 5
of the 10 phenyl hydrogen atoms. The positional parameters of all
such hydrogen atoms were calculated, assuming the normal phenyl
ring stereochemistry. The scattering of these atoms was included in
all subsequent structure factor calculations but neither their
positional nor thermal parameters were varied. The refinement
converged at R 0.053 and R' 0.056. In the final cycle of refinement
all parameters shifted by $< 0.9\sigma$. There were only expected features
in the final difference synthesis; the peak function values ranged
from +1.1 to -1.0 e $\overset{o}{A}^{-3}$, except for two values of +6.2 and -4.6 e $\overset{o}{A}^{-3}$
which were associated with the position of the metal atom. In the
final electron density synthesis the minimum peak height for a
carbon atom was 7.1 e $\overset{o}{A}^{-3}$.

Complex (II). - (a) Diffractometric Intensities

Refinement of a scale factor and of the positional and isotropic
thermal parameters of the rhenium atom led to R 0.27. When the
non-hydrogen atoms of the phosphine, nitrosyl and chloride ligands
were included, R decreased to 0.13. Anisotropic temperature factors
were then assigned to the rhenium, phosphorus and chlorine atoms,
giving R = 0.11. A difference synthesis revealed that a sixth
metal co-ordination site was occupied. However, the electron density
associated with this ligand appeared rather diffuse, and there was
only one function maximum at 3.5 e $\overset{o}{A}^{-3}$. There were difficulties in
the identification of this ligand since the sample had been
recrystallised from a variety of solvents in an attempt to obtain

a specimen of suitable dimensions and quality for an X-ray struc-

tural analysis. Initially, it was assumed that the sixth ligand was

a water molecule. However, this assumption proved unsatisfactory

in that it led to an unrealistic Re-O single bond length of 2.43 $\overset{o}{A}$.

Furthermore, the thermal parameters, U, of the nitrosyl atoms were

rather abnormal throughout the refinement. Thus, the nitrogen and

oxygen atoms had U values close to 0.03 and 0.19 $\overset{o}{A}{}^2$. Furthermore,

interchange of the nitrogen and oxygen atoms of the nitrosyl ligand

led to somewhat more acceptable thermal parameters of 0.13 and $0.06 \overset{o}{A}{}^2$,

respectively. These observations strongly suggested that the

structural model was partially incorrect.

(b) Photographic Intensities

With a view to obtaining the structure amplitudes of additional

high-angle reflexions, and hence better resolution, a set of

intensities was obtained by photographic methods. The observed

structure amplitudes were put on an approximately absolute scale

by comparison with the amplitudes calculated for the approximate

structural model already obtained. Refinement of layer scale factors

and the positional and isotropic thermal parameters of the non-

hydrogen atoms led to R 0.13. These parameters were found to be in

good agreement with those derived from the diffractometric

intensities. The atoms of the nitrosyl group and of the unidentified

ligand were then removed from the structural model: R increased to

0.16. The individual layer scale factors were then fixed at their

current values; an overall scale factor was introduced and an

anisotropic temperature factor was assigned to the rhenium atom.

R decreased to 0.13. A difference synthesis indicated that the

additional ligand consisted of two (non-hydrogen) atoms; peak

function values were 2.2 and 3.4 e $Å^{-3}$. Contrastingly, the corres-

ponding values of the ligand considered to be nitrosyl were 2.8 and

1.8 e $Å^{-3}$ for the nitrogen and oxygen atoms, respectively. It was

considered that a sixth co-ordination site was occupied by a methanol

molecule; this formulation was consistent with the variety of

solvents employed in the sample preparation and with the observed

density measured by flotation in aqueous ZnI_2 solution. At this stage

the electron density was apparently consistent with alternative

models for the two metal co-ordination sites (denoted A and B):

(i) the original model with A = bent NO and B = CH_3OH (possibly

disordered);[10] and (ii) A = CH_3OH and B = linear NO. Refinement

of each model was carried out.

(a) _Model (i)_. - When the nitrosyl atoms were included in the

refinement with isotropic thermal parameters R and R' were 0.12 and

0.14, respectively. The thermal parameters of these atoms were

again abnormal (_vide_ _supra_).

(b) _Model (ii)_. - Isotropic thermal parameters were assigned to the

nitrosyl atoms. R and R' became 0.12 and 0.14. Thus, distinction

between the models on the basis of the R-ratios[11] was impossible.

However, the second model did lead to physically reasonable thermal

parameters: U(N) = 0.09 and U(O) = 0.12 $Å^2$. Furthermore, the

Re-N and N-O bond lengths, respectively 1.70(6) and 1.18(8) $Å$, were

for the first time in accord with expectation (_cf._ l(Re-N) = 1.94(5) $Å$

and l(N-O) = 1.37(7) $Å$, previously). Accordingly, all further

refinement was carried out with this model. When the methanol carbon

and oxygen atoms were included in the refinement R and R' decreased

significantly to 0.095 and 0.11, respectively. Furthermore, the thermal parameters of these atoms, namely U(O) 0.11 and U(C) 0.10 $\overset{o}{A}{}^{2}$, were unexceptional and the Re-methanol dimensions were in the range expected (vide infra).

Despite the long exposures used, the photographic technique gave fewer usable structure amplitudes than the diffractometric experiment and the two data sets contained a high proportion of common reflexions. The refinement was, therefore, continued with the (presumably more accurate) diffractometric measurements. The positions of the hydrogen atoms of the phenyl groups were inferred from stereochemical considerations and the scattering of these atoms was included in subsequent structure factor calculations but neither the assumed thermal parameters nor the fractional atomic co-ordinates were varied. Refinement of a scale factor, anisotropic temperature factors of the rhenium, phosphorus and chlorine atoms, and isotropic thermal parameters of the remaining non-hydrogen atoms led to R 0.086 and R' 0.078. In the final cycle of refinement all parameters varied by < 0.2 σ. The standard deviation of an observation of unit weight was 1.8. However, mean values of $w\Delta^{2}$ showed no apparent trend when analysed as a function of $|F_{0}|$ or $\sin\theta$, indicating that the weighting scheme was satisfactory. The extreme function values (1.9 and -1.4 e $\overset{o}{A}{}^{-3}$) in the final difference synthesis were associated with the position of the metal atom.

Observed and calculated structure amplitudes (diffractometric set for II) are listed in the Appendix (pp. 190 - 210,(I), and 211 - 224,(II)]. Atomic parameters are given in Tables 5.1 and 5.2 and a selection of derived functions is presented in Tables 5.3 - 5.6. The atomic

labelling schemes are indicated and views of the molecular structures
are shown in Figures 5.2 and 5.3.

The computer programs employed have been described previously.[12]

5.3. RESULTS AND DISCUSSION

The crystals of both structures are built from discrete monomeric

molecules. The interactions between adjacent molecules are of the

van der Waals type;[13] selected intermolecular contacts are given

in Tables 5.3(d) and 5.4(d).

The Co-ordination of the Metal Atoms - The molecules of the title

complexes have distorted octahedral metal co-ordination geometries.

In each complex an equatorial plane is defined by the metal atom,

mutually-_trans_ $PMePh_2$ ligands, and mutually-_trans_ chloro and nitrosyl

ligands. The axial _trans_ co-ordination sites are occupied by two

chloro ligands in (I) and by chloro and methanol ligands in (II).

There are a number of short intramolecular contacts, involving

chlorine and phosphine carbon atoms (Tables 5.3(c) and 5.4(c)). The

most noteworthy are: $Cl(1)\cdots C(1)$ 3.56, $Cl(2)\cdots C(1)$ 3.45,

$Cl(1)\cdots C(12)$ 3.42, $Cl(1)\cdots C(21^*)$ 3.42 and $Cl(1)\cdots C(22^*)$ 3.20 $\overset{o}{A}$

in (I); and $Cl(1)\cdots C(1)$ 3.54, $Cl(1)\cdots C(2)$ 3.48, $Cl(2)\cdots C(1)$

3.50, and $Cl(2)\cdots C(2)$ 3.46 $\overset{o}{A}$ in (II). Of the remaining contacts,

there are only four of interest in (I): $N\cdots C(1)$ 3.48, $N\cdots C(21^*)$

3.29, $N\cdots C(22^*)$ 3.23, and $O\cdots C(22^*)$ 3.20 $\overset{o}{A}$.   Since these values

are not unduly short, any steric strain is expected to be small and

this is, indeed, observed. Thus, the angles subtended at the rhenium

atom by mutually-_cis_ ligand donor atoms lie in the narrow range

87-93°. Moreover, individual donor atoms of (I) are displaced only

slightly by up to 0.03 $\overset{o}{A}$ from the metal co-ordination planes (Table

5.5).

Replacement of one of the mutually-_trans_ chloro ligands of (I) by

a phosphine leads to the related complex _cis_-_mer_-$[ReCl_2(NO)(PMe_2Ph)_3]$

(III). The substitution of a chloride by phosphine, thereby producing a meridional arrangement of phosphine groups, is expected to produce some increase in steric strain in the primary metal co-ordination sphere. The interbond angles in (III) confirm this prediction. Thus, the angles subtended at the metal atom by cis ligands cover a wider range [84-96°] than is observed for (I).[14]

Substitution of a phosphine ligand of (III) by a methanol molecule, with retention of the metal configuration, leads to complex (II). The interbond angles within the $ReCl_2(NO)(PMePh)_2$ fragment of (II) are similar to those of (III): those involving mutually-cis ligands lie in the range 84.0(4) to 94(1)°. However, the angles O(1)-Re-P(1) 99.6(7)°, O(1)-Re-Cl(2) 80.0(8)°, and O(1)-Re-N 102(2)°, all involving the methanol oxygen atom, deviate more from the ideal octahedral value of 90° than any of the angles in (III) involving cis-ligand donor atoms. A possible explanation is intramolecular hydrogen bonding: the O(1)···Cl(2) distance of 2.78 Å is ca. 0.4 Å shorter than the sum of the van der Waals radii[13] of oxygen (1.4 Å) and chlorine (1.8 Å) atoms and within the range typical of O-H···Cl hydrogen bonds.[15]

The Rhenium-Phosphine Bonding. - The Re-P (trans to P) bond lengths in (I) and (II), respectively 2.511(1) Å and 2.49(2) Å (mean), are in good agreement. They are comparable to corresponding distances in related complexes: 2.462(3) Å (mean) in (III);[1] and 2.459(3) Å (mean), 2.470(1) Å, and 2.484(5) Å (mean), in the rhenium-imino complexes $[ReCl_3(L)(PEt_2Ph)_2]$ (L = $NC_6H_4COCH_3$ and NC_6H_4OMe)[16] and $[ReCl_3(NCH_3)(PEtPh_2)_2]$.[17]

The Rhenium-Chloride Bonding. - Re-Cl (trans to Cl) distances in

the literature cover a wide range, being dependent on, inter alia,

the metal oxidation state and ligand-ligand interactions. The bond

length observed in (I), 2.350(2) Å, is within the above range and,

in particular, is very similar to the values found in the related

complexes $[ReCl_3(MeCN)(PPh_3)_2]$ (2.35(1) and 2.36(1) Å),[18]

$[ReCl_3(PMe_2Ph)_3]$ (2.353(6) Å),[19] and in the anion $[ReCl_4(NO)(py)]^-$

(2.353 - 2.379(2) Å).[20] The Re-Cl (trans to NO) distances in (II)

and (III), respectively 2.40(1) and 2.436(3) Å, are also in good

agreement. However, the corresponding dimension for (I) [2.311(4)

Å] is ca. 0.1 Å shorter than these values. This contraction may

arise from systematic error: Ibers has reported systematic variations

of bond lengths in complexes which display an analogous halogen/

carbonyl disorder.[21]

The Re-Cl (trans to MeOH) bonded distance in (II) is 2.41(1) Å, which

is comparable to the Re-Cl (trans to NO) bond lengths in (II) and

(III), indicating that the trans-influences of nitrosyl and methanol

ligands are similar.

The Rhenium-Nitrosyl Bonding. - The Re-N-O interbond angles in the

complexes (I) - (III) [178(2)°, (I); 179(4)°, (II); and 179(1)°,

(III)] do not differ significantly from 180°. Hence, the nitrosyl

ligands may be described formally as NO^+ 3-electron donors. Moreover,

the Re-N and N-O bond lengths [1.79(2), 1.21(2) Å; 1.60(4),

1.20(5) Å; and 1.775(10), 1.182(14) Å, respectively in (I), (II)

and (III)] are similar and in the range expected for NO^+ derivatives

of third-row transition metals.[22] In particular, they are in fair

agreement with corresponding values found in the anions $[ReCl_4(NO)(py)]^-$

$[1.749(6), 1.171(9)$ Å$]^{20}$ and $[ReBr_4(NO)(EtOH)]^-$ $[1.723(15), 1.19(2)$ Å$]$.[23]

The Rhenium-Methanol Interaction. - A methanol molecule is co-ordinated to the metal atom in (II) with a Re-O distance of 1.88(3) Å. Structural data for ligating alcohol molecules are scarce. However, the above bond length is indicative of a fairly strong metal-oxygen σ-bond. It may be compared with the sum of the covalent radii[24] of the metal and oxygen atoms (ca. 1.95 Å), with Re-O(sp^3) distances in the derivatives $[NEt_4][ReBr_4(NO)(EtOH)]$ and $[ReO(H_2O)Cl_2tu_2]Cl$ (2.161(5) and 2.23(1) Å, respectively),[23, 25] and with Re = O double bond distances (ca. 1.80 Å).[26] Furthermore, the O(sp^3)-C(sp^3) O(1)···C(3) bonded distance $[1.40(5)$ Å$]$ appears normal,[26] and the M-O(H)-C(sp^3) angle of 124(3)° is comparable to those observed in the anion $[ReBr_4(NO)-$(EtOH)]^-$ $[132.1(13)°]$[23] and in a uranium derivative $[121.9(11)°]$.[27]

The Phosphine Ligands. - The geometry of each phosphine ligand is normal.[28] Thus the Re-P-C and C-P-C interbond angles display the expected deviations from a regular tetrahedral configuration. Moreover, the P-C(Ph), P-C(Me), and C(Ph)-C(Ph) bond lengths are in the ranges expected. Thus, the mean P-C(Ph) distances are 1.812(4) Å and 1.82(3) Å, respectively, in (I) and (II); the corresponding P-C(Me) bond lengths are 1.822(6) Å and 1.84(3) Å (mean), respectively. These values are similar to those found in other monotertiary phosphine derivatives of third-row transition metal ions.[29] Furthermore, the mean C(Ph)-C(Ph) distances in (I) and (II) are, respectively, 1.39(1) and 1.38(1) Å which agree well with the spectroscopic value for benzene.[26] The C-C-C interbond angles are close to 120°, as expected, and the phenyl rings are planar within experimental error.

5.4.   REFERENCES.

1. R. W. Adams, J. Chatt, N. E. Hooper, and G. J. Leigh, J.C.S. Dalton,
        1974, 1075.

2. W.R. Busing and H. A. Levy, Acta Cryst., 1967, 22, 457.

3. See Sec. 1.3.

4. M. J. Buerger, 'Crystal-Structure Analysis,' Wiley, New York, 1960,
        Ch. 6.

5. Ref. 4, Ch. 7.

6. 'International Tables for X-Ray Crystallography,' vol. IV, Kynoch Press,
        Birmingham, 1974.

7. D. T. Cromer and J. T. Waber, Acta Cryst., 1965, 18, 104.

8. R. F. Stewart, E. R. Davidson, and W. T. Simpson, J. Chem. Phys.,
        1965, 42, 3175.

9. D. T. Cromer, Acta Cryst., 1965, 18, 17.

10. Group B is linearly co-ordinated to rhenium, whereas a Re-O(H)-C(sp^3)
        interbond angle is expected to be ca. 130° (ref. 23)

11. W. C. Hamilton, 'Statistics in Physical Science,' Ronald Press,
        New York, 1964, pp. 157-162; Acta Cryst., 1965, 18, 502.

12. Sec. 2.3.2.

13. L. Pauling, 'The Nature of the Chemical Bond,' Cornell University
        Press, Ithaca, New York, 1960.

14. Dr. K. W. Muir, personal communication.

15. W. C. Hamilton and J. A. Ibers, 'Hydrogen Bonding in Solids,'
        W. A. Benjamin, New York, 1968.

16. D. Bright and J. A. Ibers, Inorg. Chem., 1968, 7, 1099.

17. D. Bright and J. A. Ibers, ibid., 1969, 8, 703.

18. M. G. B. Drew, D. G. Tisley, and R. A. Walton, Chem. Comm., 1970, 600.

19. L. Aslanov, R. Mason, A. G. Wheeler, and P. O. Whimp, ibid., 30.

20. G. Ciani, D. Giusto, M. Manassero, and M. Sansoni, J.C.S. Dalton,
        1978, 798.

21. N. C. Payne and J. A. Ibers, Inorg. Chem., 1969, 8, 2714.

22. B. A. Frenz and J. A. Ibers, Med. Tech. Publ. Co., Int. Rev. Sci.,
    Inorg. Chem., Ser. One, 1972.

23. G. Ciani, D. Giusto, M. Manassero, and M. Sansoni, J.C.S. Dalton,
    1975, 2156.

24. J. C. Slater, J. Chem. Phys., 1964, 41, 3199.

25. T. Lis, Acta Cryst., 1976, B32, 2707.

26. L. E. Sutton, 'Tables of Interatomic Distances,' Chem. Soc. Special
    Publ. No. 18, 1965.

27. G. Bandoli, D. A. Clemente, U. Croatto, M. Vidali, and P. A. Vigato,
    J.C.S. Dalton, 1973, 2331.

28. M. A. Bush, A. D. U. Hardy, Lj. Manojlović-Muir, and G. A. Sim,
    J. Chem. Soc. (A), 1971, 1003.

29. B. Jovanović, Lj. Manojlović-Muir, and K. W. Muir, J. Chem. Soc.
    Dalton, 1974, 195.

TABLE 5.1.

(a) Fractional co-ordinates $(\times 10^4)$ and vibrational parameters

in $[ReCl_3(NO)(PMePh_2)_2]$,(I)

Atom	x	y	z	$U \times 10^3 \mathrm{\AA}^2$
Re	0	0	0	*
N**	340(17)	2085(25)	1712(23)	63(3)
O**	624(14)	3503(20)	2878(19)	66(3)
Cl(1)**	504(3)	2713(5)	2196(4)	38.7(5)
Cl(2)	1524(2)	-320(2)	1700(2)	*
P	2325(1)	1434(1)	-991(1)	*
C(1)	3963(7)	2807(8)	741(8)	46(1)
C(11)	2232(6)	2894(6)	-1709(6)	36(1)
C(12)	1835(7)	4209(9)	-632(9)	49(1)
C(13)	1785(8)	5385(10)	-1121(10)	56(1)
C(14)	2105(8)	5238(10)	-2681(10)	55(1)
C(15)	2513(8)	3952(10)	-3751(10)	57(1)
C(16)	2556(7)	2773(8)	-3274(8)	48(1)
C(21)	2856(5)	-71(6)	-2711(6)	35(1)
C(22)	1835(6)	-1198(8)	-4262(8)	44(1)
C(23)	2192(8)	-2366(9)	-5614(9)	52(1)
C(24)	3564(8)	-2450(9)	-5436(9)	54(1)
C(25)	4571(8)	-1359(9)	-3900(9)	52(1)
C(26)	4228(7)	-161(8)	-2537(8)	44(1)

* These atoms were assigned anisotropic temperature factors of the

form $\exp\left[-2\pi^2 \sum_i \sum_j U_{ij} a_i^* a_j^* h_i h_j\right]$. The final values of the U_{ij} parameters

$(\times 10^4)$ are:

TABLE 5.1 (Cont'd)

Atom	U_{11}	U_{22}	U_{33}	U_{12}	U_{13}	U_{23}
Re	315(1)	275(1)	268(1)	125(1)	38(1)	133(1)
Cl(2)	455(6)	486(7)	500(7)	180(5)	-29(5)	272(6)
P	283(5)	297(5)	303(5)	106(4)	48(4)	136(4)

** Site occupancies of these atoms are 0.5.

TABLE 5.1 (Cont'd)

(b) Calculated fractional co-ordinates $(\times 10^3)$ and assumed isotropic

vibrational parameters for hydrogen atoms; each hydrogen atom is

numbered according to the carbon atom to which it is attached.

Atom	x	y	z	$U \times 10^3 \, \text{Å}^2$
H(12)	159	432	52	60
H(13)	150	633	-33	67
H(14)	208	609	-303	66
H(15)	278	389	-488	68
H(16)	286	184	-408	58
H(22)	81	-115	-439	54
H(23)	145	-319	-674	62
H(24)	381	-330	-642	65
H(25)	557	-142	-378	64
H(26)	497	65	-142	54

TABLE 5.2.

(a) Fractional co-ordinates ($\times 10^3$) and vibrational parameters in $[\text{ReCl}_2(\text{NO})(\text{MeOH})(\text{PMePh}_2)_2]$, (II)

Atom	x	y	z	$U \times 10^2 \text{Å}^2$
Re	115.2(1)	182.4(1)	209.2(2)	*
P(1)	36.1(6)	288.5(8)	22.5(14)	*
P(2)	211.7(5)	101.9(8)	396.3(13)	*
Cl(1)	196.2(5)	233.5(8)	121.7(11)	*
Cl(2)	145.9(6)	299.3(8)	388.7(13)	*
N	95(2)	106(3)	86(5)	10(1)
O(1)	64(1)	153(2)	314(3)	6(1)
O(2)	80(1)	50(2)	-7(4)	9(1)
C(1)	73(2)	398(3)	34(5)	8(2)
C(2)	287(2)	168(3)	494(5)	8(1)
C(3)	29(2)	74(3)	293(5)	9(2)
C(11)	14(2)	252(3)	-163(5)	7(1)
C(12)	46(2)	275(3)	-254(6)	11(2)
C(13)	26(3)	243(4)	-398(7)	12(2)
C(14)	-27(3)	189(4)	-456(5)	11(2)
C(15)	-62(2)	164(3)	-378(5)	9(2)
C(16)	-38(2)	201(3)	-228(5)	9(2)
C(21)	-45(2)	320(3)	34(5)	7(1)
C(22)	-54(2)	287(3)	158(5)	10(2)
C(23)	-119(3)	310(4)	149(6)	13(2)
C(24)	-167(2)	352(3)	31(6)	10(2)
C(25)	-152(2)	382(3)	-76(5)	10(2)
C(26)	-90(3)	363(3)	-88(6)	11(2)
C(31)	199(2)	57(3)	548(4)	5(1)

TABLE 5.2 (Cont'd)

Atom	x	y	z	$U \times 10^2 \text{Å}^2$
C(32)	167(2)	103(3)	615(5)	6(1)
C(33)	156(2)	76(3)	740(5)	8(1)
C(34)	183(2)	-6(3)	796(4)	7(1)
C(35)	215(2)	-56(3)	739(6)	10(2)
C(36)	224(2)	-30(3)	620(5)	7(1)
C(41)	236(2)	8(3)	312(4)	6(1)
C(42)	297(2)	9(3)	300(5)	9(2)
C(43)	309(2)	-64(4)	229(5)	10(2)
C(44)	263(3)	-127(3)	168(5)	11(2)
C(45)	206(2)	-130(3)	188(5)	8(2)
C(46)	191(2)	-58(3)	246(5)	9(2)

* These atoms were assigned anisotropic temperature factors of

the form $\exp\left[-2\pi^2\sum_i\sum_j U_{ij}a_i^*a_j^*h_ih_j\right]$. The final values of the U_{ij}

parameters $(\times 10^2)$ are:

Atom	U_{11}	U_{22}	U_{33}	U_{12}	U_{13}	U_{23}
Re	4.6(1)	6.0(1)	5.9(1)	-0.4(2)	2.5(1)	-0.5(2)
P(1)	6(1)	8(1)	8(1)	1(1)	3(1)	0(1)
P(2)	5(1)	7(1)	7(1)	-1(1)	3(1)	-1(1)
Cl(1)	5(1)	11(1)	6(1)	0(1)	3(1)	1(1)
Cl(2)	8(1)	8(1)	8(1)	-2(1)	3(1)	-1(1)

TABLE 5.2 (Cont'd)

(b) Calculated fractional co-ordinates ($\times 10^3$) and assumed isotropic vibrational parameters for hydrogen atoms; each hydrogen atom is numbered according to the carbon atom to which it is attached.

Atom	x	y	z	$U \times 10^2 \mathring{A}^2$
H(12)	86	321	-207	12
H(13)	54	257	-456	13
H(14)	-42	170	-569	12
H(15)	-103	122	-424	10
H(16)	-67	185	-169	10
H(22)	-18	248	244	11
H(23)	-129	294	241	13
H(24)	-215	359	26	10
H(25)	-187	424	-158	10
H(26)	-80	380	-183	12
H(32)	150	165	571	7
H(33)	129	112	784	9
H(34)	178	-28	891	8
H(35)	232	-116	790	10
H(36)	250	-71	578	9
H(42)	332	59	343	10
H(43)	355	-67	221	11
H(44)	273	-175	105	11
H(45)	177	-187	160	9
H(46)	142	-52	234	10

TABLE 5.3

Selected interatomic distances (Å) and angles (°) in (I)

(a) **Bond lengths**

Re-Cl(1)	2.311(4)	C(11)-C(12)	1.40(1)
Re-Cl(2)	2.350(2)	C(12)-C(13)	1.40(2)
Re-P	2.511(1)	C(13)-C(14)	1.37(1)
Re-N	1.79(2)	C(14)-C(15)	1.38(1)
		C(15)-C(16)	1.39(1)
N-O	1.21(2)	C(16)-C(11)	1.38(1)
		C(21)-C(22)	1.40(1)
P-C(11)	1.819(8)	C(22)-C(23)	1.38(1)
P-C(21)	1.809(5)	C(23)-C(24)	1.39(1)
Mean	1.812(4)	C(24)-C(25)	1.38(1)
P-C(1)	1.822(6)	C(25)-C(26)	1.39(1)
		C(26)-C(21)	1.39(1)
		Mean	1.39(1)

TABLE 5.3 (Cont'd)

(b) Interbond angles

Cl(1)-Re-Cl(2)	89.9(1)	C(11)-P-C(21)	105.9(3)
Cl(1)-Re-P	87.0(1)		
Cl(2)-Re-N	90.4(8)	C(11)-C(12)-C(13)	120.6(7)
Cl(2)-Re-P	89.3(1)	C(12)-C(13)-C(14)	120.2(8)
N-Re-P	88.4(6)	C(13)-C(14)-C(15)	119.8(10)
N-Re-Cl(1)	178.5(5)	C(14)-C(15)-C(16)	120.3(8)
		C(15)-C(16)-C(11)	120.8(7)
Re-N-O	178(2)	C(16)-C(11)-C(12)	118.4(7)
		C(21)-C(22)-C(23)	120.5(7)
Re-P-C(11)	115.8(2)	C(22)-C(23)-C(24)	120.2(6)
Re-P-C(21)	113.5(2)	C(23)-C(24)-C(25)	119.7(7)
Mean	115(1)	C(24)-C(25)-C(26)	120.4(8)
Re-P-C(1)	111.0(2)	C(25)-C(26)-C(21)	120.0(5)
		C(26)-C(21)-C(22)	119.1(5)
C(1)-P-C(11)	103.1(3)	Mean	119.9(2)
C(1)-P-C(21)	106.6(3)		
Mean	105(2)		

TABLE 5.3 (Cont'd)

(c) Intramolecular non-bonded distances[**]

$PMePh_2$

C(1)⋯C(12)	3.39	C(16)⋯C(21)	3.12
C(1)⋯C(26)	3.13	C(16)⋯C(22)	3.28
C(11)⋯C(22)	3.41		

$Cl⋯PMePh_2$

Cl(1)⋯C(1)	3.56	Cl(2)⋯C(1)	3.45
Cl(1)⋯C(12)	3.42	Cl(2)⋯C(11*)	3.51
Cl(1)⋯C(21*)	3.42	Cl(2)⋯C(12*)	3.59
Cl(1)⋯C(22*)	3.20		

$NO⋯PMePh_2$

N⋯C(1)	3.48	N⋯C(22*)	3.23
N⋯C(21*)	3.29	O⋯C(22*)	3.20

[**] Co-ordinates of the starred atoms are related to those of the corresponding unstarred ones by the transformation $(\bar{x}, \bar{y}, \bar{z})$.

TABLE 5.3 (Cont'd)

(d) Intermolecular non-bonded distances

$O\cdots C(23^{I})$*   3.23 $C(1)\cdots C(14^{III})$ 3.60

$Cl(1)\cdots C(15^{II})$ 3.61 $C(1)\cdots C(15^{III})$ 3.64

$C(1)\cdots C(13^{III})$ 3.76

* The Roman numeral superscripts refer to the following co-ordinate transformations:

 I x, 1+y, 1+z   III 1-x, 1-y, -z

II x,   y, 1+z

TABLE 5.4

Selected interatomic distances (Å) and angles (°) in (II)

(a) **Bond lengths**

Re-P(1)	2.51(1)	C(14)-C(15)	1.37(9)
Re-P(2)	2.47(1)	C(15)-C(16)	1.45(7)
Mean	2.49(2)	C(16)-C(11)	1.30(6)
Re-Cl(1)	2.41(1)	C(21)-C(22)	1.42(8)
Re-Cl(2)	2.40(1)	C(22)-C(23)	1.44(9)
Re-N	1.60(4)	C(23)-C(24)	1.35(7)
Re-O(1)	1.88(3)	C(24)-C(25)	1.32(9)
		C(25)-C(26)	1.45(9)
O(1)-C(3)	1.40(5)	C(26)-C(21)	1.35(6)
N-O(2)	1.20(5)	C(31)-C(32)	1.34(7)
		C(32)-C(33)	1.41(7)
P(1)-C(1)	1.85(5)	C(33)-C(34)	1.41(6)
P(2)-C(2)	1.82(4)	C(34)-C(35)	1.30(8)
Mean	1.84(3)	C(35)-C(36)	1.32(8)
P(1)-C(11)	1.76(5)	C(36)-C(31)	1.50(6)
P(1)-C(21)	1.89(5)	C(41)-C(42)	1.40(8)
P(2)-C(31)	1.77(5)	C(42)-C(43)	1.39(8)
P(2)-C(41)	1.84(5)	C(43)-C(44)	1.35(7)
Mean	1.82(3)	C(44)-C(45)	1.35(9)
		C(45)-C(46)	1.34(7)
C(11)-C(12)	1.40(9)	C(46)-C(41)	1.37(6)
C(12)-C(13)	1.38(8)	Mean	1.38(1)
C(13)-C(14)	1.34(8)		

TABLE 5.4 (Cont'd)

(b)   Interbond angles

Cl(1)-Re-Cl(2)	90.0(4)	C(1)-P(1)-C(11)	106(2)
Cl(1)-Re-N	88(2)	C(1)-P(1)-C(21)	99(2)
Cl(1)-Re-P(1)	85.2(4)	C(2)-P(2)-C(31)	102(2)·
Cl(1)-Re-P(2)	84.0(4)	C(2)-P(2)-C(41)	107(2)
Cl(2)-Re-O(1)	80.0(8)	Mean	104(2)
Cl(2)-Re-P(1)	86.7(4)	C(11)-P(1)-C(21)	107(2)
Cl(2)-Re-P(2)	86.8(4)	C(31)-P(2)-C(41)	105(2)
N-Re-O(1)	102(2)	Mean	106(1)
N-Re-P(1)	92(1)		
N-Re-P(2)	94(1)		
O(1)-Re-P(1)	99.6(7)	C(11)-C(12)-C(13)	123(5)
O(1)-Re-P(2)	89.8(7)	C(12)-C(13)-C(14)	120(6)
Cl(1)-Re-O(1)	168.6(6)	C(13)-C(14)-C(15)	122(5)
Cl(2)-Re-N	178(2)	C(14)-C(15)-C(16)	114(4)
P(1)-Re-P(2)	167.4(5)	C(15)-C(16)-C(11)	127(5)
		C(16)-C(11)-C(12)	114(4)
		C(21)-C(22)-C(23)	112(4)
Re-N-O(2)	179(4)	C(22)-C(23)-C(24)	124(6)
Re-O(1)-C(3)	124(3)	C(23)-C(24)-C(25)	119(6)
		C(24)-C(25)-C(26)	124(4)
Re-P(1)-C(1)	113(1)	C(25)-C(26)-C(21)	113(5)
Re-P(2)-C(2)	114(1)	C(26)-C(21)-C(22)	127(5)
Mean	114(1)	C(31)-C(32)-C(33)	126(4)
Re-P(1)-C(11)	110(1)	C(32)-C(33)-C(34)	114(4)
Re-P(1)-C(21)	120(2)	C(33)-C(34)-C(35)	125(5)
Re-P(2)-C(31)	115(1)	C(34)-C(35)-C(36)	121(5)
Re-P(2)-C(41)	112(1)	C(35)-C(36)-C(31)	121(5)
Mean	113(2)	C(36)-C(31)-C(32)	114(4)

TABLE 5.4 (Cont'd)

C(41)-C(42)-C(43)	116(4)	C(44)-C(45)-C(46)	116(5)
C(42)-C(43)-C(44)	122(5)	C(45)-C(46)-C(41)	124(5)
C(43)-C(44)-C(45)	122(5)	C(46)-C(41)-C(42)	119(4)
Mean	119(1)		

TABLE 5.4 (Cont'd)

(c) Intramolecular non-bonded distances

PMePh$_2$

C(1)···C(12)	3.24	C(16)···C(21)	3.22
C(1)···C(26)	3.29	C(16)···C(26)	3.28
C(2)···C(32)	3.46	C(31)···C(46)	3.39
C(2)···C(36)	3.76	C(36)···C(41)	3.21
C(2)···C(42)	3.16	C(36)···C(46)	3.46
C(11)···C(26)	3.18		

Cl···PMePh$_2$

Cl(1)···C(1)	3.54	Cl(2)···C(1)	3.50
Cl(1)···C(2)	3.48	Cl(2)···C(2)	3.46

NO···PMePh$_2$

N···C(11)	3.23	N···C(46)	3.23
N···C(41)	3.30	O(2)···C(46)	3.12

MeOH···PMePh$_2$

C(3)···C(22)	3.70	O(1)···C(22)	3.16
C(3)···C(31)	3.51	O(1)···C(31)	3.23
C(3)···C(32)	3.35	O(1)···C(32)	2.95
C(3)···P(2)	3.74		

MeOH···NO

C(3)···N	3.02

MeOH···Cl

O(1)···Cl(2)	2.78

TABLE 5.4 (Cont'd)

(d) Intermolecular non-bonded distances

$C(1)\cdots C(25^{I})$*	3.72	$O(2)\cdots C(3^{II})$	3.39
$C(1)\cdots C(26^{I})$	3.69	$C(3)\cdots C(14^{III})$	3.63
$C(3)\cdots C(15^{II})$	3.75	$C(33)\cdots C(13^{III})$	3.64

* The Roman numeral superscripts refer to the following co-ordinate transformations:

I $-x,\ 1-y,\ -z$ III $x,\ y,\ 1+z$

II $-x,\ -y,\ -z$

TABLE 5.5

Equations of least-squares planes of (I) in which x, y, z refer to fractional co-ordinates. Deviations of selected atoms from the plane are given in square brackets.

Plane 1:   Re, P, P', Cl(2), Cl(2')*

$$-2.424 \ x +6.245 \ y +3.349 \ z = 0$$

[Symmetry requires exact coplanarity]

Plane 2:   Re, Cl(1), Cl(2), Cl(2'), N

$$6.584 \ x +3.146 \ y -5.311 \ z +0.002 = 0$$

[Re 0.002, Cl(1) 0.021, Cl(2) 0.002, Cl(2') 0.002, N -0.027]

Plane 3:   Re, P, P', Cl(1), N

$$6.790 \ x -6.508 \ y +6.514 \ z +0.001 = 0$$

[Re 0.001, P 0.001, P' 0.001, Cl(1) 0.008, N -0.010]

Plane 4:   C(11) - C(16)

$$7.658 \ x +1.017 \ y +1.550 \ z -1.736 = 0$$

[P 0.036, C(11) 0.002, C(12) -0.001, C(13) 0.004, C(14) -0.008,
  C(15) 0.008, C(16) -0.005]

Plane 5:   C(21) - (26)

$$1.313 \ x +7.770 \ y -6.440 \ z -2.061 = 0$$

[P -0.004, C(21) 0.004, C(22) -0.007, C(23) 0.003, C(24) 0.004,
  C(25) -0.006, C(26) 0.002]

Angles (°) between planes:

(1)-(2)	87.5	(2)-(3)	89.3
(1)-(3)	89.9	(4)-(5)	66.3

TABLE 5.5 (Cont'd)

* Co-ordinates of the primed atoms are derived from those of the corresponding unprimed ones by the transformation $(\bar{x}, \bar{y}, \bar{z})$.

TABLE 5.6

Least-squares planes and lines of (II)

Plane 1:   Re, P(1), P(2), Cl(2), N

19.467 x +5.196 y −6.547 z −1.924 = 0

[Re −0.103, P(1) 0.131, P(2) 0.132, Cl(2) −0.073, N −0.087]

Plane 2:   Re, P(1), P(2), Cl(1)

0.005 x +11.614 y +5.799 z −3.429 = 0

[Re −0.097, P(1) 0.053, P(2) 0.054, Cl(1) −0.010, O(1) 0.169]

Plane 3:   Re, N, Cl(1), Cl(2)

9.950 x −8.990 y +4.074 z −0.349 = 0

[Re 0.010, N −0.006, Cl(1) 0.000, Cl(2) −0.004, O(1) 0.314]

Plane 4:   C(11) − (16)

−11.039 x +12.076 y −1.073 z −3.072 = 0

[P(1) −0.010, C(11) −0.013, C(12) 0.006, C(13) 0.004, C(14) −0.007, C(15) −0.001, C(16) 0.012]

Plane 5:   C(21) − (26)

3.720 x +13.149 y +3.607 z −4.154 = 0

[P(1) −0.145, C(21) 0.015, C(22) −0.012, C(23) 0.022, C(24) −0.036, C(25) 0.038, C(26) −0.027]

Plane 6:   C(31) − (36)

14.793 x +6.469 y +2.583 z −4.722 = 0

[P(2) 0.093, C(31) 0.000, C(32) 0.004, C(33) −0.005, C(34) 0.003, C(35) 0.002, C(36) −0.003]

TABLE 5.6 (Cont'd)

Plane 7: C(41)-(46)

$$1.254 \ x \ -7.348 \ y \ +7.541 \ z \ -2.571 \ = \ 0$$

[P(2) -0.066, C(41) 0.016, C(42) 0.004, C(43) 0.007, C(44) -0.037,

C(45) 0.057, C(46) -0.047]

Line 8:   Re, O(1)

$$x \ = \ 0.090 \ +0.027t, \ y \ = \ 0.168 \ +0.016t, \ z \ = \ 0.262 \ -0.056t.$$

Angles ($^{\circ}$) between planes/line:

(1)-(2)	87.2	(2)-(8)	81.9
(1)-(3)	89.2	(3)-(8)	84.4
(1)-(8)	78.0	(4)-(5)	65.4
(2)-(3)	89.7	(6)-(7)	68.4
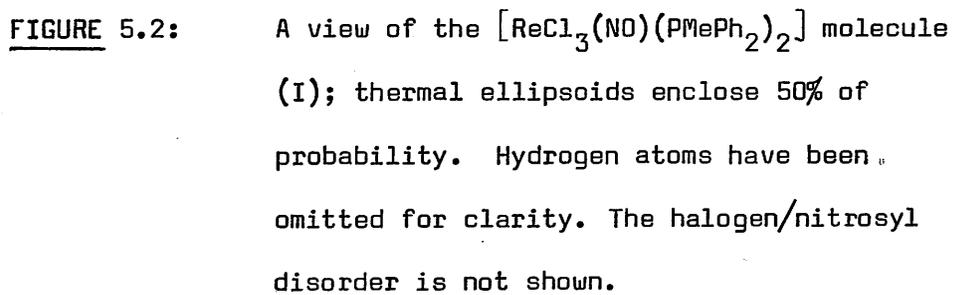
FIGURE 5.2:   A view of the $[ReCl_3(NO)(PMePh_2)_2]$ molecule

(I); thermal ellipsoids enclose 50% of

probability. Hydrogen atoms have been

omitted for clarity. The halogen/nitrosyl

disorder is not shown.
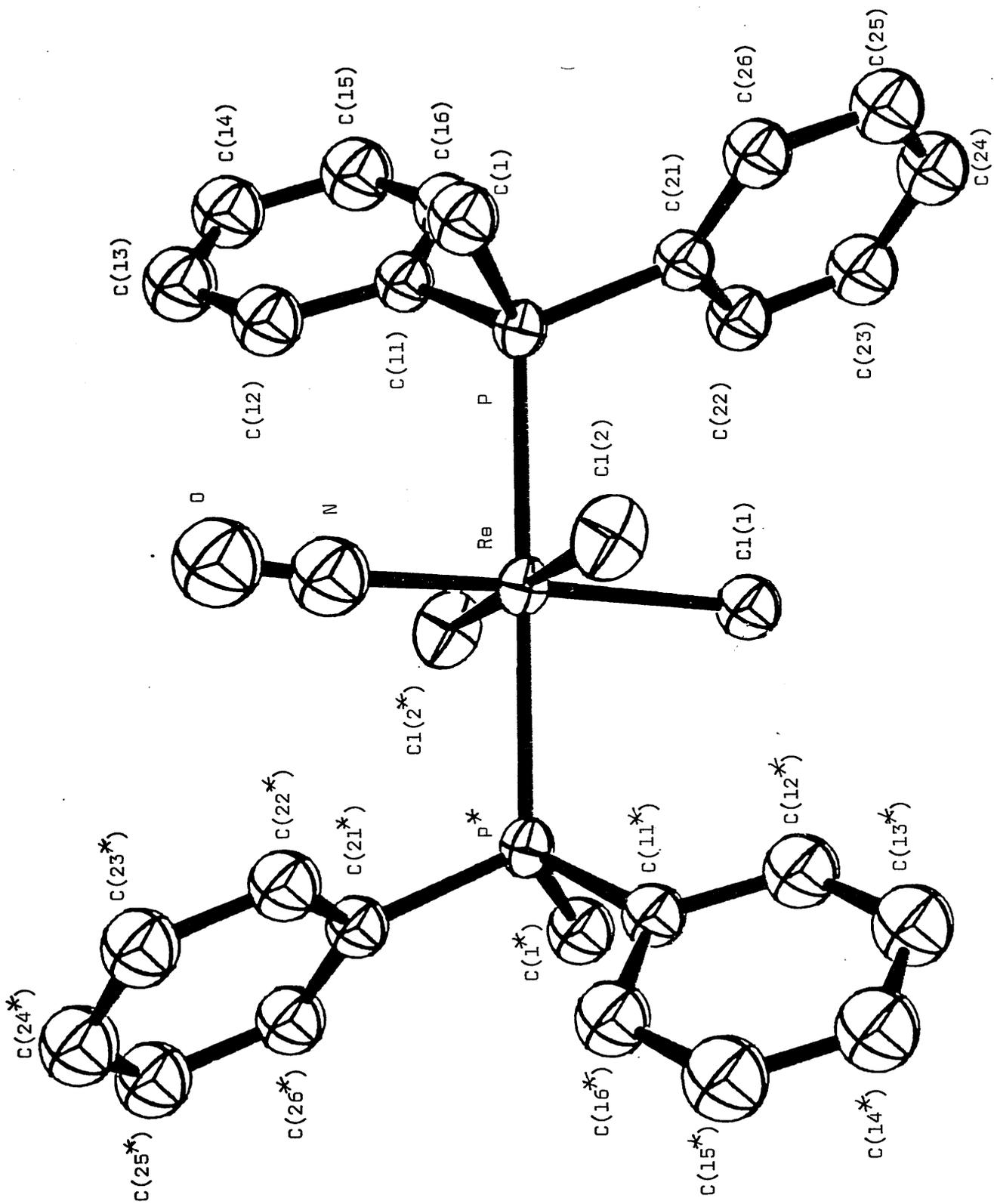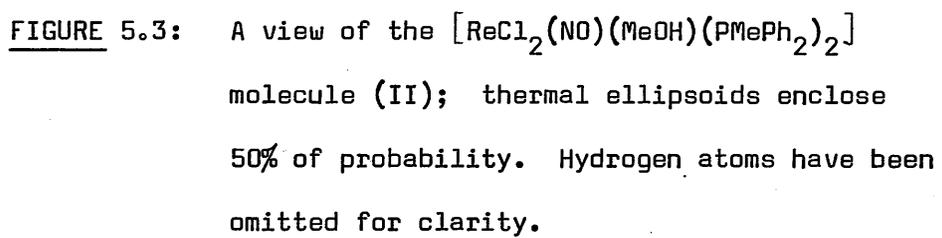
FIGURE 5.3: A view of the $[ReCl_2(NO)(MeOH)(PMePh_2)_2]$

molecule (II); thermal ellipsoids enclose

50% of probability. Hydrogen atoms have been

omitted for clarity.